Study on Development of Latent Heat Storage at Various Middle High Temperature Range

March, 2018

Than Tun Naing

Graduate School of

Natural Science and Technology

(Doctor's Course)

Okayama University

Abstract

In recent years, energy demand has increased due to the high-energy consumption in domestic and industrial sectors. People's living standards have improved due to the development of science and technology but in addition to the depletion of fossil resources. Fossil fuels have served and fulfilled all human needs of energy for a long era. These fossil fuels caused significant damage to the environment as it leads to global warming, climate change, acid rain etc. In addition, the prices of fossil fuels have increased and are expected to continue in coming years because of the increase in energy demand.

The effective use of alternative energy such as solar power generation and wind power generation that are environmentally friendly are expected. However, these alternatives are susceptible to weather and supplies are unstable. Thus, a thermal storage system that temporarily store energy is required. On the other hand, some factories discard the waste heat energy into the environment from the exhaust system. It leads to air-pollution, global warming and there are a lot of wasted energy that people cannot use. If these types of wasted heat energy can be stored and used somewhere at the desirable time, it will be very useful for human being life and can decrease the unnecessary environmental impact. For these reasons, thermal storage technology plays a very important role. The purpose of this research is to develop the latent heat storage technology and to effectively utilize unused wasted energy that caused by exhausted heat from factories as a heat source of latent heat storage system that recovers the wasted heat energy in the temperature range of 100$\sim$400°C.

A number of different approaches have been developed to solve this wasted heat energy problem by using different latent heat storage materials that have different melting temperatures. Many researchers present the solidification and melting of the latent heat

storage materials by using differential scanning calorimetry(DSC). In this dissertation, we constructed a latent heat storage system for research purpose and three different latent heat storage materials were observed with different melting temperature range of the wasted heat energy.

For the melting temperature range of 300∼400°C, the mixtures of NaCl: KCl: LiCl were used. Firstly, many different wt% of the mixtures were studied to get the required melting temperature by using the electric furnace. After getting the latent heat storage mixture, we tested the corrosiveness of some construction materials and selected the appropriate material to construct the experimental device. There are corrosiveness problems because of high temperature. Corrosiveness test of construction materials with latent heat storage mixture were performed by using some anti-corrosive spray, paint and argon gas. For this mixture, some construction materials could be used for experiment device but they were too expensive. And most of the construction materials could not be used because of corrosiveness problems with the latent heat storage material and high melting temperature. We found some difficulties to construct the experiment devise for this temperature range.

The second part of this dissertation presents the latent heat storage material mixture for the melting temperature range of 200∼300°C. The mixture of NaOH: LiOH were used for this melting temperature range. Firstly, many different mol% of mixtures were studied to get the required melting temperature by using the electric furnace. After getting the latent heat storage mixture, corrosiveness test were performed with some construction materials in order to select the appropriate material to construct the experimental device. According to the corrosiveness test results, we designed and constructed the experimental device by using the stainless steel SS316L. We must use the argon gas to decrease the corrosiveness problems of the construction materials and latent heat storage material mixtures. This device contains the test-section, heating system, and the cooling system. In this system, indirect heat exchange system was used between latent heat storage material mixture and heat transfer oil. By using this device, the melting and solidification process and behavior of this latent heat storage material mixture were investigated.

The last part of this dissertation describes an approach to develop a latent heat storage system using middle-temperature waste heat of 100∼200°C from factories. Direct contact melting and solidification behaviors between the heat-transfer fluid and the latent heat storage material mixture were observed. The mixture consisted mannitol and erythritol (C_m = 70 mass %, C_e = 30 mass %) as a phase-change material (PCM). The weight of the PCM was 3.0 kg and the flow rates of the oil, f_{oil}, were 1.0, 1.5, or 2.0 kg/min. While making the solidification process, the solidification height increases as the flow rate of heat transfer oil increases. There was a flow out problem of PCM from the test-section with the heat transfer oil at high flow rate of oil. We attempted to control the solidified height of the PCM mixture during the solidification process,by installing a perforated partition plate in the PCM region inside of the heat storage vessel. PCM coated oil droplets were broken by the perforated partition plate, preventing the solidified height of the PCM from increasing. The solidification and melting processes were repeated using metal fiber. It was found that installing the metal fiber were more effective than installing the perforated partition plate to prevent the flow out problem of the PCM. While using the perforated partition plate and metal fiber, the amount of heat release were slightly lessened than without of that. To increase the amount of heat release during the solidification process, the effects of metal fiber diameter, the proportion of fibers, and the position of the fibers within the PCM region were also investigated. As a result, the most effective conditions employed metal fibers with a diameter of 0.2 mm. The numerical calculation was performed to predict the temperature of the mixture and compared it with the experimental results . As a results, the temperature trends of the numerical calculation were nearly the same with the experimental results.

Acknowledgements

The success of this research work in this thesis became possible due to a lot of help from many people during my Ph.D. study at Okayama University. Firstly, I would like to express my deepest gratitude to my advisor, Professor Akihiko Horibe, for his valuable guidance, encouragement, patience, motivation, and support in completing the research work in this thesis.

I wish to express my thanks to Professor Naoto Haruki and Assistant Professor Yutaka Yamada for their suggestions and comments throughout my Ph.D. research. Their kind guidance, encouragement, and patience have been a great support throughout my research.

I would like to thank my thesis committee members, Professor Eiji Tomita and Professor Shinichiro Yanase, for their encouragement, insightful comments and reviewing this dissertation. I feel proud and honored that you have accepted to be on my committee.

In this study, as co-researcher with Mr. Yoshitaka Takase, and Mr. Nobumasa Suzuki who performed the work with the author, Mr. Mazakazu Shinoda and Mr. Shiro Sugitani who cooperated in all processes from the production of the experimental apparatus to the implementation of the experiment and the data arrangement. I wish to express my gratitude here for their efforts to make this research fruitful.

I wish to express my thanks to Mr. Tatsuya Imai. It is one of the most fun memories when we were talking at the Heat Transfer Laboratory. I will remember your word that I am ever ready for Naing San for preparing the experimental device. I deeply thanks for helping not only in the workshop but also for daily life in Japan.

I also would like to thank all previous and current student members of Heat Transfer Laboratory, who have been very helpful not only in the laboratory but also in personal mat-

ters. I also would like to thank the staff from Centre of Global Partnerships and Education for their kind help during my stay at Okayama University.

The writing of this dissertation became possible due to the financial support by Japan International Cooperation Agency (JICA), Heat Transfer Laboratory and Okayama University.

Finally, I would like to offer my special thanks to my family, my wife, who always give encouragement, support, and good advice.

Contents

List of Figures

List of Tables

List of Symbol

C_m : mannitol mass %

C_e : erythritol mass%

Q : the amount of heat (kJ)

f : flow rate of oil (kg/min)

C_p : specific heat (kJ/kgK)

t : time (min)

T : temperature (°C)

ΔT : temperature difference (°C)

L : latent heat (kJ/kg)

m : mass (kg)

ϕ : the ratio of heat with experiment and theoretical

P : the rate of heat(kJ/s)

h : enthalpy(kJ/kg)

Subscripts

M : melting process

S : solidification process

oil : heat transfer fluid oil

PCM : phase change material

l : liquid

s : solid

e : end of process

b : beginning of process

m : melting

f : finishing time

th : theoretical value

ts : test section

in : inlet

out : outlet

Mix : mixture

a : ambient

Chapter 1

Introduction

1.1 Introduction

In recent years, energy demand has increased due to the high-energy consumption in domestic and industrial sectors. People's living standards have improved due to the development of science and technology but in addition to the depletion of fossil resources. Fossil fuels have served and fulfilled all human needs of energy for a long era. These fossil fuels caused significant damage to the environment that leads to global warming, climate change, acid rain etc. In addition, the value of fossil fuels have increased and are expected to continue through the coming years because of the increase in energy demand.

The effective use of alternative energy such as solar power generation and wind power generation that are environmentally friendly are expected. However, these alternatives are susceptible to weather and supply are unstable, thus temporarily store energy and require a storage system to supply it when needed. If these types of waste heat energy can be stored somewhere and used at the desirable time, it will be very useful for human life and be able to decrease the unnecessary environmental impact. For these reasons, thermal storage technology plays a very important role. To store these wasted heat energy, it can use sensible heat storage, latent heat storage, and chemical heat storage. Researchers on thermal storage systems have been actively conducted, including latent heat storage systems that utilize sensible heat storage that stores heat due to temperature changes of substances, latent heat

generated when a substance undergoes a phase change, chemical thermal storage utilizing chemical reaction and so on. Sensible heat storage is stable and safe, but the thermal storage density is small, chemical storage can store a lot of heat, but reactions at high temperature and high pressure are required, and stability lacks. Therefore, attentions are paid to latent heat storage from the viewpoint of stability and heat storage capacity, and research has been actively carried out.

1.2 Background and Motivation

Thermal energy storage plays an important role for effective use of thermal energy and has applications in diverse areas, such as building heating or cooling systems, solar energy collectors, power and industrial waste heat recovery [1]. The term latent heat storage applies to the storage of heat as the latent heat of fusion in suitable substances that undergo melting or freezing at desired temperature level [2]. The wide range of Phase Change Material (PCM) applications in the construction, electronic, biomedical, textile and automotive industries are presented, and future research directions are indicated. In recent years, the integration of PCMs in thermal storage systems has been a topic of interest in research and development within the heat transfer and renewable energy communities [3]. Solar energy is available during the day only, and its application requires efficient thermal energy storage so that the excess heat collected during sunshine hours may be stored for later use during the night [4]. Major examples of the applications of PCMs include thermal storage of solar energy. Performance of PCM for solar thermal energy storage was conducted using a commercially available flat-plate solar thermal collector [5] [6]. In order to increase the efficiency of the solar air collector and to improve their thermal efficiency in terms of operating time, hot outlet air temperature and starting operation time, the performance of a compact phase change material solar air heater collector based on latent heat storage energy was investigated [7].

Advanced-structure heat sinks with multi-layer PCMs and hybrid passive heat sinks combined with active cooling are also introduced. The PCM-based thermal management system is powerful in ensuring electronic devices, Li-ion batteries and photovoltaic cells working

safely and efficiently [8]. The rapid commercialization of PCMs for heating, ventilation, and air-conditioning(HVAC) applications, has paved way for effective utilization of ambient thermal fluctuations temperature regulation in residential and commercial buildings [9]. The application of PCM in heating and domestic hot water systems can reduce greenhouse gas emission and electrical power consumption [10]. The experimental studies related to PCMs usage in hot water tank and central thermal storage were performed [11], [12]. With the rapid development of construction industry, more and more lightweight building materials are applied in high-rise buildings. PCMs with their high heat storage capacity have been considered for the building thermal storage [13]. The review focuses on PCM technologies developed to serve the building industry. Various PCM technologies tailored for building applications are studied with respect to technological potential to improve indoor environment, increase thermal inertia and decrease energy use for building operation [14].

An optimal design for a PCM underfloor heating system is proposed to reduce energy consumption in apartment buildings and thermal storage performance of the proposed system is evaluated experimentally [15] Latent heat thermal energy storage (LHTES) are becoming more and more attractive for space heating and cooling of buildings. The application of LHTES in buildings has the following advantages: the ability to narrow the gap between the peak and off-peak loads of electricity demand; the ability to save operative fees by shifting the electrical consumption from peak periods to off-peak [16]. Many considerations are discussed in this paper including physical considerations about building envelop and PCM [17]. Thermal energy storage used for air conditioning systems and the application of PCMs in different parts of the air conditioning network, air distribution network, chilled water network, microencapsulated slurries, thermal power and heat rejection of the absorption cooling. It is expected that the design of latent heat thermal energy storage will reduce the cost and volume of the air conditioning systems and networks [18].

Heat storage materials which can store wasted heat at medium-temperature around 200∼400°C were discussed. Wasted heats around 200∼400°C are emitted as exhaust gases from an internal combustion engine, co-generation, high-temperature process and solar sys-

tems. Amount of exhaust gas emission are quite large and needed to utilize well for energy efficiency improvement [19]. A phase change material acting as thermal mass is attached to one side of the thermoelectric generators while the other side is placed on the aircraft structure. The application area under investigation for this paper is the pylon aft fairing, located near the engine of an aircraft, with temperatures reaching on the inside up to 350°C [20] . The work on thermal energy storage materials, development of PCMs classification, working principle of PCMs and working of PCMs in clothing were studied. The review also summarizes the evaluation of textiles containing PCM and different applications Paraffinic hydrocarbon are widely used in textiles than other PCM due to its outstanding properties such as noncorrosiveness, chemical, and thermal stability and low under cooling [21]. The use of latent heat thermal energy storage for thermally buffering vehicle systems is reviewed. Vehicle systems with transient thermal profiles are classified according to operating temperatures in the range of 0∼800°C. A comprehensive overview of phase change materials covering the relevant operating range are given, including selection criteria and a detailed list of over 700 candidate materials from a number of material classes [22]. Thermal energy storage forms a key component of a power plant for improvement of its dispatch ability. Though there have been many reviews of storage media, there are not many that focus on storage system design along with its integration into the power plant [23].

The continuous increase in the level of greenhouse emissions gas and the climb in fuel prices are the main driving forces behind efforts more effectively utilize various sources of renewable energy. One of the options is to develop energy storage devices, which are as important as developing new sources of energy. The storage of energy in suitable forms, which can conventionally be converted into the required form, is a present-day challenge to the technologists [24]. With a global concern about energy and carbon dioxide emissions, renewable energies has attracted extensive attention. One of the crucial aspects is waste heat recovery and thermal energy storage. Phase change materials have unique merits in latent heat thermal energy storage, due to its capability of providing a high-energy density storage by solidifying/melting at a constant temperature [25].

Motivated as shown above reasons, thermal energy storage technology is essential for energy required problem and to protect the environment impact. New heat storage materials are required as much as we can at various temperature zone to store wasted heat energy. In this research, three different heat storage materials are investigated for different temperature range and construct the latent heat storage system for research purpose.

1.3 Purpose of this study

As shown in the previous section, the latent heat storage technology is widely used large ranges of utilization. One of the problems of the latent heat storage material is that the melting temperature of this material is fixed and cannot be changed. Even though there is a waste heat source at a certain temperature, there is a possibility that the heat source may be wasted if there is no heat storage material usable at this temperature. In order to solve this problem, many types of research should be made to get the new heat storage materials for various temperature. The purpose of this research is to develop the latent heat storage technology and to effectively utilize unused wasted energy that received by exhaust heat from factories as a heat source of latent heat storage system. Another hand, this latent heat storage system can be used to protect the global warming to minimize the different electricity between day and night, and to minimize the depletion of fossil fuel. To recover the wasted heat energy in the temperature range (100∼400°C) discarded from the factories, our research purpose is to determine the new heat storage material mixtures at the temperatures of 150°C, 250°C, and 350°C, and to construct the latent heat storage system. And then study the solidification and melting behaviors, the temperature histories during the heat stored and released process, and the amount of heat required for melting and solidification of each material mixture according to the temperature range.

1.4 Structure of this thesis

This paper consists of all six chapters. The chapters contained in this dissertation can be briefly summarized as follows:

Chapter 1 describes introduction and the background information that leads to conduct the research in this thesis.

Chapter 2 presents the thermal energy storage system and required properties and classification of energy storage materials.

Chapter 3 describes the selection of heat storage material mixture that melts about the melting temperature of 300∼400°C. Corrosiveness test of construction material with this heat storage material mixture were performed. And also used anti-corrosiveness sprays and argon gas to determine the corrosiveness of construction materials.

Chapter 4 contains the construction of latent heat storage system of the mixture that melts at the melting temperature of 200∼300°C. In addition, the melting and solidification behaviors of this mixture was described.

Chapter 5 includes the melting and solidification behaviors of heat storage material mixture that has the melting temperature of 100∼200°C. While using a mixture of erythritol and mannitol, there is a problem of flow out from the system at the high flow rate of heat transfer fluid oil. The methods are investigated to protect the flow out problem of heat storage material mixture. The numerical calculation is performed to predict the temperature of heat storage mixture and compared to experimental results.

Finally, **Chapter 6** summarizes the results described in each chapter and concludes this dissertation and future work.

Chapter 2

Thermal Energy Storage Technology

In order to efficiently utilize thermal energy or to increase the efficiency of heat-utilizing equipment, it is necessary to supply the required amount of thermal energy at the desirable time. The thermal storage system is used between thermal energy supply and demand. By effectively storing and supplying unused energy such as waste heat from factories, it is considered to be an environmentally friendly system that can convert these energy into usable energy at the desire place and time [26]-[27].

Solar energy has a disadvantage that the amount of energy that can be utilized depending on the climate changes greatly. To effectively utilize natural energy like solar energy, therefore, it is necessary to store thermal energy intermittently and store it appropriately. It is considered that the thermal storage tank installed in the solar water heater used in the private sector has a big influence on the efficiency of the whole system. In addition, in order to effectively use waste heat, the heat storage system is also considered to be very important. To efficiently use the late-night electric power from the power demand difference between the day and night, the heat storage system is a very efficient method. Latent heat thermal energy storage (TES) using phase change materials (PCM) is an effective way of storing thermal energy because of its high energy storage density and the nearly isothermal melting and solidification processes at the phase change transition temperature of the PCM [28].

Generally, in the thermal energy utilization system, the operating temperature is deter-

mined according to the waste heat temperature. The heat storage technology in the thermal storage system is an important technology to make the whole energy utilization system efficiently operate. In contrast, the thermal storage system requires the initial investment cost as disadvantage, but unused waste energy can be used as energy supply and reduction effect of greenhouse gas can be directly obtained.

2.1 Thermal energy storage system

The most common way to classify the thermal heat storage method is to distinguish it from sensible heat storage, latent heat storage, and chemical storage according to the stored thermal energy form. The thermal storage system can be used at low temperature (100°C or less), medium temperature (150∼250°C), and high temperature (250°C or higher), and can be distinguished in short-term and long-term thermal storage according to the duration of thermal storage.

The sensible heat storage is a system that uses heat capacity of a substance to store heat energy due to the temperature difference. The experimental investigation studies the performance of a small size sensible heat energy storage unit made of gypsum rocks[29]. Since the principle of thermal storage is simple, there are few technical problems and it is stable such as water, gravel, brick etc. There is an advantage that there are a lot of heat storage materials. However, since the heat storage capacity per unit volume, per unit mass, is small, in addition to the necessity of selecting a huge heat storage device and a heat capacity material with large heat capacity, the heat storage is performed at a temperature higher than the use temperature, which leads to larger heat loss. There are drawbacks. Also, since the efficiency largely changes due to the temperature change of the heat storage facility and the system, it is necessary to have a device for regulating the temperature during heat storage and heat release and a high-performance heat insulating facility.

The latent heat storage utilizes latent heat generated when a substance undergoes a phase change or transition, has a larger heat storage capacity per unit volume, unit mass as compared with sensible heat storage. In the phase change process, since there is no

temperature change, when using the latent heat storage material, the storage capacity per unit volume is large and the volume and weight of the heat storage tank can be greatly reduced compared with the sensible heat storage device. In addition, since heat storage and heat released are performed in the required temperature range, it is expected to be useful in scenes requiring a constant temperature heat source. Latent heat storage method that stores heat energy by using latent heat absorbed or released when changing the phase of the material is a very effective heat storage method.

The chemical storage is a system that utilizes a reversible chemical reaction, temporarily stores thermal energy as chemical energy, and causes a reverse reaction when necessary to convert it to thermal energy [30][31].There are thermochemical reactions, photochemical reactions, adsorption reactions, electrochemical reactions, etc. As chemical reactions, and heat can be stored at a higher density than latent heat storage. In addition to being able to preserve heat for a long period even at room temperature, it also has the feature that it can correspond to a wide temperature range by selecting the reaction condition and can also carry out heat transfer. However, there are many heterogeneous reaction systems in chemical heat storage, and chemical thermal storage materials are expensive. In addition, the reactions require high temperature and high pressure at the time of regeneration. Thus, in order to use it, it is necessary to accurately grasp thermo-physical properties and reactions and to produce highly reliable devices.

2.2 The utilization of the heat storage technology

The utilization of the heat storage technology is in the following systems [32]:

1. PCMs have been widely used in latent heat thermal storage systems for heat pumps, solar engineering, and spacecraft thermal control application.

2. Medical applications: Transportation of blood, operating tables, hot-cold therapies, treatment of asphyxia.

3. PCM applications such as in solar cooking, solar power plants, thermal energy storage.

4. PCMs are also used in textiles.
5. In the case of a power failure to conventional cooling systems, PCMs minimize use of diesel generators, and this can translate into enormous savings across thousands of telecom sites in tropics.
6. Thermal storage of solar energy.
7. Passive storage in bioclimatic building/architecture (HDPE paraffin).
8. Cooling: use of off-peak rates and reduction of installed power, ice bank.
9. Heating and sanitary hot water: using off-peak rate and adapting unloading curves.
10. Safety: temperature maintenance in rooms with computers or electrical appliances.
11. Thermal protection of food: transport, hotel trade, ice-cream, Food agroindustry, wine, milk products (absorbing peaks in demand), greenhouses.
12. Thermal protection of electronic devices (integrated in the appliance) and medical applications: transport of blood, operating tables, hot-cold therapies.
13. Cooling of engines (electric and combustion).
14. Thermal comfort in vehicles.
15. Softening of exothermic temperature peaks in chemical reactions.
16. Spacecraft thermal systems.
17. Solar power plants.

2.3 Heat Storage Method

A heat exchanger is a device used to transfer heat between a solid object and a fluid, or between two or more fluids. Heat exchange method of heat storage system is roughly classified into two. One is an indirect contact latent heat storage technology where heat

storage material filled in heat storage tank exchanges heat with heat transfer medium via heat transfer walls such as shell and tube. Other is direct contact latent heat storage technology that performs heat exchange by making direct contact of heat storage material and heat transfer medium.

(1) Indirect Contact Heat Storage

The fluids may be separated by a solid wall to prevent mixing or they may be indirect contact. The indirect contact has a structure in which a heat exchanger is enclosed in a heat storage tank, and the heat storage material and the heat transfer medium are connected via a heat transfer wall or tube that performs indirect heat exchange. They are widely used in space heating, refrigeration, air conditioning, power stations, chemical plants, petrochemical plants, petroleum refineries, natural-gas processing, and sewage treatment. The heat transfer tube is required to have excellent heat transfer characteristics and not to corrode the heat storage material and the heat transfer medium. Furthermore, since the heat storage material and the heat transfer medium do not come into contact with each other, it is safe to use even substances that react with each other, and the reliability is high because the heat storage material does not flow out. As a disadvantage, since heat exchange is performed via a heat transfer tube, the heat exchange rate is low, and it takes time to store heat and release heat.

(2) Direct contact heat storage

Direct contact heat exchangers involve heat transfer between hot and cold streams of two phases in the absence of a separating wall. In the direct contact, heat transfer medium flows directly into the heat storage tank and performs heat exchange directly with the heat storage material and heat transfer medium. In order to adopt this method, it is necessary that the chemical reaction of both heat storage material and heat transfer oil do not occur, the density of the heat storage material must be higher than the heat transfer oil in order to prevent outflow of the heat storage material. An advantage is that since there is no conduit which becomes thermal resistance compared with an indirect contact, it has high heat exchange rate and can store heat at high density. Construction is very simple and does not hesitate the corrosiveness problem of tube and wall. The lightweight of the direct-contact heat exchanger

enables its use as not only a stationary system but also a heat transport system [33][34]. On the other hand, as a disadvantage, there are a possibilities that the heat storage material flows out outside of the heat storage tank together with the heat transfer medium, the pressure inside the tank fluctuates, and the heat storage material tends to deteriorate easily.

2.4 Phase Change Material

Phase Change Material (PCM) is a substance with a high heat of fusion which, melts and solidifies at a certain temperature, and is capable of storing or releasing large amounts of energy. Phase change materials are latent heat storage substance, in which energy is stored and released in the process of changing the state i.e. either by solid to liquid or liquid to solid. While storing heat in the storage material, the material begins to melt when the phase change temperature is reached. The temperature then stays constant until the melting process is finished. The process is called latent heat process that only the phase change is occurring at the constant temperature while storing and releasing the heat energy. The process is called sensible heat process that does not change the phase and only changing the temperature while storing and releasing the heat energy.

2.4.1 Required properties for phase change material

There are some items to be considered when selecting the latent heat storage material and are summarized as follows [35]-[41]:

(1) Large heat storage capacity per unit volume/unit mass

When storing a certain amount of energy, if the heat storage capacity per unit volume/unit mass is large, the filling amount of the heat storage material can be reduced, so that the size of the device can be decreased. And it leads to a reduction in the overall cost. In particular, the source and location of waste heat are different, and when transporting thermal energy, storage capability becomes important from the viewpoint of cost reduction by weight reduction. Specifically, substances having a high latent heat amount generated

during phase change and substances having a large specific heat are preferable for storing sensible heat generated upon temperature change near the melting point.

(2) Large thermal conductivity

The speed of heat transfer during heat storage and heat released greatly affects the efficiency of the system. High thermal conductivity causes the temperature gradient required for charging the storage material is small.

(3) Phase change at a constant temperature

The PCM needs to freeze and melt cleanly over as a small temperature range as possible. Water is ideal in this respect since it freezes and melts at exactly 0°C. However, many PCMs freeze or melt over a range of several degrees, and will often have a melting point that is slightly higher or lower than the freezing point. This phenomenon is known as hysteresis. If melting and solidification are performed over a wide temperature range, phase separation may occur due to the density difference between the solid phase and the liquid phase of the heat storage material, and the composition may change. In addition, when storage and release process at a constant temperature is not performed, it is inefficient considering from the viewpoint of energy utilization.

(4) Volume change during phase change is small

If the volume expansion coefficient is large, the burden on the device increases, and in the worst case, there is a risk of damage for heat storage vessel and the heat storage material flowing out.

(5) There is no toxicity or flammability

PCMs are often used in applications whereby they could come in contact with people, for example in food cooling or heating applications, and others such as heating and cooling purpose of building temperature. For this reason, they should be safe for human body. Because of the danger of the heat storage material flowing out from the heat storage tank, it is required that it be harmless to the human body as much as possible and not to be inflammable because of its fire problem. Also, in high-temperature range, there are substances that generate harmful gases by heating, so special care are required.

(6) Chemically stable and not corrosive

The chemical reaction rate is fast in the high-temperature range, and corrosion of the heat storage container is also easy to proceed. Therefore, it is desirable to have high compatibility with containers and high stability.

(7) Having a melting point suitable for use temperature

In order to utilize latent heat, it is necessary that the phase change temperature of the heat storage material and the temperature in use are close. It is thought that efficient operation becomes difficult if the temperature difference increases.

(8) Economical

It doesn't matter how well a substance can perform if the PCM is prohibitively expensive. PCMs can range in price from very cheap (e.g. water) to very expensive (e.g. pure linear hydrocarbons). It is desirable that the heat storage material is cheap, but in the case where a highly efficient heat storage system can be constructed even with an expensive material, since there is a possibility that the overall cost can be suppressed.

(9) Low degree of supercooling

Supercooling is observed with many eutectic solutions and salt hydrates. The PCM in its liquid state can be cooled below its freezing point while remaining a liquid. Supercooling occurs at the time of heat released, heat recovery at the target temperature becomes difficult. Therefore, a method to release supercooling by placing crystals of a nucleating agent should be important.

(10) Repeatability

PCMs are usually used many times, and often have an operational lifespan of years in which they will be subjected to thousands of freeze/melt cycles. It is very important that the PCM is not prone to chemical or physical degradation over time which will the energy storage capability of the PCM.

2.4.2 Classification of PCM

There are a large number of PCMs (organic, inorganic and eutectic), which can be identified as PCMs from the point of view melting temperature and latent heat of fusion. However, except for the melting point in the operating range, a majority of PCMs do not satisfy the criteria required for an adequate storage media. As no single material can have all the required properties for an ideal thermal storage media, one has to use the available materials and try to make up for the poor physical properties by an adequate system design. For example, metallic fins can be used to increase the thermal conductivity of PCMs, supercooling may be suppressed by introducing a nucleating agent in the storage material, and incongruent melting can be inhibited by the use of a PCM of suitable thickness. For their very different thermal and chemical behavior, the list of each sub-group, which affect the design of latent heat storage systems using PCM of that sub-group are mentioned as follow [42]-[44]:

Organic: Organic materials are further described as paraffin and non-paraffin compounds. The paraffin compounds are formed by saturated hydrocarbons which correspond to the general formula C_nH_{2n+2}. Paraffins are known to be non-corrosive, non-toxic, have good stability upon cycling, and able to crystallize with little or no subcooling [45]. Paraffin wax is the most PCM material used in this group and it consists in a combination of different hydrocarbons obtained from the petroleum distillation. The properties of the different paraffin compounds are quite similar. However, they also have low thermal conductivity, and high volume change for phase transition, are fairly flammable, and are non-compatible with plastic containers due to the chemical similarity which can lead to softening of some polymers [46]. The thermal properties of laboratory-grade tetradecane, hexadecane and their binary mixtures, and demonstrate their potential for use as PCMs for cool storage. The thermal properties include freezing point, the heat of fusion, thermal stability and volume expansion during the phase change process [47].

The non-paraffin group contains different esters, fatty acids, alcohols, and glycols. Each of the materials has different properties. Organic materials include congruent melting means

melt and freeze repeatedly without phase segregation and consequent degradation of their latent heat of fusion, self-nucleation means they crystallize with little or no supercooling and usually non-corrosiveness. Organic PCMs are more chemically stable than inorganic substances, supercooling does not pose a significant problem. Although the initial cost of organic PCMs is higher than that of the inorganic type. And they are flammable, and they may generate harmful fumes on combustion. Paraffins, fatty acids also have low thermal conductivity, are flammable at very high temperatures, and exhibit little or no supercooling. Esters, also known as fatty acid esters, can be produced from fatty acids combined with an alcohol. They are usually non-toxic, show no supercooling, and are available in large quantities for many commercial applications

Inorganic: Inorganic materials are further classified as salt hydrate and metallic alloy. Inorganic PCMs usually have a higher heat of fusion than organic PCMs, with the exception of organic sugar alcohols. Salt hydrates are alloys of inorganic salts and water forming a typical crystalline solid of general formula $AB.nH_2O$. Salt hydrate has some attractive properties including high latent heat values, they are not flammable, and they are inexpensive and easily available to buy. Salt hydrates are inorganic PCMs that consist of salt and water in a crystal matrix when they solidify. They have a high latent heat and a melting temperature. Molten salts have a melting temperature range from 250 to 1680°C. Salt hydrates are considered one of the most important PCM groups, and their applications in TES systems have been extensively studied by many researchers. However, their unsuitable characteristics have led to the investigation of organic PCMs for this purpose. These include corrosiveness, instability, improper re-solidification, and a tendency to super cool. The metallic group includes low melting metals and metal eutectic, but it must be mentioned that they have not been really considered as PCM because of their large weight. In spite of this, there are some interesting points to remark: they have high thermal conductivity, relatively low vapor pressure and high heat of fusion per unit volume. These phase change materials do not super cool appreciably and their heats of fusion do not degrade with cycling. The ease of availability and relatively low cost of salt hydrates make them very attractive

for the commercial applications of TES. For instance, $CaCl_2.6H_2O$ and $Na_2SO_4.10H_2O$ are examples of salt hydrates that are widely available at very low cost. Compared to other PCMs, they are characterized by a lower volume change during phase transition and a relatively high thermal conductivity. Metallic alloys are inorganic PCMs of high thermal conductivity and relatively high heat of fusion compared to other PCMs. However, they have not been considered for commercial applications because of their weight drawbacks.

Eutectics: Eutectic mixtures are used to get new PCMs with improved properties and with different melting temperature. A eutectic is a minimum-melting composition of two or more components, each of which melts and freeze congruently forming a mixture of the component crystals during crystallization. Eutectic nearly always melts and freezes without segregation since they freeze to an intimate mixture of crystals, leaving little opportunity for the components to separate. Eutectic mixtures are investigated by conducting several experiments until an ideal PCM mixture is found at the required melting temperature with a desirable "sharp" melting behavior and a high enthalpy. If two or more components are found to have positive results, additional experiments are performed to find an optimum mixture and composition. This group contains three different groups: organic-organic, inorganic-inorganic and inorganic-organic, depending on the nature of the components of the composition.

2.4.3 Previous researches on latent heat storage materials

Many PCMs have been proposed in the literature for different temperature ranges, being the phase change temperature and phase change enthalpy, the main parameters provided by the authors [48]. Five solid-liquid phase change materials comprising three basic classes, paraffin waxes, salt hydrates and mixtures of fatty acids were thermo-physically characterized for thermal regulation applications in photovoltaics. The PCM was investigated using Differential Scanning Calorimetry and Temperature History Method to find their thermophysical properties of interest [49]. Different types of solar stills with latent heat storage have been reviewed and covering their different design aspects [50]. Blends of polyvinyl alcohol-

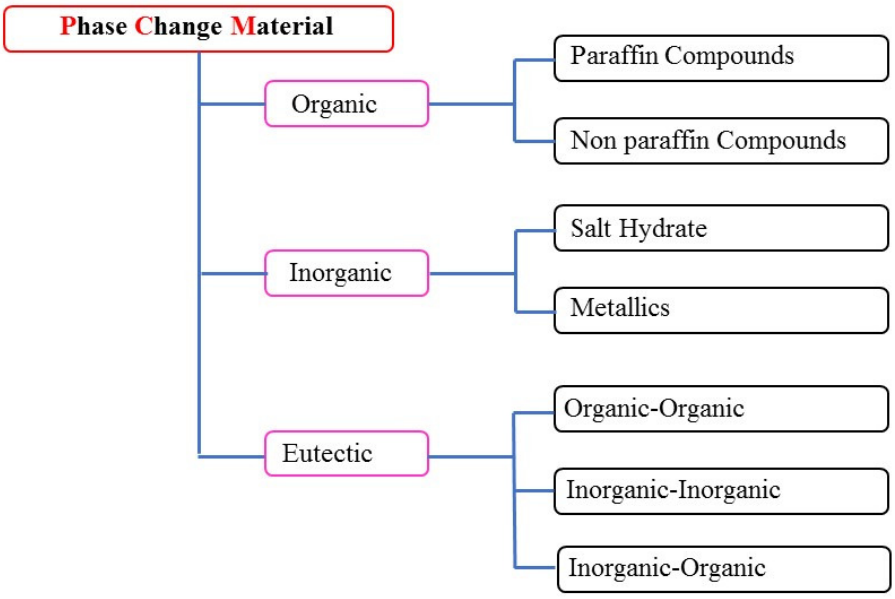

Figure 2.1: Classification of PCM [35].

stearic acid, and polyvinyl chloride-stearic acid are used as phase change material for thermal energy storage. Polymer-stearic has great potential for especially solar space and building heating applications in terms of their satisfactory thermal properties and cost-effectivity [51]. The phase change enthalpies, phase change temperatures, and thermal reliability properties of the Neopentyl glycol-dilaurate, Neopentyl glycol-dimyristate, and Neopentyl glycol -palmitate esters were measured by the DSC technique [52]. Melting and solidification process of PCMs Paraffin wax and Steric acid are investigated experimentally for the solar water heater. The objective is to explore the characteristics of the PCM when it is being melted and solidified. The experiments are performed in a glass box. Temperatures are recorded and the melting and solidification processes are pictured by using the camera [53]. Different methods of heat transfer enhancement techniques in thermal energy storage system, which is more attractive and useful to the energy conservative system were carried out [54].

In the field of concentrated power applications, molten nitrate salts, a mixture of 60 wt% $NaNO_3$ and 40wt% KNO_3, are used exclusively. Those multicomponent salt mixtures feature much lower melting points compared to Solar Salt and could be attractive materials for direct thermal energy storage for CSP applications [55]. A review has been carried out of the history of thermal energy storage with solid-liquid phase change. It contains listed over

150 materials used in research as PCMs, and about 45 commercially available PCMs. The paper lists over 230 references [56]. Heat-of-fusion storage materials for low-temperature latent heat storage in the temperature range 0∼120°C are reviewed. Organic and inorganic heat storage materials classified as paraffins, fatty acids, inorganic salt hydrates and eutectic compounds are considered. The melting and freezing behavior of the various substances is investigated using the techniques of Thermal Analysis and Differential Scanning Calorimetry [2]. Two different types of PCM are used for the experimental work; the commercially available PT-37 and n-eicosane. It was determined that the use of a thin PCM thermal energy storage package significantly improved the temperature behavior of the experimental setup, by reducing the rate of temperature increase at the heater and the back cover [57]. The performance analysis of the developed latent heat thermal energy storage system with sodium thiosulfate pentahydrate as phase change material was investigated experimentally with four different mass flow rates of heat transfer fluid [58].

Tests were performed to characterize the thermal behavior of hexadecane and tetradecane as a potential PCM to enhance the convective heat transfer performance of district cooling system. In order to vary the melting temperature of the mixture, hexadecane and tetradecane were mixed in different fractions, and their thermal behavior was experimentally evaluated [59]. Direct contact melting of hydrocarbon mixtures as phase change materials was investigated experimentally. Tetradecane and hexadecane binary mixtures, and pentadecane and octadecane binary mixtures were used as phase change materials, with various mixing ratios [60]. Heat transfer characteristics of PCM during energy storage and releases in vertical double pipe configuration were investigated. Paraffin wax with an average melting temperature of 52°C is used as the energy storage material and water is used as the heat transfer fluid (HTF). The experimental system is operated for the following set of conditions: (a) flow rates of HTF are 0.238-0.37 kg/s; (b) inlet temperatures of heating HTF are 65∼85°C, and (c) inlet temperatures of cooling HTF are 10∼20°C [61]. Differential scanning calorimetry (DSC) was used to study the phase transformations of three pure n-alkanes, namely hexadecane ($C_{16}H_{34}$), octacosane ($C_{28}H_{58}$) and hentriacontane ($C_{41}H_{84}$), and their

binary and ternary mixtures. The DSC results were used to investigate the liquid-solid phase equilibrium of n-alkane mixtures, all of which show eutectic behavior [62]. The aim of this paper is to show and perform at laboratory scale the selection of a PCM, with a phase change temperature between 120∼200°C, which will be further used in an experimental facility. Beyond the typical PCM properties, sixteen PCMs are studied here from the cycling and thermal stability point of view, as well as from the health hazard point of view [63]. Heat-transfer characteristics have been determined for the circular finned and unfinned-tube units during the freezing of magnesium chloride hexahydrate ($MgC_{12}.6H_{20}$) used as a PCM with a melting temperature of 116.7°C. The effects on the heat-transfer characteristics have been determined of the inlet temperature and the flow rate of air used as the HTF [64].

Polyalcohols, such as erythritol, mannitol, and galactitol, are good candidates as PCMs because of their relatively high melting points and high latent heats. Among them, erythritol is nontoxic, nonflammable, and noncorrosive; the melting point is around 393 K, and the latent heat is 340 kJ/kg, which is close to the heat of fusion of ice [65]. An experimental study has been conducted to investigate the processes of the PCMs (RT35) in a finned-tube heat exchanger at a constant flow rate of 0.6 L/min [66].

36 kinds of mixed carbonate molten salts were prepared by mixing potassium carbonate, lithium carbonate, sodium carbonate in accordance with different proportions. The data of melting point and latent heat are measured by the analysis of DSC curves of 36 kinds of salts, which show that the majority of ternary carbonate's melting points are close at around 400°C [67]. 3PCMs latent heat thermal storage unit filled with three types of PCMs namely, $C_{24}H_{50}$, $C_{21}H_{44}$, and $C_{18}H_{38}$ were investigated on a cascaded shell-and-tube latent heat storage system [68]. Investigations are carried out in the TES system for different phase change materials (paraffin and Stearic acid) by varying HTF flow rate experiments are performed in both charging and discharging processes [69].

Pentaerythritol is a very promising material for the latent heat-thermal energy storage in the temperature range 150∼200°C and it can be used in direct contact with the heat transfer fluids of hydrocarbon in a sealed container for long duration; the direct contact in a slurry

would be very effective for the heat transfer both in charging and discharging modes [70]. An energy storage system has been designed to study the heat transfer characteristics of paraffin wax during melting and solidification processes in a vertical annulus energy storage system. In the experimental study, three important issues are focused. The experiment has been performed for different water flow rates at a constant inlet temperature of heat transfer fluid for recovery and use of heat. Time- based variations of the temperature distributions were explained from the results of observations of melting and solidification curves. Charging and discharging processes were carried out [71].

Xylitol ($C_5H_{12}O_5$), erythritol ($C_4H_{10}O_4$) and magnesium chloride hexahydrate (MCHH, $MgCl_26H_2O$) with phase change temperatures between 90∼150°C were investigated. The sugar alcohols xylitol and erythritol indicate a large supercooling and different melting regimes [72]. Differential scanning calorimetry was applied to the evaluation of binary eutectic mixtures and compounds of NaOH with $NaNO_2$, or $NaNO_3$, as latent heat thermal energy storage materials for use in a nuclear power plant [73]. An experimental study on a vertical shell-and-tube latent heat thermal storage unit with erythritol as storage media and air as a HTF is conducted to evaluate the thermal behavior and heat transfer performance of the unit. The thermophysical properties of erythritol, such as melting temperature, melting enthalpy, thermal conductivity, and viscosity, are obtained. Increasing the inlet temperature and the mass flow rate of the HTF during charging obviously enhances the heat transfer in the PCM and shortens the charging time. In addition, increasing the mass flow rate of the HTF helps enhance heat transfer during discharging [74]. The thermal and heat transfer characteristics of stearic acid during the solidification processes were investigated experimentally in a vertical annulus energy storage system. The temperature distribution and temperature variations with time at different radial positions during the freezing processes were obtained [75].

Chapter 3

Heat Storage Material Mixture at Temperature Range 300∼400°C

Energy such as the steam and electricity are required for CO_2 capture, separation, and recovery from blast furnace gas in steel-making factories. The waste heat temperature from the exhaust gas blower of steel-making factory is about 350°C. By using this waste heat energy, recover the electricity for CO_2 capture. This waste energy is firstly stored in the heat storage device in which heat storage material is used. And then waste heat energy is released from the heat storage material and reuse this energy to recover the electricity to capture the CO_2.

In this study, we constructed a latent heat storage vessel to study the melting and solidification characteristics of latent heat storage materials with a temperature around 350°C discharged from steel factory as a heat source. Organic substances, sugar alcohols can be used as a heat storage material at 200°C or below, but it is difficult to use it at around 350°C. Among the molten salts, various substances have different characteristics when used as a heat storage material. There are substances that emit explosive gasses by heating and the substances that strongly show corrosiveness to metal and deliquescence at atmosphere, thus it is necessary to examine from various viewpoints for selection.

Therefore, in this study, for the purpose of constructing a heat storage system with a mixed molten salt having a melting point about 350°C, the characteristics of heat storage

material suitable for such temperature range were investigated. Figure 3.1 shows the proposed experimental device for this research. The phase change material mixture is inserted into the heat storage vessel (test section) and study the characteristics of this mixture. This device consists of the solidification and melting systems. The solidification system is made by the low-temperature oil bath and water cooler and the melting system is made by the plate heater that is attached at the bottom of the test-section. Firstly, the electric furnace is used to get the appropriated heat storage mixture. And then, it is needed to select the appropriated material to construct the heat storage vessel.

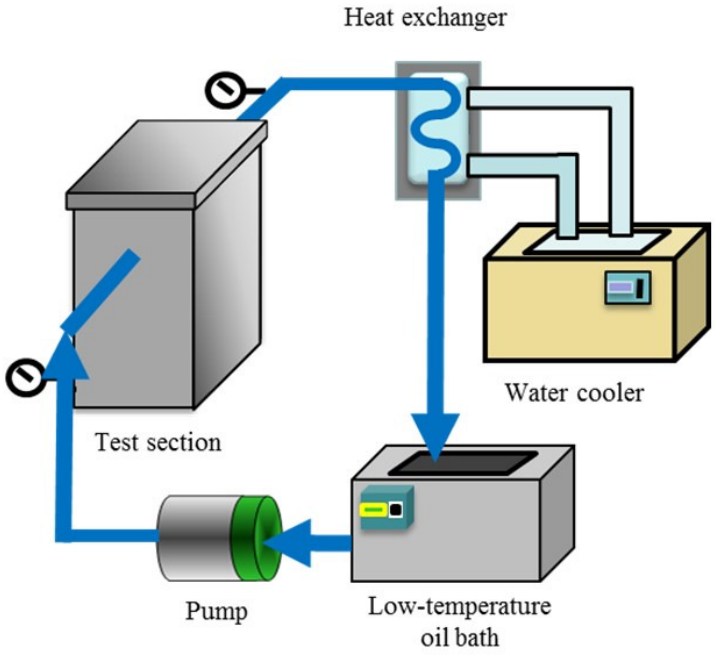

Figure 3.1: The proposed experimental device.

To get the appropriate heat storage mixture that has the melting temperature of about 350°C, the evaluation was made by adjusting the melting point of heat storage mixture by changing the mixing ratio. The NaCl:KCl:LiCl mixture can be used for 350°C melting temperature with different mixing ratios [76]. Heat storage mixture is made by mixing three different type of molten salt, Sodium chloride NaCl (melting temperature of 801°C), Potassium chloride KCl (melting temperature of 770°C) and Lithium chloride LiCl (melting temperature of 605°C) by different ratio of wt% as shown in Figure 3.2.

Figure 3.2: PCM and their melting temperature.

3.1 The Experimental Apparatus and Mixture

In order to develop a mixed latent heat storage material, it is necessary to measure physical properties such as melting point temperature and latent heat. However, in the case of molten salt, the corrosiveness to the construction material is strong, it is not easy to measure the thermo-physical properties using differential scanning calorimetry (DSC), the heat storage material can be leak out from the enclosure during melting of the heating process. Therefore, in this research, heating is performed by an electric muffle furnace, the melting temperature is calculated from the melting and solidification behaviors at that time. The experimental apparatus for measurement of melting temperature for the new PCM mixture is shown in Figure 3.3. The model of electric muffle furnace is Advantec FUW230PA and the maximum temperature is to 1150°C (±1.5°C). The inside dimension of the furnace is (W200×D300×H160) mm.

The molten salt mixture of three different salt NaCl, KCl and LiCl are mixed in a different ratio of wt% in the crucible. The height of the crucible is 65 mm. The ceramic crucible is used to protect the corrosion. The crucible with the molten salt mixture and ceramic

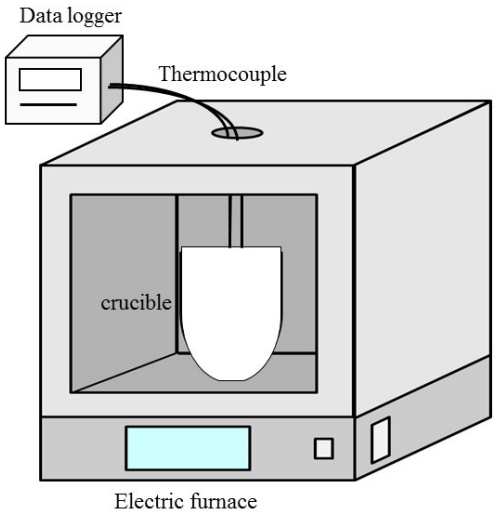

Figure 3.3: The experimental apparatus for melting point measurement of new PCM and making corrosion test.

thermocouple are set in the electric furnace as in Figure 3.3. The thermocouple is inserted from the hole located at the upper part of the electric furnace and heat is insulated by filling it in the gap with rock wool. The thermocouple is connected to the data logger and the temperature history is recorded by the data logger. Firstly, the temperature of the electric furnace set to 500°C for good mixing about 4 hours, and cooling down in the furnace to atmosphere temperature to get the good mixing of PCM mixture. After that, making the melting process by heating from 250°C to 450°C in 3 hours and keeping 450°C for 1 hour, after that continues the solidification process, by cooling down in the furnace from 450°C to 250°C. Temperature histories are recorded by the data logger.

The graph shown in Figure 3.4 is the temperature histories of melting process of four different types of molten salt mixture NaCl0%, NaCl23%, NaCl28%, and NaCl33%. NaCl0% mixture is NaCl:KCl:LiCl (0:54:46), NaCl23% mixture is NaCl:KCl:LiCl (23:46:31), NaCl28% mixture is NaCl:KCl:LiCl (28:18:54) and NaCl33% mixture is NaCl:KCl:LiCl (33:24:43) respectively. The melting temperatures of all mixtures of NaCl: KCl: LiCl are about 350°C. It was found that even though the mixing ratios of the molten salt change, the melting point of the melting temperature are almost the same. Figure 3.5 shows the melting conditions of PCM at 450°C with different ratios of NaCl: KCl: LiCl. From these photos, it was found that it was not easy to melt when increasing in NaCl% because the melting temperature is

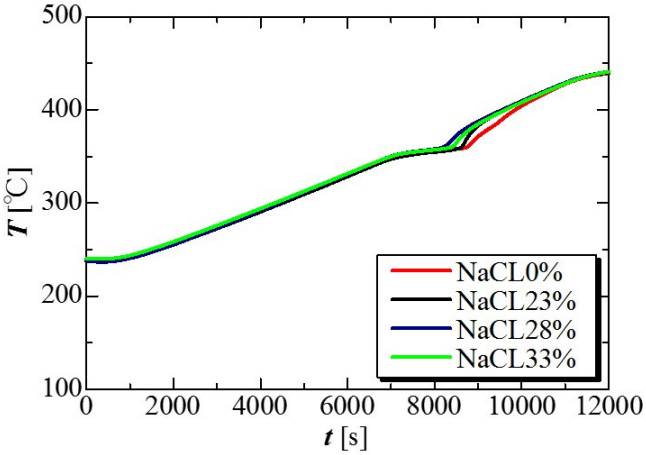

Figure 3.4: Melting process of different wt% of NaCl, KCl, and LiCl.

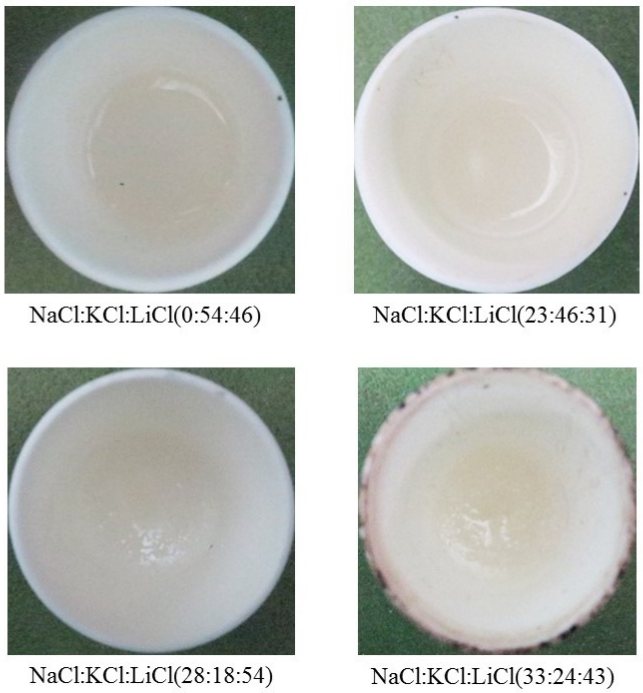

Figure 3.5: PCM conditions of different mixtures at 450°C.

very high. For this research, choose NaCl0% and NaCl23% from four different mixtures and further study of corrosion test with some material plates. For using these two mixtures, corrosion test were made with different types of material SS304, SS316, SS316L, SS310, copper, brass, carbon steel, aluminum, nickel, titanium, and molybdenum. After that also make the test of the corrosiveness condition of constructive materials by using some corrosion and heat resistance paints and spray. Corrosion can be caused by both of oxygen and heat storage

material mixture vapor. Thus, corrosion test makes again by inserting the argon gas instead of oxygen inside of the electric furnace.

3.2 Corrosion Test without Using Any Paint and Spray

For making corrosion tests, we also used the experiment apparatus of Figure 3.3. The plates size is 10 mm× 80 mm and the thickness of the plate is 2 mm as shown in Figure 3.6. This size of the plate was chosen to know the condition of the plates on the inside and outside of the liquid PCM mixture after finishing the corrosion test. The cover plate is made of stainless steel SS304, and the cover plate has holes for inserting a thermocouple and a test plate. NaCl:KCl:LiCl mixture of 40 g is inserted into the crucible and heating to 500°C for good mixing and cooling down to atmosphere temperature at the inside of the furnace. The 40 g of liquid mixture has the height of 20 mm and when the plate is inserted into the crucible, 20 mm of plate immerse into the liquid PCM and the left of another portion is outside of the liquid PCM. Firstly, plates are not inserted into the crucible and kept over the cover plate and heated up to 450°C in 2 hours to check heating effects. After that plates are inserted at 450°C into the crucible and made solidification process by cooling down from 450°C to 250°C in the furnace and melting process by heating from 250°C to 450°C in 3 hours and keeping 450°C for 1 hour and repeated these two processes twice and after that, heating it to 450°C and took out the plate outside of the crucible and took the photo. After cleaning with water, and we took photos again. Pictures of the PCM condition were captured and compare the condition of PCM at 450°C before and after of corrosion test.

Figure 3.7 shows the plates condition of stainless steel SS304,SS316, and SS316L(a) before the test (b) after the twice of melting and solidification and before cleaning with water and (c) after cleaning with water. While cleaning with water, do not use any brush, and only pour water and shake slowly. These three plates have the same composition but only different in the percentage of the composition. The difference is SS304 contains 18% chromium and 8% nickel while SS316 contains 16% chromium, 10% nickel and 2% molybdenum. The molybdenum is added to help resist corrosion to chlorides like sea water and salts. The

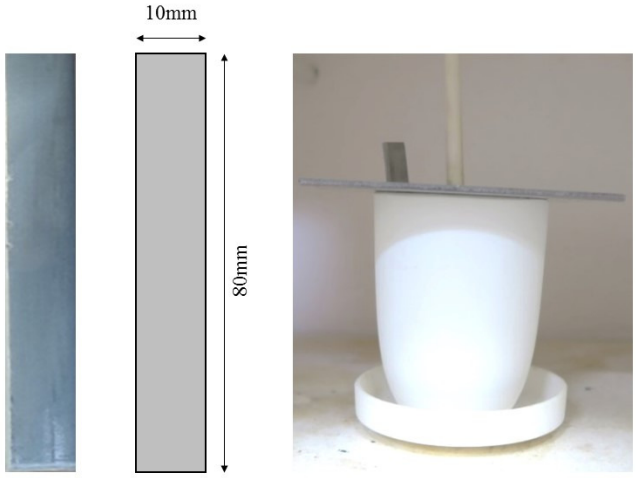

Figure 3.6: The plate and crucible setting for corrosion test.

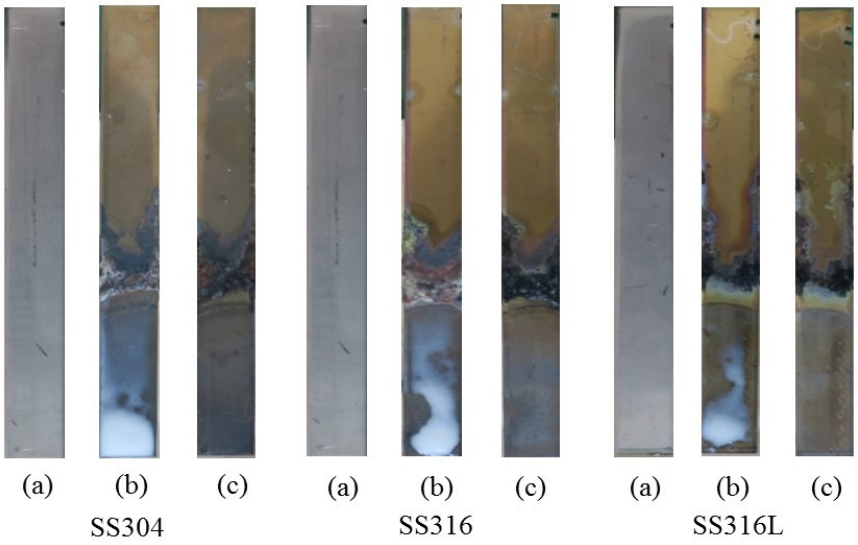

Figure 3.7: Plates condition of SS304, SS316, SS316L.

difference between SS316 and SS316L stainless steel is that SS316L has a 0.03% max carbon and is good for welding whereas SS316 has a mid-range level of carbon 0.08%. The higher nickel and molybdenum content in this grade allows it to demonstrate better overall corrosion resistant properties than SS304. The type of PCM mixture of this test is NaCl: KCl: LiCl (0:54:46) wt% of 40 kg mass mixture. The composition of three steel plates is nearly the same. Thus, making the corrosion test with same crucible and the same time. It is found that the plate inside of the liquid PCM has no corrosion. Corrosion was found at the interface of the liquid PCM and air region. Corrosion can be caused by the vapor of PCM and oxygen.

There has no oxygen inside of the PCM. Thus, corrosion effect has not occurred at the inside of the liquid PCM region. The SS316L plate has the less corrosion effect than the SS304 and SS316. Figure 3.8 shows the comparison of the liquid PCM condition before and after corrosion test. The color of the liquid PCM has changed after the corrosion test.

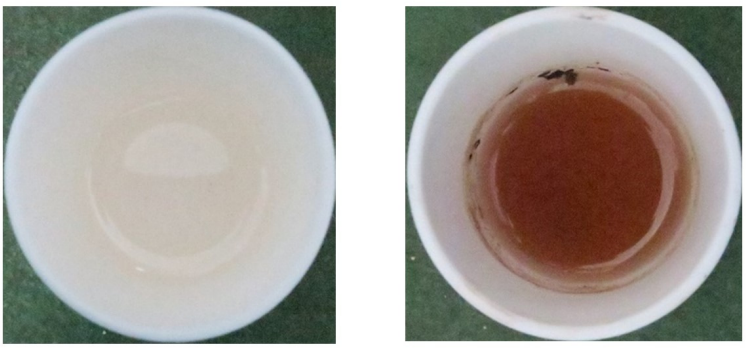

Figure 3.8: PCM conditions with and without steel plates.

Figure 3.9 shows the plates condition of copper, brass, carbon steel and SS310 (a) before the test (b) after the twice of melting and solidification and before cleaning with water and (c) after cleaning with water. The oxidation of copper material can occur quickly when heating in high temperature. This effect causes the thin black layer over the plate. When making the corrosion test, this layer and vapor of liquid PCM are mixes together. The plate that inside of the liquid PCM has not corrosion and the plate that outside of the liquid PCM cover by dark black layer. Some part of this layer can dissolve in the liquid PCM and the liquid PCM color change after making the corrosion test.

Brass is the alloy material of copper and zinc. Because of this copper material, the brass plates have oxidation layer over it when heating. This layer change very hard layer over the plate after mixing with the vapor PCM and this layer is sticky to the plate and do not dissolve in the liquid PCM. Because of this reason, PCM color does not change after the corrosion test in Figure 3.9. And the plate inside of liquid PCM has not changed and has not corrosion.

Carbon steel or plain-carbon steel is a metal alloy. It is a combination of two elements, iron and carbon. Other elements are present but quantities are too small to affect its prop-

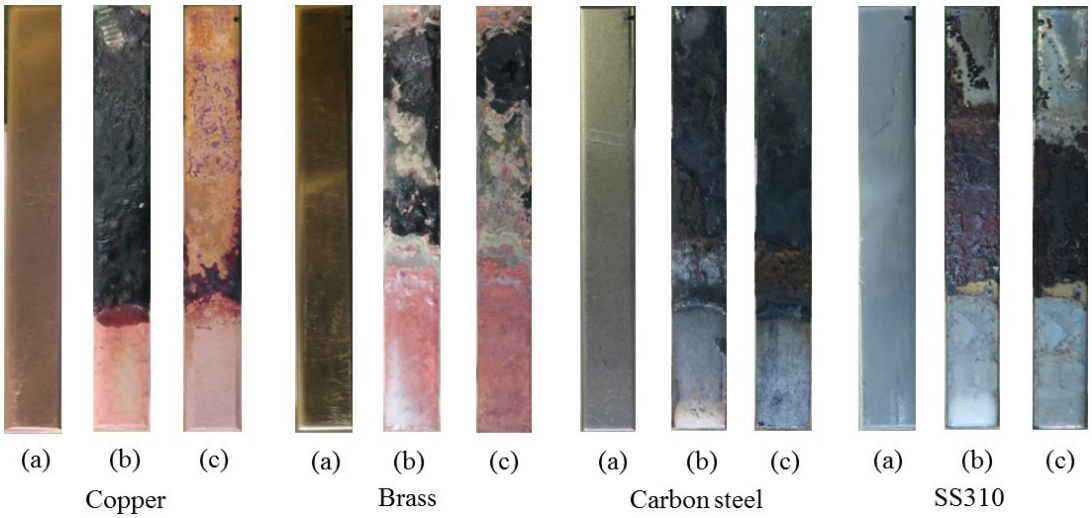

Figure 3.9: Condition of copper, brass, carbon steel and SS310 plates before and after the corrosion test(a)before the test, (b) after the test before cleaning and, (c) after cleaning.

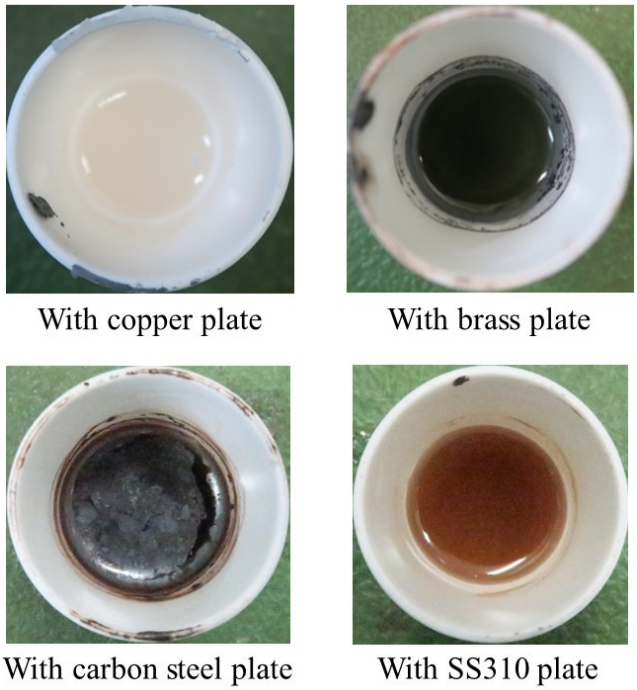

Figure 3.10: PCM conditions with test of copper, brass, carbon steel and SS310 plates.

erties. The only other elements allowed in plain-carbon steel are: manganese (1.65% max), silicon (0.60% max), and copper (0.60% max). The carbon steel plate has very corrosion after making the corrosion test with PCM at high temperature. The PCM color very changes after the test. Stainless steels have good strength, resistance to corrosion and oxidation at

elevated temperatures. SS310 is used to a temperature up to 1100°C. But this plate also has the corrosion after the test with PCM mixture. Carbon steel has more corrosiveness than SS310 plate. The color of PCM change after the test with this plate. Figure 3.10 shows the liquid PCM conditions with a test of copper, brass, carbon steel and SS310 plates.

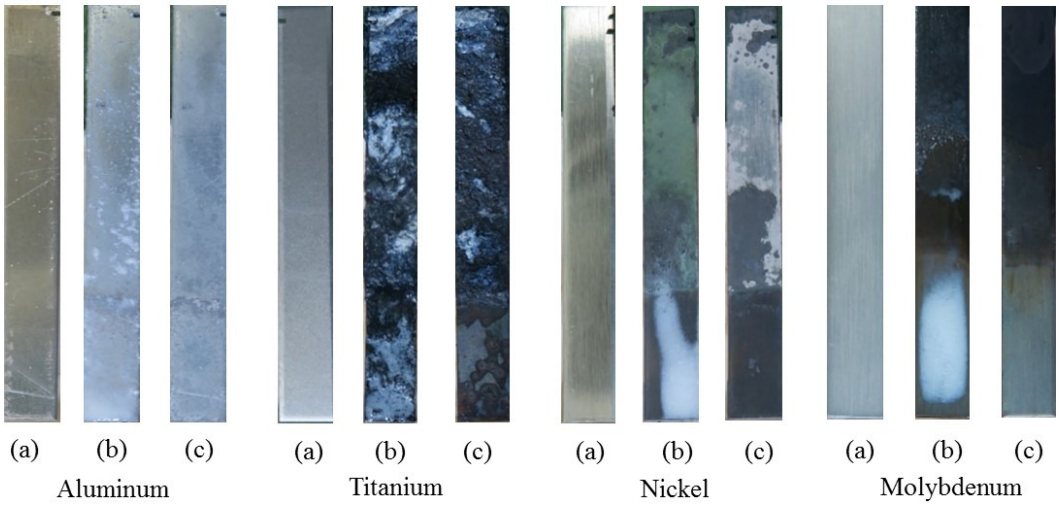

Figure 3.11: Condition of aluminum, titanium, nickel and molybdenum plates (a)before the test, (b) after the test before cleaning and, (c) after cleaning.

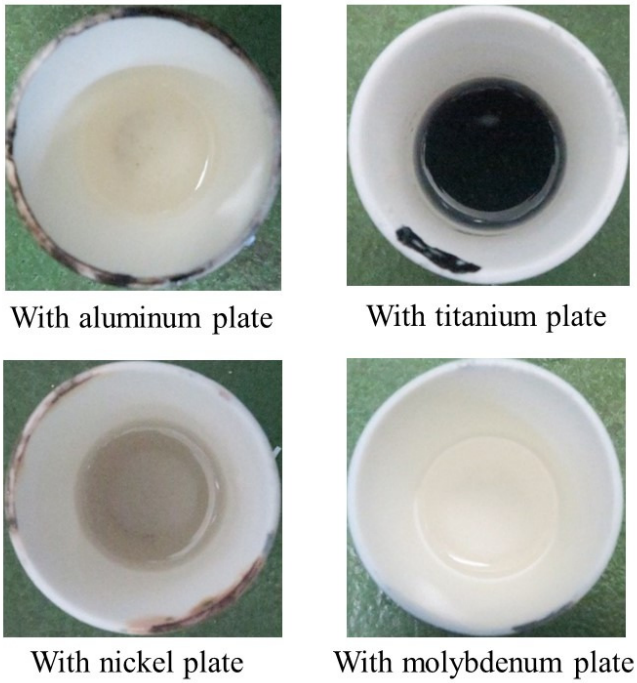

Figure 3.12: PCM conditions with test of aluminum, titanium, nickel, and molybdenum.

Figure 3.11 shows the condition of aluminum, titanium, nickel, and molybdenum plates before and after the corrosion test. Unlike iron and steel, aluminum does not rust or corrode in moist conditions. Its surface is protected by a natural layer of aluminum oxide. This prevents the metal below from coming into contact with air and oxygen. After the test, the aluminum plate has only surface corrosion. Titanium metal is used as an alloying agent with metals including aluminum, iron, molybdenum, and manganese. Titanium is used in several products such as drill bits, bicycles, golf clubs, watches and laptop computers. It is a metal with a silver color, low density, and high strength. Titanium is resistant to corrosion in sea water, and chlorine, but a little bit expensive. After the test, it is found that titanium had very corrosiveness because of high temperature. Nickel is a silvery metal that resists corrosion even at high temperatures. Nickel resists corrosion and is used to plate other metals to protect them. It is, however, mainly used in making alloys such as stainless steel. Nichrome is an alloy of nickel and chromium with small amounts of silicon, manganese, and iron. After the test, nickel has only surface corrosion, but a little change in plate color. Nickel does not decompose as it oxidizes but forms a layer of nickel oxide that prevents further oxidation from occurring. Molybdenum plate has not corrosiveness. It is found that Nickel and molybdenum are good for construction the experimental device, but we need to consider the economic point of view because of the cost of this material is quite expensive. Figure 3.12 shows the liquid PCM conditions after the test of aluminum, titanium, nickel, and molybdenum plates. The color of PCM does not change with aluminum and molybdenum, a little change with nickel, and quite change with the titanium. Figure 3.13 shows the temperature histories of PCM with different material plates. It was found that the temperature histories with different material plates were the same trend and it was not found any change.

After finishing these experiment, it is found that most of the plate has corrosiveness and it is concluded that PCM vapor and oxygen is most efficient for corrosion and we would like to continue the corrosion test with some anti-corrosion spray and paint.

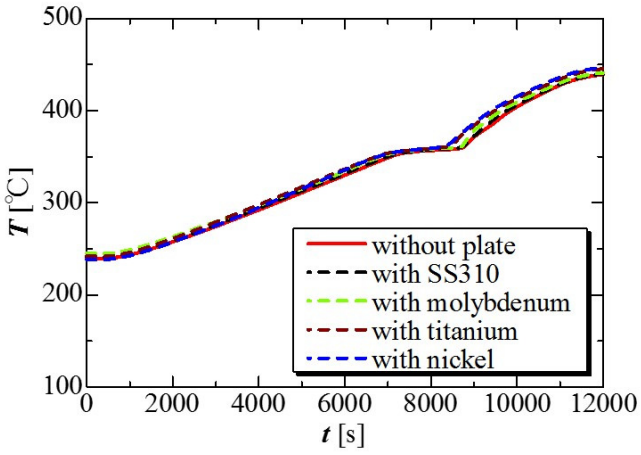

Figure 3.13: Temperature histories of PCM with different material plates.

3.3 Corrosion Test with Using Some Spray and Paint

In this section, for preventing the corrosiveness of the construction material, some anti-corrosive spray and paint were used. Firstly, make the corrosion test SS304, SS316 and SS 316L stainless steel plate with one type of high heat primer spray Rust Oleum. This High Heat Primer spray bonds to bare metal and helps create a smooth top coat finish. It is specially formulated to prevent rust and is recommended for use on automotive engines and other metal surfaces which reach intermittent temperatures up to 1093°C. All plates are spraied and dried at atmosphere naturally. After that, sprayed plates are not inserted directly into the PCM and heated up to 450°C outside of the PCM. After heating the plates at 450°C, all plates are inserted into the crucible. The bottom portion of about 20 mm of plates are immersed inside the PCM and other portions are outside of PCM. After that solidification process is made by cooling from 450°C to 250°C and melting process are made by heating up from 250°C to 450°C in 3 hours and keeping 450°C for 1 hour. This two solidification and melting is made twice and takes the photos of plates condition. After heating to 450°C, the spray is not sticky to the SS316 plate.

Figure 3.14 shows the results after the corrosion test of SS304, SS316, and SS316L steel plates with Rust Oleum of high heat primer spray. Figure 3.14(a) before the test, only dry condition, Figure 3.14(b) after heating to 450°C, Figure 3.14 (c) after making the corrosion

test before the cleaning and Figure 3.14(d) after making the corrosion test after the cleaning. Plates are cleaned with water. After the test, plates outside the PCM has not corrosion and not change, but plates inside the PCM, the spray is eroded by PCM. Thus, this type of spray cannot be used to prevent the corrosion. Figure 3.15 shows the PCM conditions after the corrosion test with SS304, SS316, and SS316L with one type of High Heat Primer spray Rust Oleum. The PCM color has changed after the test.

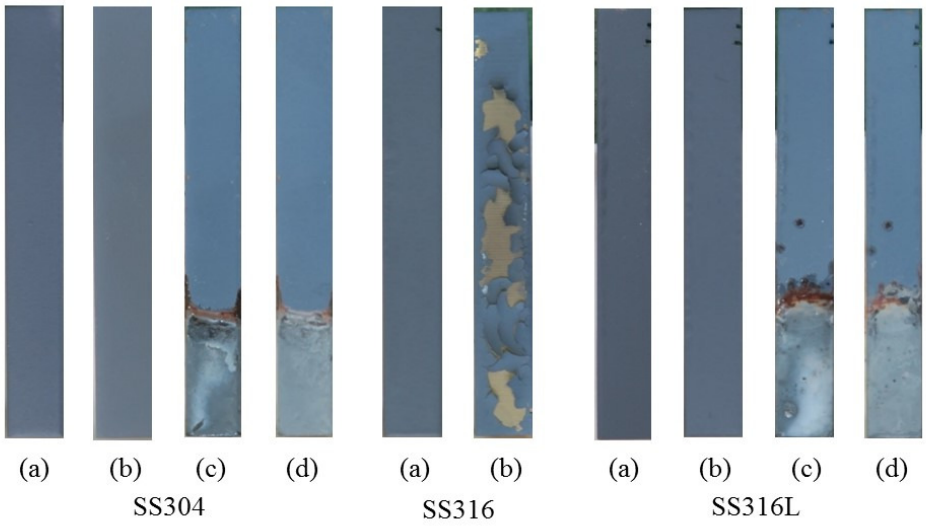

Figure 3.14: Plates condition of SS304, SS316 and SS316L plates with spray Rust Oleum.

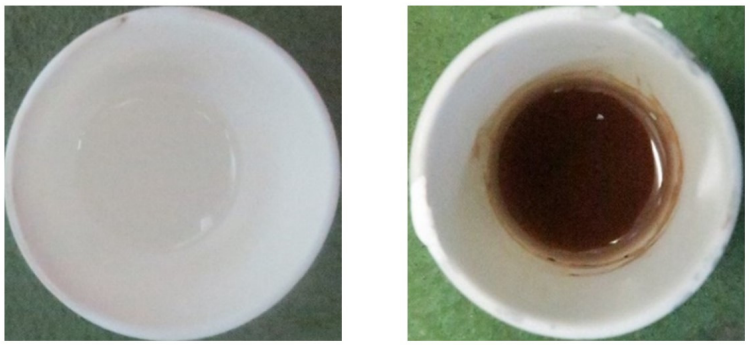

Figure 3.15: PCM condition with test of SS304, SS316, and SS316L with spray Rust Oleum.

Cerakoto Alumina spray has a heat-resistant upper limit of 1800°C. For exceeding the heat-resistant upper limit of the binder, alumina is free coating the surface of the main component with discoloration powder. High-purity alumina Al_2O_3 is a main ingredient.

Although the film is excellent in insulation and corrosion resistance, heat resistance and abrasion resistance are inferior to ceramic paint. It is used for purposes such as insulation, masking, prevention of adhesion of molten metal, demolding and so on. Firstly, spray over the plates and keep dry naturally and after that spray again and keep dry. After drying, the plate is heated to 450°C and at that time plates were not inserted into the PCM. When testing with this type spray, it is not sticky to the plate after only heating to 450°C in 2 hours and before inserting to the liquid PCM condition. The spray is easily removed from the plate with tissue paper. Figure 3.16 shows the plate condition of SS304 with type Cerakoto Alumina spray (a) after drying (b) after heating 450°C in 2 hours and (c) after pushing with tissue paper. This type of spray cannot be used to prevent the corrosion.

Figure 3.16: Plate conditions of SS304 with Cerakoto Alumina spray.

The main component of Cerakoto paint Figure 3.17 is silica SiO_2, to form a dark brown hard film. It is resistant to thermal and mechanical shocks, has the flexibility to thermal expansion, high heat resistance upper limit. It is suitable for protection of ceramics zirconia, magnesia with high thermal expansion coefficient from steel, stainless steel, aluminum, copper, manganese alloy, chromium steel, nickel alloy. It can be used heat-resistant temperature 1500°C. It was a little difficult to paint uniformly. Firstly paint to the plate and dry naturally. After that painted plates were heated to 450°C in 1 hour not inserted into the PCM. After that inserted into the liquid PCM and made the solidification process by cooling

down from 450°C to 250°C and melting process by heating from 250°C to 450°C for 3 hours and keeping 450°C for 1 hour. Figure 3.17 shows the plates condition of SS304, SS316 and SS316L with this type of paint (a) before test after drying (b) after heating 450°C in 1 hour and (c) after corrosion test. It is found that when testing with this type of paint, the paint easily melts and easily dissolve into the liquid PCM and PCM can be easily changed to the very dirty condition. Figure 3.18 shows the PCM condition after corrosion test with this type of paint. This type of paint cannot be used to protect the corrosiveness.

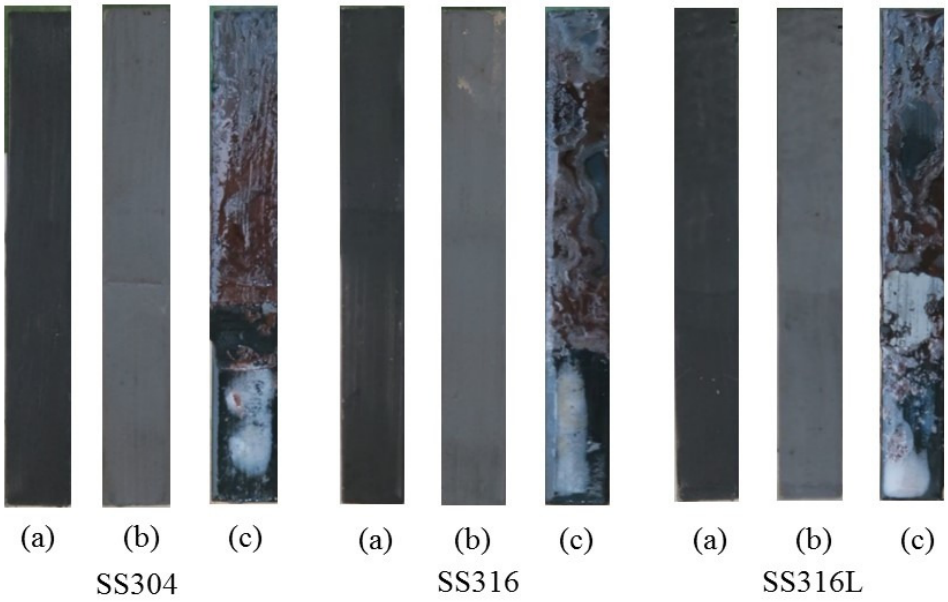

Figure 3.17: Plates condition of SS304, SS316 and SS316L plates with Cerakoto paint.

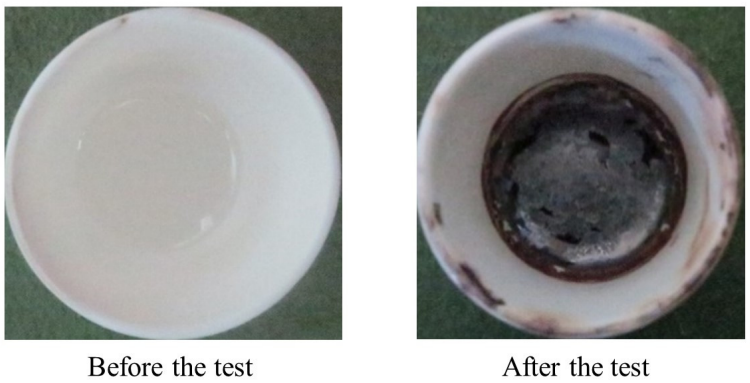

Figure 3.18: PCM condition with test of SS304, SS316, and SS316L with Cerakoto paint.

Kure Heat and corrosion resistant spray is used like hot mufflers and engines, it prevents

the occurrence of rust and corrosion. The heat-resistant temperature after spraying is 600°C. When testing this spray, it needs to heat 200°C for 1 hour after drying for 1 hr. Plate outside the PCM is good condition. Figure 3.19 shows the plate conditions of SS304, SS316, and SS 316L with Kure Heat and corrosion resistant spray (a) before test (b) after test before cleaning and (c) after cleaning with water. Plate inside the liquid PCM is good condition after one or two-time experiment but it will be eroded and corroded by PCM if making many repeated cycles. Thus, this type of spray cannot be used to prevent the corrosiveness. Figure 3.20 shows the PCM condition before and after making the corrosion test. It was found that PCM color does not change after the corrosion test.

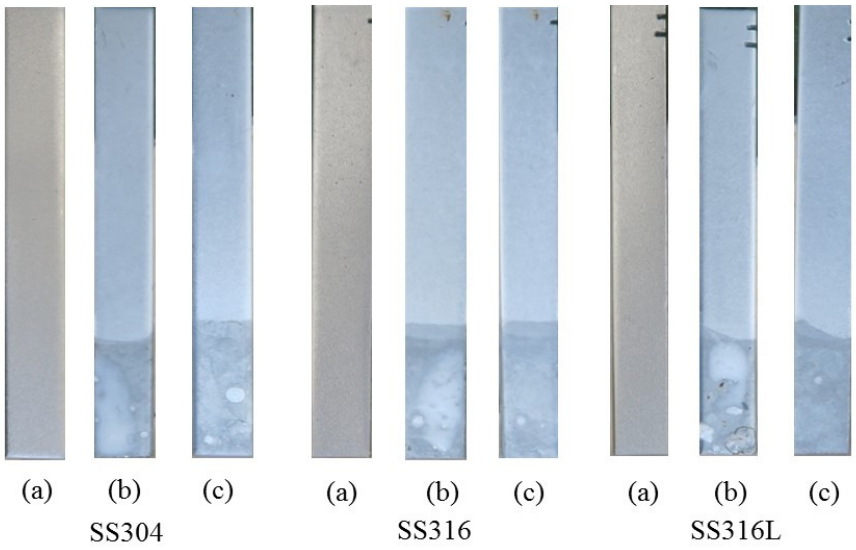

Figure 3.19: Plates condition of SS304, SS316 and SS316L plates with Kure Heat and corrosion resistant spray.

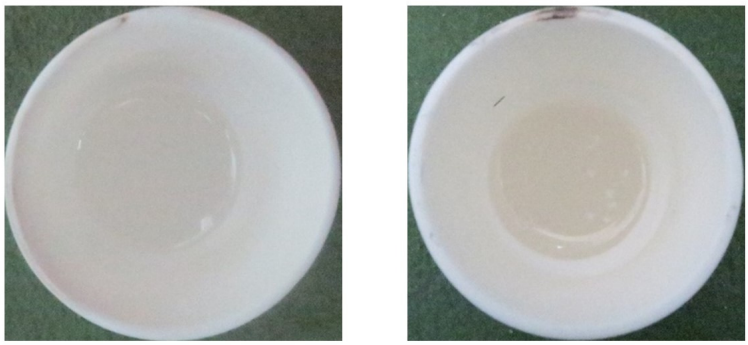

Figure 3.20: PCM condition with test of SS304, SS316, and SS316L with Kure Heat and corrosion resistant spray.

3.4 Corrosion Test by Using Argon Gas

Mixing with oxygen is also one case for corrosiveness. While making the corrosion test, there has oxygen inside of the electric furnace. To prevent this problem, argon gas was inserted inside of the electric furnace while performing the corrosion test. Figure 3.21 shows the experimental device for corrosion test with argon gas. Argon gas is denser than air and it can displace oxygen and close to the bottom during inserting the argon gas.

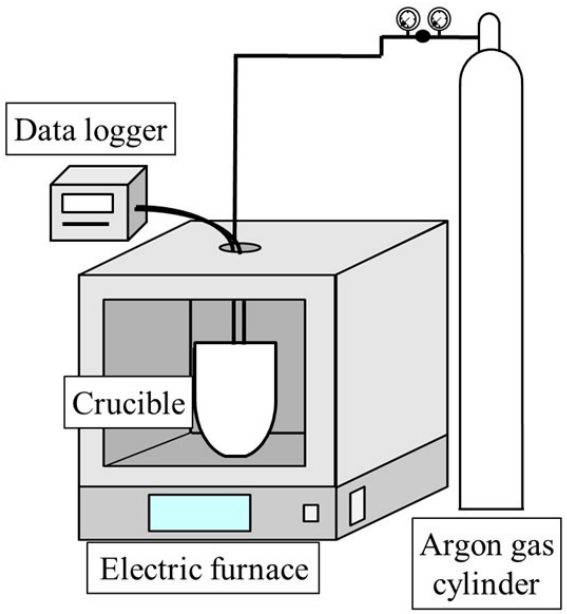

Figure 3.21: Experimental device for corrosion test with argon gas.

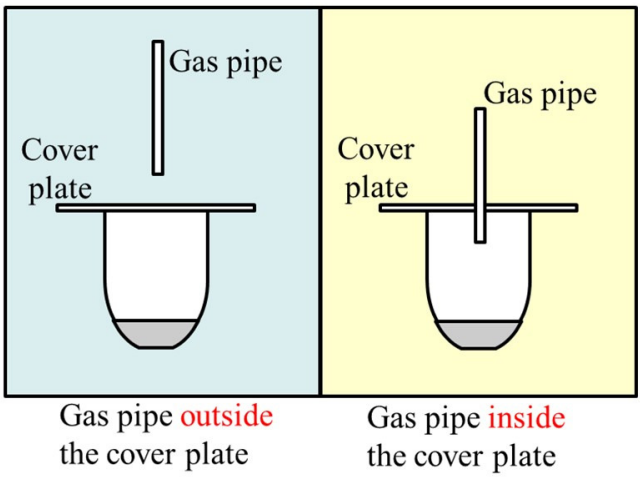

Figure 3.22: Gas pipe setting.

When performing the corrosion test, two pipes setting were chosen for inserting gas as shown in Figure 3.22, argon gas pipe only keeping over the cover plate and inserting inside of the crucible. A corrosion test was made by solidification process, cooling from 450°C to 250°C and melting process, heating from 250°C to 450°C in 3 hours and keeping 450°C for 1 hour. Argon gas inserted continuously both melting and solidification process.Figure 3.23 shows the plates condition of SS304, SS316 and SS316L with NaCl: KCl: LiCl (0:54:46) (a) before the test, (b) after test without argon gas, (c)after test with argon gas and (d)after test with argon gas inside crucible. Comparing with (b)and (c), corrosiveness of plate with argon gas is slightly decreased but nearly the same. At argon gas inserting inside of crucible, the corrosion decreases and there was no corrosion of plate inside of crucible. But the edges of plates that were outside of the cover plate had a little corrosion.

Figure 3.24 shows the PCM condition before the test, after the test without inserting argon gas, after the test with gas and after the test with gas inside of the crucible. The PCM color very changes without gas, a little change with gas and nearly the same with gas inside of the crucible. Figure 3.25 shows the melting processes of corrosion test without, with gas and with gas inside of the crucible. With gas means the argon gas pipe is not inserted into the crucible, only kept over the cover plate outside of crucible and with gas inside means the argon gas pipe is inserted into the crucible undercover plate. The melting temperatures of all processes are nearly the same. It is not affected the temperature histories by inserting

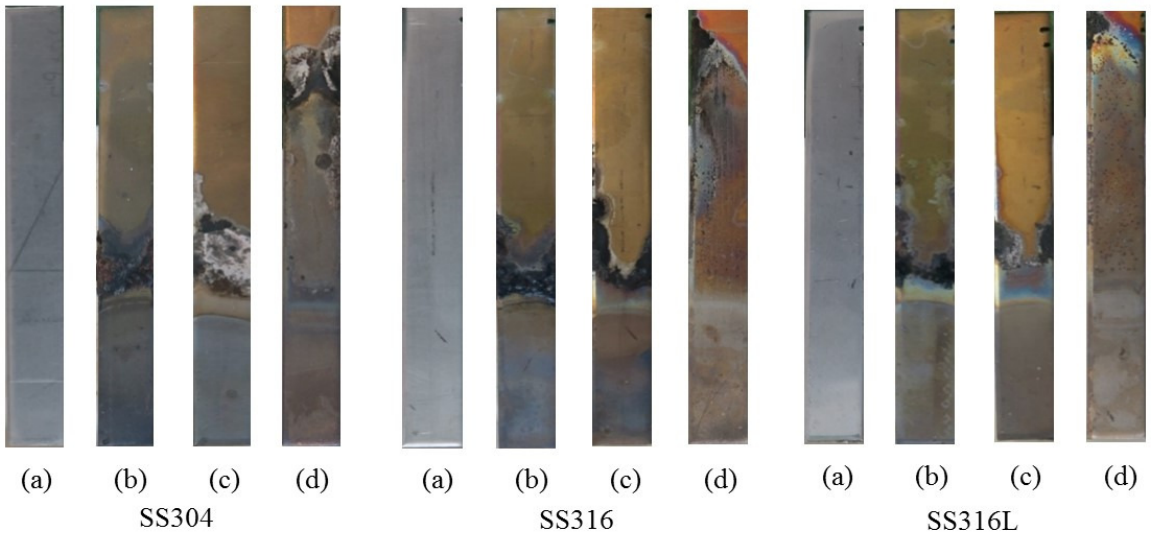

Figure 3.23: Plates conditions after corrosion test with argon gas.

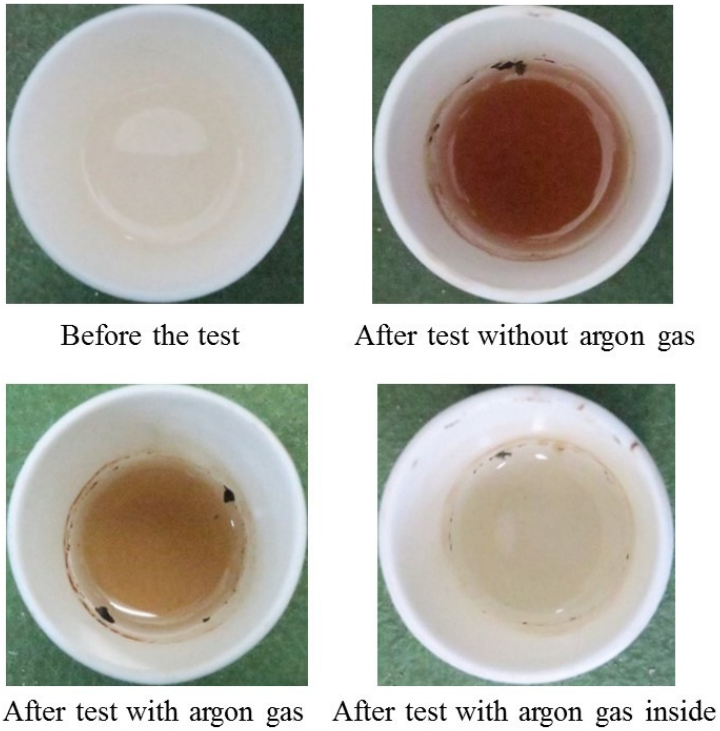

Figure 3.24: PCM conditions after test with argon.

argon gas.

When performing the corrosion test without and with inserting argon gas by using the experimental device of Figure 3.3, there has no significant to understand corrosion effect because the door of this device has leakage and there has a hole in the upper part of this

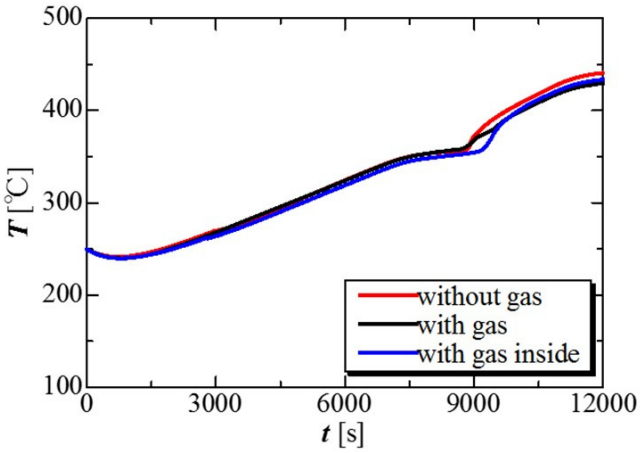

Figure 3.25: Temperature histories of melting process with argon gas.

device. Oxygen can enter through this leakage and hole. Because of these reasons, make the corrosion test again by using the vacuum furnace of Figure 3.26. The model of this vacuum furnace is FT-01VAC-50. This furnace is space, temperature, and energy saving device and it can heat up to maximum 1200°C, and can be used with A.C 100 V, 0.8 kW. This device includes controllable heater, high purity transparent quartz chamber, programmable controller, vacuum pump, and digital gas control unit. The temperature can be controlled by connecting to the computer.

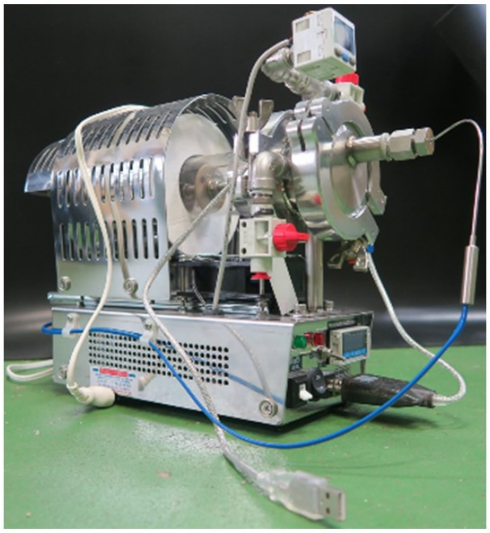

Figure 3.26: Vacuum furnace.

SS304 and SS316L with the size of 10 mm × 35 mm are used for corrosion test. The

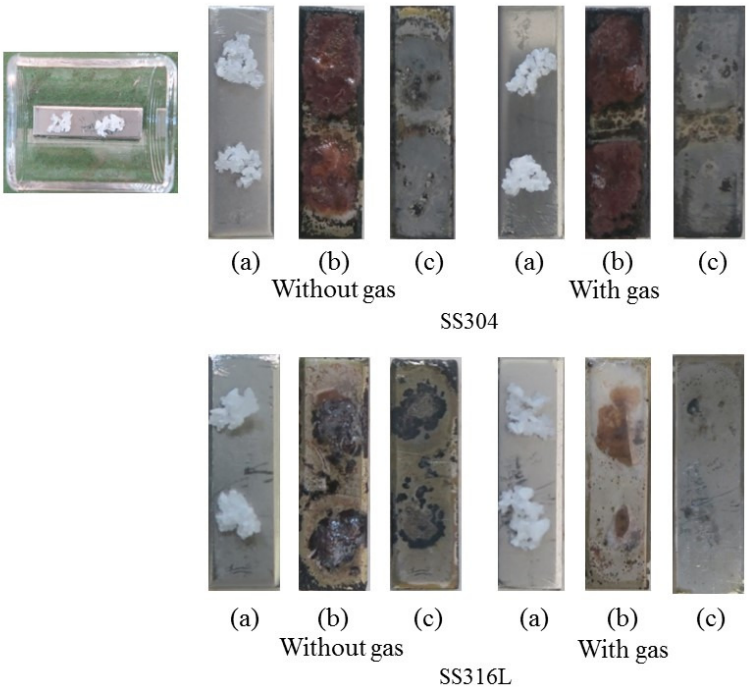

Figure 3.27: Plates condition with NaCl0%.

thickness of the plates are 2 mm. The mixture is NaCl: KCl: LiCl (0:54:46) and (23:46:31) wt% and the mass of PCM mixture is 0.1 g. Corrosion test is made without and with inserting argon gas. Melting and solidification process is like heating from 0°C to 300°C in 2 hours, heating from 300°C to 400°C in 1 hour, keeping 400°C for 30 min, cooling from 400°C to 300°C in 1 hour and cooling from 300°C to 0°C in 2 hours. Argon gas does not insert continuously. Test plates and mixtures were inserted into the glass bowl and this bowl is inserted into the quartz chamber of the vacuum furnace. The vacuum furnace is shown in Figure 3.26. At the beginning of the corrosion test, air is blown out from the inside of the quartz chamber by using the small vacuum pump and inserted argon gas at once inside of the quartz chamber of vacuum furnace before starting the test. After that started the corrosion test by making the melting and solidification process of PCM mixture. After finishing the test, test plate were taken out and took photos of plate condition with a digital camera. The plate was cleaned with water, and took the photo of plate condition again. Figure 3.27 and 3.28 show the corrosion test result of SS304 and SS316L without and with inserting argon gas by using the small vacuum furnace. The PCM is 0.1 g of NaCl: KCl: LiCl (0:54:46)

and (23:46:31) wt% mixture. Plates are compared (a) before the test, (b) after test before cleaning and (c) after cleaning with water. It is found that the corrosion effect decreases with inserting the argon gas. Comparing SS304 and SS316L, the corrosion effect less in SS316L. And the corrosion effect slightly highers with the NaCl23% than the NaCl0%.

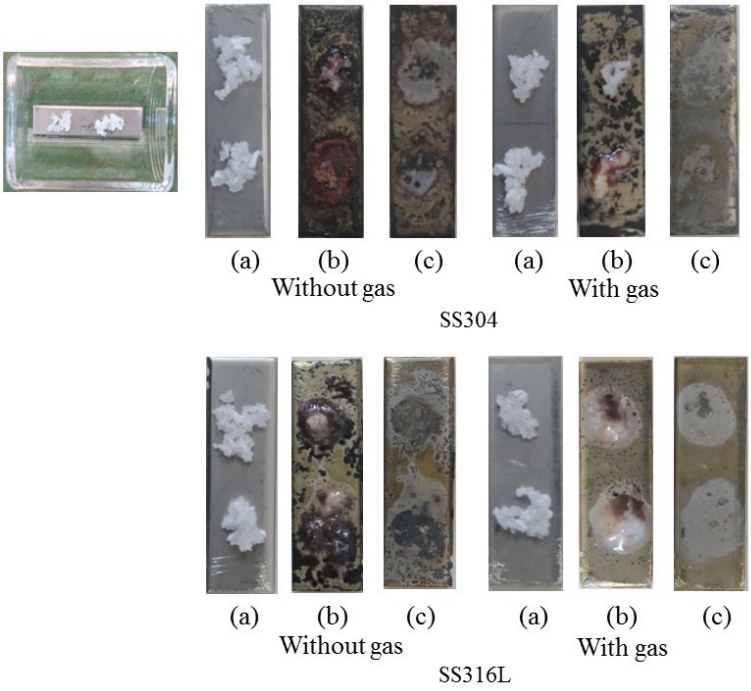

Figure 3.28: Plates condition with NaCl23%.

At this time, after finishing the corrosion test with the PCM mixture of 0.1 g, the mass of the PCM mixture increases to 1 g, and the mixture of the NaCl0% is used. In this time, the experiment is made in two conditions, the plates were immersed inside of the PCM mixture and only kept the plates over the PCM mixture. Figure 3.29 shows the result of the plates condition after the test without inserting argon gas. Plates are compared (a) before the test, (b) after test before cleaning and (c) after cleaning with water. Both of plates SS304 and SS316 have not corrosiveness after the test. Because both of plates immerse inside of the PCM mixture and they have no chance to contact with any oxygen and gas. Figure 3.30 shows SS304 Plates condition with NaCL0%without and with argon gas at the beginning of the test. Plates are only kept over the PCM mixture and the mixture is NaCl0% of 1 g. It is found that the plate has corrosiveness without inserting argon gas and the effect of

corrosiveness decrease with inserting the argon gas.

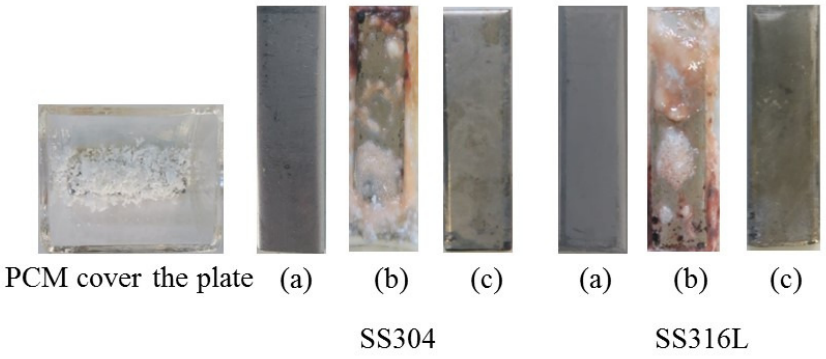

Figure 3.29: Plates condition with NaCl0% without gas.

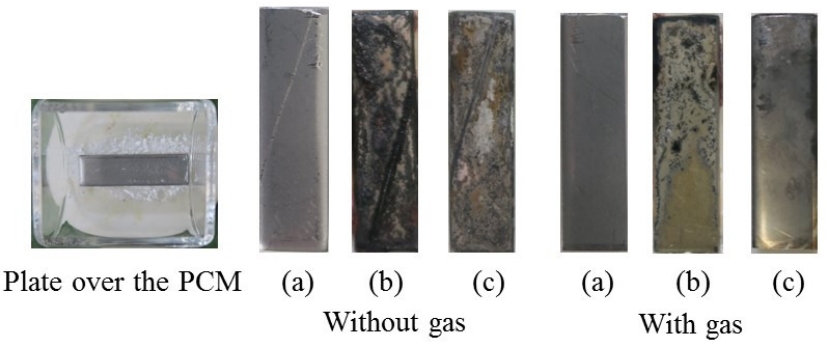

Figure 3.30: SS304 Plates condition with NaCl0%.

3.5 Summary

In this Chapter, contains selection of phase change materials to store the waste heat energy from the factories for the temperature range 300∼400°C. NaCl:KCl:LiCl (0:54:46)wt% and NaCl:KCl:LiCl (23:46:31)wt% were selected as heat storage material mixtures. For using these two mixtures, corrosiveness test with different types of material SS304, SS316, SS316L, SS310, copper, brass, carbon steel, aluminum, nickel, titanium, and molybdenum were performed. After that, the test of the corrosiveness condition of constructive materials by using some corrosion and heat resistance paints and spray were also performed. Corrosion can be caused by both oxygen and heat storage material mixture vapor. Thus, corrosion

test performed again by inserting the argon gas instead of oxygen inside the electric furnace. Although the nickel and molybdenum can be used as construction material for the latent heat storage system, they are very expensive and it would not match from the economically point of view. Most of materials have corrosiveness problem with the heat storage material because of high temperature operating condition. Electric furnace has some leakage from the upper hole and door while making the corrosiveness test. Thus, corrosiveness test was performed again by using small vacuum furnace and argon gas. As results, the corrosiveness of test plate decreased by using argon gas. Further corrosiveness tests are needed to construct the latent heat storage system for this temperature range because of high temperature.

Chapter 4

Heat Storage Material Mixture at Temperature Range 200∼300°C

Industrial waste heat refers to energy that is generated in industrial processes without being put to practical use. Sources of waste heat include hot combustion gases discharged to the atmosphere, heated products exiting industrial processes, and heat transfer from hot equipment surfaces. The exact quantity of industrial waste heat is poorly quantified, but various studies have estimated that as much as 20 to 50% of industrial energy consumption is ultimately discharged as waste heat. While some waste heat losses from industrial processes are inevitable, facilities can reduce these losses by improving equipment efficiency or installing waste heat recovery technologies. Waste heat recovery entails capturing and reusing the waste heat in industrial processes for heating or for generating mechanical or electrical work. The example uses for waste heat include generating electricity, preheating combustion air, preheating furnace loads, absorption cooling, and space heating. Heat recovery technologies frequently reduce the operating costs for facilities by increasing their energy productivity. Many recovery technologies are already well developed and technically proven; however, there are numerous applications where heat is not recovered due to a combination of market and technical barriers. Various sources indicate that there may be significant opportunities for improving industrial energy efficiency through waste heat recovery. A comprehensive investigation of waste heat losses, recovery practices, and barriers is required in

order to better identify heat recovery opportunities and technology needs. Such an analysis can aid decision makers in identifying research priorities for promoting industrial energy efficiency.

Recovering industrial waste heat can be achieved via numerous methods. The heat can either be reused within the same process or transferred to another process. Ways of reusing heat locally include using combustion exhaust gases to preheat combustion air or feedwater in industrial boilers. By preheating the feedwater before it enters the boiler, the amount of energy required to heat the water to its final temperature is reduced. Alternately, the heat can be transferred to another process; for example, a heat exchanger could be used to transfer heat from combustion exhaust gases to hot air needed for a drying oven. In this manner, the recovered heat can replace fossil energy that would have otherwise been used in the oven. Such methods for recovering waste heat can help facilities significantly reduce their fossil fuel consumption, as well as reduce associated operating costs and pollutant emissions.

Today, latent heat storage system is a very effective method to reuse the waste heat energy as desirable time and place. In this chapter, the latent heat storage material at 220°C is discussed. Firstly, the appropriate material for this temperature was chosen, and then consider the corresponding construction material for this mixture. After that, design and construct the experimental apparatus, and study the melting and solidification behaviors of this storage material by using this experimental apparatus.

A large number of inorganic salt mixtures and several single salts with a melting temperature in the range 200∼350°C was studied, and the system KNO_3-$NaNO_3$ is discussed in detail in terms of their thermo-physical properties in the liquid and solid phase [77]. There was the study to evaluate the melting point and thermal stability of conventional salt systems, such as the Solar Salt (60% $NaNO_3$- 40% KNO_3, $T_m = 220$°C) and HITEC (7%$NaNO_3$- 53% KNO_3- 40 % $NaNO_2$, T_m= 142°C), and a novel eutectic mixture. The physical and chemical properties of the studied salts were evaluated by Differential Scanning Calorimetry (DSC) [78].

4.1 Selection of Heat Storage Material

In the temperature range over 200°C, it is difficult to use organic substances and sugar alcohols that mainly used in the low to mid temperature range, and molten salt and alloys are used for the temperature range of 200∼300°C. However, when using alloys, it is difficult to load heat storage material and take out after use, so it is essential to study. Therefore, in this research, we focused on molten salt and select latent heat storage material with phase change temperature in the temperature range from 200∼300°C. Table 4.1 shows latent heat storage material candidates having a phase change temperature in a temperature range of 200∼300°C. Among them LiOH, NaOH,LiCl, and KOH are used to store the waste heat energy in this chapter.

Table 4.1: Heat storage materials in the temperature range of 200∼300°C [76], [79].

Material	Composition (mol%)	Phase change temperature (°C)	Latent- heat (kJ/kg)
$NaOH\text{-}NaNO_2$	20-80	230	278
	73-27	237	206
$NaOH\text{-}NaNO_3$	81.5-18.5	257	292
	59-41	273	273
	28-72	248	222
LiOH-LiCl-KCl	62-36.5-1.5	282	300
LiOH-LiCl	63 -37	264	339
LiOH-LiCl	65.5-34.5	274	339
LiOH-NaOH	30-70	210	362
LiOH-KOH	29-71	227	285

The picture of KOH, LiOH, NaOH, and LiCl are shown in Figure 4.1. Potassium hydroxide is an inorganic compound with the formula KOH and is commonly called caustic potash.Its melting temperature is 360°C. This colorless solid is a prototypical strong base. It has many industrial and niche applications, most of which exploit its corrosive nature and its reactivity toward acids. Lithium hydroxide is an inorganic compound with the formula LiOH. It is a white hygroscopic crystalline material. It is soluble in water and slightly soluble in ethanol and is available commercially in a hydrous form and as the monohydrate ($LiOH.H_2O$), both of which are strong bases. It is the weakest base among the alkali metal hydroxides. It has the melting temperature of 462°C. Lithium hydroxide is mainly consumed

for the production of lithium greases. Sodium hydroxide, also known as lye and caustic soda, is an inorganic compound with formula NaOH. It is a white solid ionic compound consisting of sodium cations Na+ and hydroxide anions OH^-. It has the melting temperature of 318°C. Sodium hydroxide is used in many industries in the manufacture of pulp and paper, textiles, drinking water, soaps and detergents and as a drain cleaner. Lithium chloride is a chemical compound with the formula LiCl. The salt is a typical ionic compound. The melting temperature of it is 605°C. Lithium chloride is mainly used for the production of lithium metal by electrolysis of a LiCl/KCl melt at 450°C. LiCl is also used as a brazing flux for aluminum in automobile parts. It is used as a desiccant for drying air streams.

Figure 4.1: Pictures of heat storage materials.

4.2 Melting Point Measurement

In order to develop a mixed latent heat storage material, it is necessary to measure physical properties such as melting point temperature and latent heat. However, in the case

of inorganic salt hydroxide, the corrosiveness to the construction material is strong, it is not easy to measure the thermo-physical properties using differential scanning calorimetry (DSC), the heat storage material can leak out from the enclosure during melting of the heating process. Therefore, in this research, heating is performed by an electric muffle furnace, the melting temperature is calculated from the melting and solidification behaviors at that time. The experimental apparatus for melting point measurement of the new PCM mixture is shown in Figure 4.2. The model of electric muffle furnace is Advantec FUW230PA and the maximum temperature is to 1150°C ($\pm 1.5°C$).

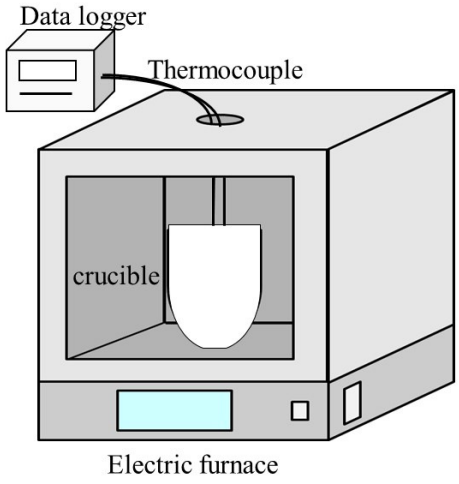

Figure 4.2: The experimental apparatus for melting point measurement.

The inside dimension of the furnace is (W200× D300× H160) mm. The inorganic salt each mixture is mixed in a different ratio of mol% in the crucible. The height of the crucible is 65 mm. The ceramic crucible is used to protect the corrosion. The crucible with the inorganic salt mixture and ceramic thermocouple are set in the electric furnace as in Figure 4.2. The thermocouple is inserted from the hole located in the upper part of the electric furnace and heat is insulated by filling it in the gap with rock wool. The thermocouple is connected to the data logger and the temperature history is recorded by the data logger. Firstly, the temperature of the electric furnace set to 500°C for good mixing about 4 hours, and cooling down in the furnace to atmosphere temperature to get the good mixing of PCM mixture. After that, making the melting process by heating from 150°C to 350°C in 3 hours and keeping 350°C for 1 hour, after that continues the solidification process, by cooling down in

the furnace from 350°C to 150°C. Temperature histories are recorded by the data logger.

4.2.1 LiOH-LiCl Mixture

Table 4.2 shows the mixing ratio in the LiOH: LiCl mixture and the measured the phase change temperature. Experimental conditions are set as stable at 150°C, the temperature is raised to 350°C in 3 hours, and the temperature is maintained for 1 hour. The temperature histories of LiOH: LiCl (60.5:39.5) and (40:60) mol% are shown in Figure 4.3 and Figure 4.4. As can be seen from this figure, the phase change temperatures are 275°C and 300°C respectively. It is difficult to adjust the melting point as a heat storage material around 250°C, and lithium chloride is relatively expensive per mass and corrosion problem to the construction material. Thus, it is considered unsuitable for practical use of this mixture.

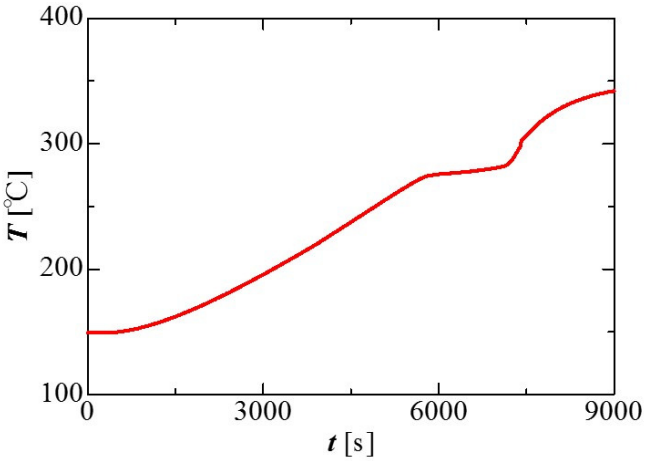

Figure 4.3: Temperature history of LiOH: LiCl (60.5:39.5)mol%.

Table 4.2: LiOH: LiCl mixtures and its melting temperature.

Mixture	LiOH (mol%)	LiCl (mol%)	Melting temperature (°C)
1	60.5	39.5	275
2	40	60	300

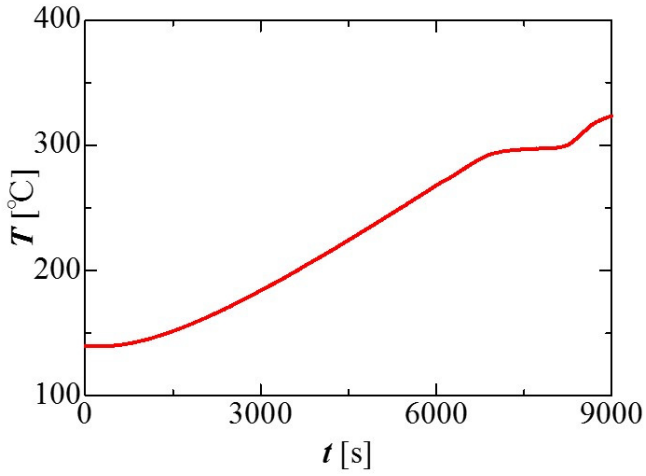

Figure 4.4: Temperature history of LiOH: LiCl (40:60) mol%.

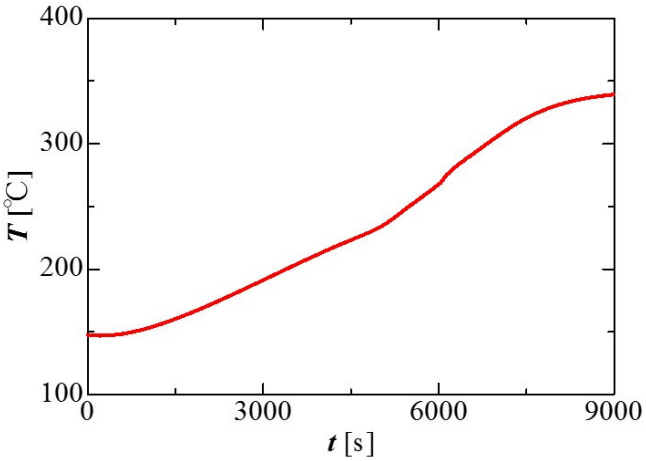

Figure 4.5: Temperature history of LiOH: KOH (29:71) mol%.

4.2.2 LiOH-KOH Mixture

According to Table 4.3, LiOH and KOH mixture (29:71) mol% mixture is used for the melting temperature of 227°C. Experimental conditions are set as stable at 150°C, the temperature is raised to 350°C in 3 hours, and the temperature is maintained for 1 hour. The temperature histories of LiOH: KOH (29:71) mol% are shown in Figure 4.5. In this figure cannot show the latent heat process for melting temperature. Thus, this mixture cannot be used for latent heat storage system.

4.2.3 NaOH-LiOH Mixture

Table 4.1 shows the mixing ratio in the NaOH: LiOH mixture and the measured the phase change temperature. Experimental conditions are set as stable at 150°C, the temperature is raised to 350°C in 2 hours, and the temperature is maintained for 1 hour. The temperature histories of NaOH: LiOH (70:30), (60:40) and (50:50) mol% are shown in Figure 4.6, Figure 4.7, and Figure 4.8 respectively.

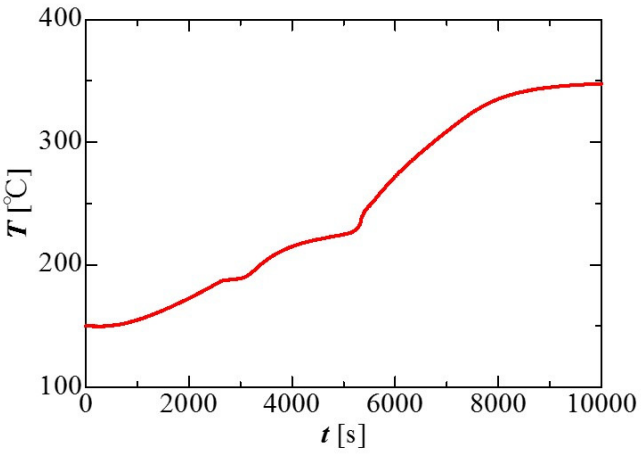

Figure 4.6: Temperature history of NaOH: LiOH (70:30) mol%.

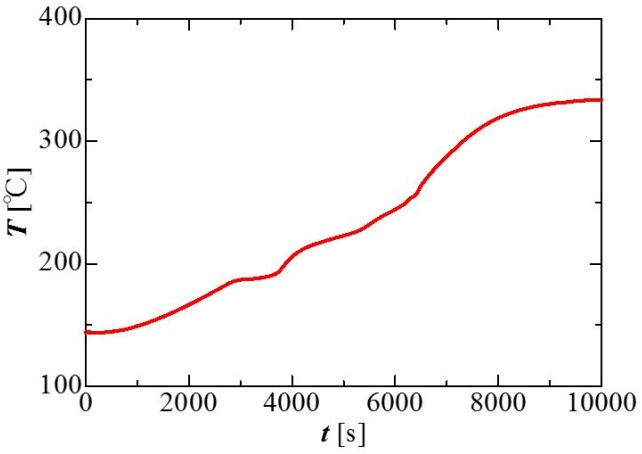

Figure 4.7: Temperature history of NaOH: LiOH (60:40) mol%.

In the literature, it has been found that it has a melting point at 210°C with a mixing ratio of NaOH: LiOH = 70: 30. Therefore, the proportion of lithium hydroxide will be raised to develop a heat storage material having a melting point of 250°C because the

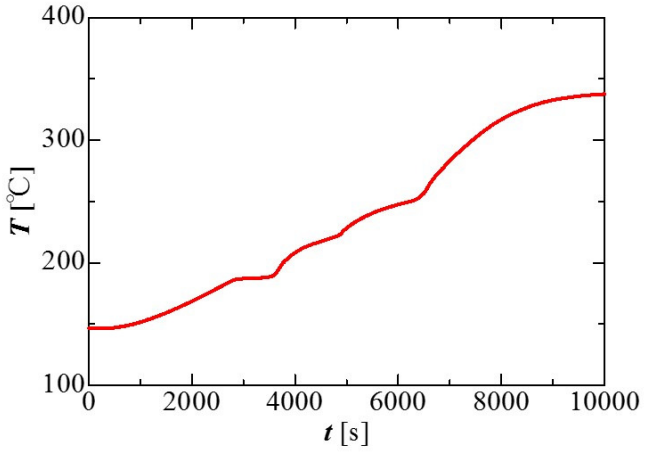

Figure 4.8: Temperature history of NaOH: LiOH (50:50) mol%.

melting temperature of lithium hydroxide is higher than the melting temperature of sodium hydroxide. From the result of the temperature histories of three different ratio mixtures, it was found that the melting temperature of all are nearly the same and the NaOH: LiOH (70:30) mol% mixture shows the most clearly latent heat process and the proportion of LiOH is the least in this mixture. The price of lithium hydroxide is high. Because of this reason, these mixture are chosen for this research and it will be continuous corrosiveness test with some construction materials for construction the experimental device to study the melting and solidification behavior of this mixture.

Table 4.3: NaOH: LiOH mixtures and its melting temperature.

Mixture	NaOH (mol%)	LiOH (mol%)	Melting temperature (°C)
1	70	30	220
2	60	40	220
3	50	50	220

4.2.4 Corrosion Test with NaOH: LiOH Mixture

For performinging corrosion test, also use the electric furnace of Figure 4.2. The size of the plate is 10 mm×80 mm and the thickness of the plate is 2 mm as shown in Figure 4.9. These size of plates was chosen to know the condition of the plates on the inside and outside of the liquid PCM mixture after finishing the corrosion test. The cover plate is made of

stainless steel SS304, and the cover plate has holes for inserting a thermocouple and a test plate. NaOH: LiOH (70:30)mol% mixture of 40 g is inserted into the crucible and heating to 500°C for good mixing and cooling down to atmosphere temperature at the inside of the furnace. The 40 g of liquid mixture has the height of about 20 mm and when the plate is inserted into the crucible, 20 mm of plate immerse into the liquid PCM and the left of another portion is outside of liquid PCM.

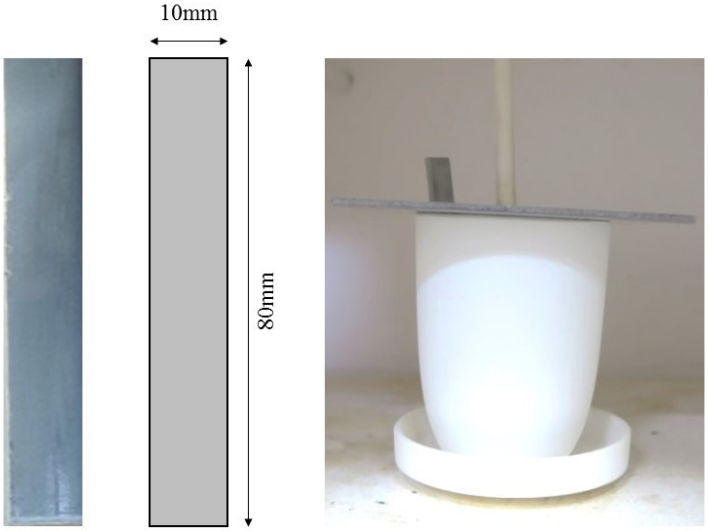

Figure 4.9: Plate and setting for corrosion test.

Firstly, plates are not inserted into the crucible and kept over the cover plate and heating up to 350°C in 1 hour to check heating effect. After that at 350°C plates are inserted into the crucible and make solidification process cooling down from 350°C to 150°C in the furnace and melting process heating from 150°C to 350°C in 2 hours and keeping 350 for 1 hour and repeat these two processes twice and after that, heating to 350°C and take out the plate outside of the crucible and take the photos. After it is cleaned with water, then surface condition was captured by camera. Pictures of the PCM condition were captured and compared the condition of PCM at 350°C before and after of corrosion test.

Figure 4.10 shows the plates condition of stainless steel SS304, SS316 and SS316L (a) before the test (b) after the twice of melting and solidification and before cleaning with water and (c) after cleaning with water (e) after performing the corrosion test fourth times. When cleaning with water, do not use any brush, only pour with water and shake slowly.

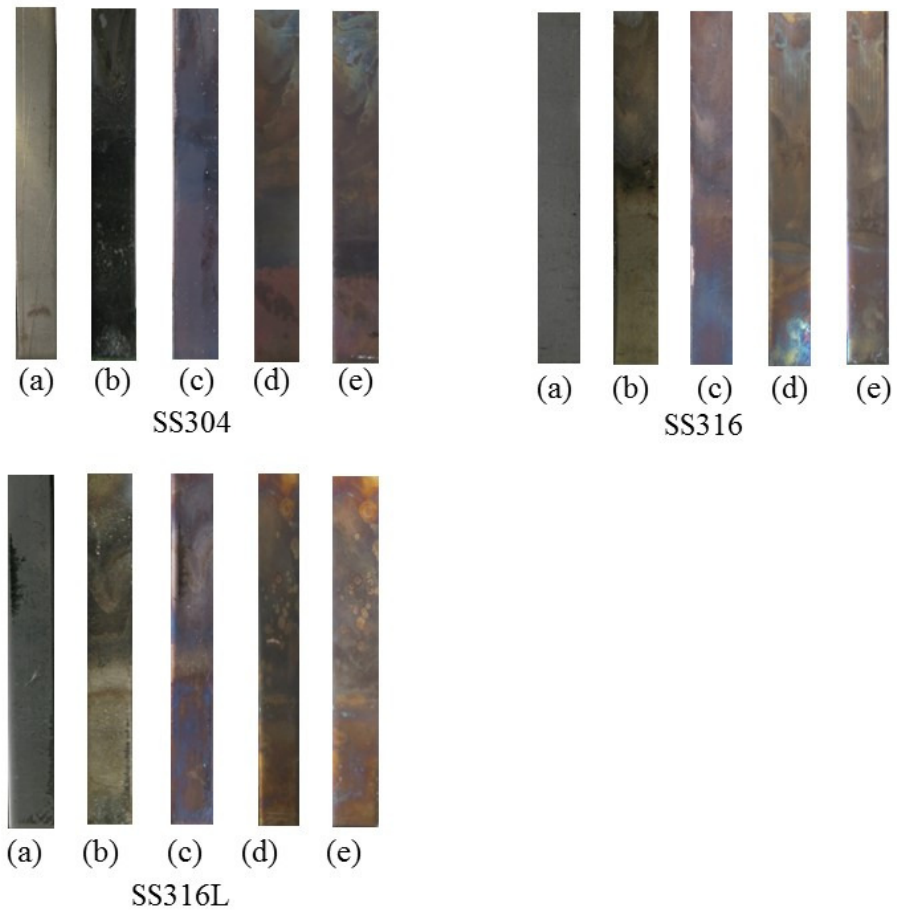

Figure 4.10: Plates condition of SS304, SS316, and SS3161.

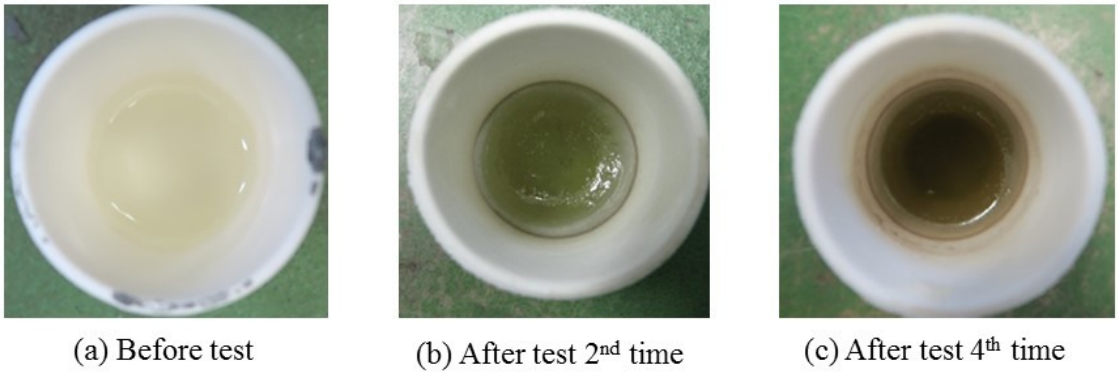

Figure 4.11: The PCM condition of NaOH: LiOH after corrosion test.

These three plates have the same composition but only different in the percentage of the composition. The difference is SS304 contains 18% chromium and 8% nickel while SS316 contains 16% chromium, 10% nickel and 2% molybdenum. The molybdenum is added to

help resist corrosion to chlorides like sea water and salts. The difference between SS316 and SS316L stainless steel is that SS316L has a 0.03% max carbon and is good for welding whereas SS316 has a mid-range level of carbon 0.08%. The higher nickel and molybdenum contents in this grade allows it to demonstrate better overall corrosion resistant property than SS304.

The type of PCM mixture of this test is NaOH: LiOH (70:30) mol% of 40 kg mass mixture. The composition of three steel plates is nearly same. Thus, performing the corrosion test inside the same crucible and the same time. It seems that only surface corrosion occurs all over the plates. However, due to the short time of corrosion experiments, repeated corrosion tests were carried out taking into consideration that such results were obtained. Next, the state of the specimen when repeating the corrosion test with each stainless steel in NaOH: LiOH = 70: 30 mol% mixture is also shown in Figure 4.10 (d) and (e) of second and fourth time of the test. From this photo, it cannot be confirmed visually that any piece of corrosion progresses. The plate has only color change and it can say that surface corrosion. Figure 4.11 shows the PCM condition of NaOH: LiOH mixture before the corrosion test, after the test second time, and after the test fourth time respectively. It is found that the PCM color changing is increased with the increased number of test.

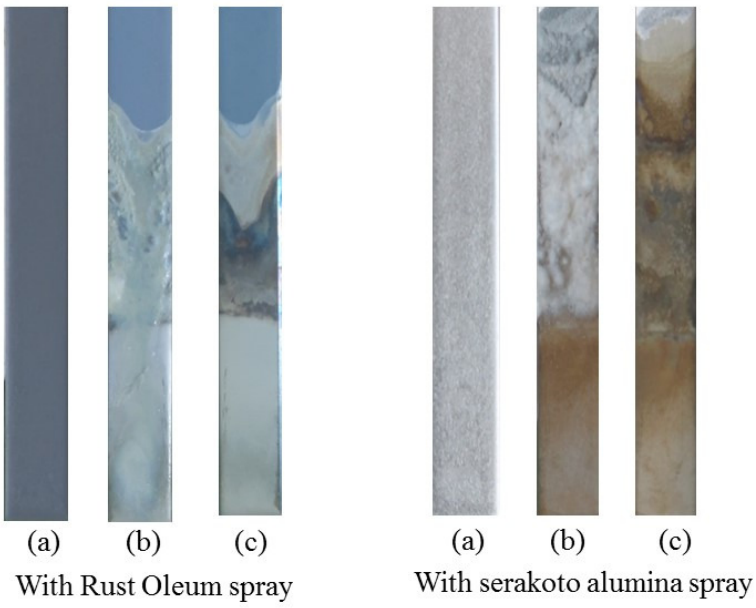

Figure 4.12: Plates condition with NaOH: LiOH with some spray.

In this section, for preventing the corrosiveness of the construction material, some anti-corrosive spray and paint were used. Firstly, make the corrosion test SS316L stainless steel plate with one type of high heat primer spray Rust Oleum. This High Heat Primer spray bonds to bare metal and helps to create a smooth surface. It is specially formulated to prevent rust and is recommended for use on automotive engines and other metal surfaces which reach intermittent temperatures up to 2000°F (1093°C). Cerakoto Alumina spray has a heat-resistant upper limit of 1800°C. For exceeding the heat-resistant upper limit of the binder, alumina is free coating the surface of the main component will discoloration powder. High-purity alumina (Al_2O_3) is a main ingredient. Although the film is excellent in insulation and corrosion resistance, heat resistance and abrasion resistance are inferior to ceramic paint. It is used for purposes such as insulation, masking, prevention of adhesion of molten metal, demolding and so on.

All plates are spray and dry at atmosphere naturally. After that sprayed plates are not inserted directly into the PCM and heated up to 450°C outside of the PCM. After heating the plates 450°C, all plates are inserted into the crucible. The bottom portion of about 20 mm of plates are immersed inside the PCM and other portions are outside of PCM. After that solidification process is made by cooling from 450°C to 250°C and melting process are made by heating up from 250°C to 450°C in 3 hours and keeping 450°C for 1 hour. This two solidification and melting is made twice and takes the photos of plates condition. Figure 4.12 shows the results after the corrosion test SS316L steel plates with Rust Oleum and Cerakoto Alumina sprays. Figure 4.12 (a) before the test, only dry condition, Figure 4.12 (b) after performing the corrosion test before the cleaning and Figure 4.12 (c) after the cleaning. Plates are clean with water. After the test, plates outside the PCM has not corrosion and not change, but plates inside the PCM, the spray is eroded by PCM. Thus, these types of spray cannot be used to prevent the corrosion.

Figure 4.13 shows the plates condition of nickel and a copper plate (a) before the test (b) after the twice of melting and solidification and before cleaning with water and (c) after cleaning with water. After heating the plates 450°C, all plates are inserted into the crucible.

The bottom portion of about 20 mm of plates are immersed inside the PCM and other portions are outside of PCM. After that solidification process is made by cooling from 450°C to 250°C and melting process are made by heating up from 250°C to 450°C in 3 hours and keeping 450°C for 1 hour. The solidification and melting is made twice and takes the photos of plates condition. It was found that there has no significant corrosion at nickel plate but the color of plate change after the test. Copperplate has the brown color of a thin layer over the plate because of oxidation condition after heating. This plate also no significant corrosion but the color of the plate changed after the test.

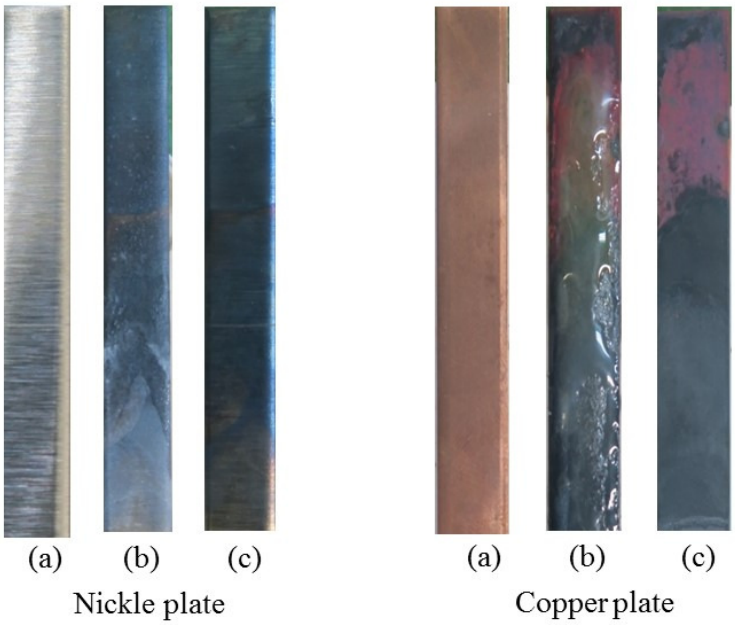

Figure 4.13: Nickel and copper plates condition with NaOH: LiOH.

Mixing with oxygen is also one reason of corrosion. While making the corrosion test, there has oxygen inside the electric furnace. To prevent the oxidation, argon gas was inserted inside the electric furnace while carrying out of the corrosion test. Figure 3.21 is also used as experimental device for corrosion test with argon gas. Argon gas is denser than air and it can displace oxygen and close to the bottom during inserting the argon gas. A corrosion test was carried out in the solidification process, cooling from 450°C to 250°C and melting process, heating from 250°C to 450°C in 3 hours and keeping 450°C for 1 hour. Argon gas inserted continuously both melting and solidification process. Figure 4.14 shows the plates

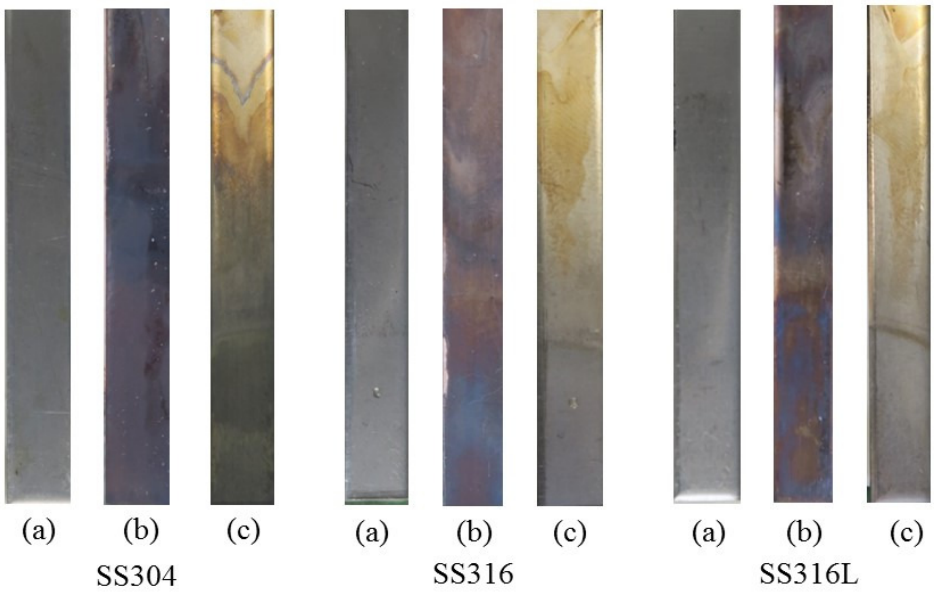

Figure 4.14: Stainless steel and NaOH: LiOH with argon gas.

condition of SS304, SS316 and SS316L with NaOH:LiOH (a) before the test, (b) after test without argon gas, and (c)after test with argon gas. While Comparing with (b)and (c), corrosiveness of plate with argon gas is slightly decrease. In this research, SS316L is used to construct the experimental device and argon gas will be inserted into the test section while making the experiment.

4.3 Design Consideration of Experimental Apparatus

In the previous section, NaOH: LiOH (70:30)mol% mixture has been selected as heat storage material mixture. After that, by using this mixture, it made the corrosiveness test with some construction material. As result, the test section will be constructed with the SS316L and while making the experiment, argon gas will be inserted into the test section to protect the corrosiveness of construction material. In this section, it will describe the design consideration of experimental apparatus. At first, the size of the test section is calculated from the 500 g of a mixture of NaOH: LiOH (70:30) mol%. The mol% of each material changes to mass% of each material and after that changes again to vol% of each material and calculate the total volume of the mixture. In that time, there has the problem, such as in

stock LiOH is very expensive and LiOH.H_2O can be bought easily and cheaper than LiOH. Thus, the size of the test section calculated again by NaOH and LiOH.$H_2$0 mixture. At that time, the size of the test section is W100 mm×D50 mm×H60 mm . The structure of the LiOH is like powder, although the structure of the NaOH is a solid crystal. Thus, it cannot be inserted into the test section before making the mixture. Because of this reason, the size of the test section will be constructed W100 mm ×D50 mm×H100 mm (. The construction material is SS316L and with the thickness of plate 5 mm. Sapphire glass plate (ϕ 70 mm, thickness 5 mm) was used on both side surface of the test section to take the photo of melting and solidification behaviors of the heat storage material mixture. There have three holes at the upper plate of the test section, one hole for argon gas insertion and to attach the pressure gauge and pressure relief valve, two holes for the thermocouples to measure the material temperature of PCM at the middle and lower portion of the test section. The plate heater was used for heating and cooling system was constructed separately.

4.4 Experimental Apparatus and Method

4.4.1 Test Section and Heating System

Test section with the heating system is shown in Figure 4.15. An experimental device used two different systems for heating of heat storage and cooling of heat released. After finishing the heating of heat storage process, the heating system was taken out from the test section and connected the cooling system to the test section to perform the cooling process. The heat storage system is composed of the vacuum pump, an argon gas cylinder, power meter, heater (RS 510 manufactured by Sakaguchi Denki Co., Ltd.), data logger and test section. The test section and heating system shown as Figure 4.15. Power meter, Voltage regulator, Vacuum pump, Argon gas cylinder, Pressure gauge, Data logger and, Pressure release valve were shown as 2∼8, respectively.

Figure 4.16 shows details of the test section. Pressure gauge, Pressure release valve, Copper spring coil pipe to prevent the heat flow to a pressure gauge, Graphite sheet (Perma-

Foil), Sapphire glass, Copperplate, Main heater, SS304 plate, and Guard heater were shown as 1∼9. Sapphire glass (ϕ 70 mm, thickness 5 mm) was used in front and rear surface of the test section. It is able to us to observe the melting and solidification behavior of the heat storage material, it is easy to observe the upper and lower parts of the heat storage material. Pyrex glass cannot be used because of corrosiveness with the heat storage material and high temperature. While installing the sapphire glass and the test part, it is necessary to prevent leakage of the heat storage material and cracking the side glass plate by tightening, thus, it can be used in ultra-high temperature range and is not corroded by NaOH, Perma-Foil grade PF, manufactured by Toyo Carbon Co., Ltd. was used. A plate heater (Super Rapid Heater, capacity 250 W, 50 mm×100 mm, manufactured by Sakaguchi Denki Co., Ltd.) was installed outside the bottom of the container via a copper plate (50 mm × 100 mm × 5 mm).

The main heater that adjust the output by the transformer so that the temperature distribution can be controlled constant through the copper plate. The temperature was measured at the copper plate by inserting a thermocouple (ϕ 1.0 mm, manufactured by Sakaguchi Electric Co., Ltd., K type) into the groove inscribed in the lower part of the test part and the copper plate, so that the surface temperature of the lower part of the test part was controlled at constant. In order to prevent heat loss to the lower part of the heat transfer surface, installation of a guard heater (Super Rapid Heater, capacity 250 W, 50 mm×100 mm, manufactured by Sakaguchi Electric Co., Ltd.) was also used. This guard heater is inserted between the main heater and an outer stainless-steel plate (100 mm×60 mm×5 mm), and the output of the guard heater is finely adjusted by using a voltage regulator. The thermocouples were installed on both sides and the temperature of the thermocouples can keep the same. Thus, most of the heat from the main heater can supply to the test section.

A vacuum pump (maximum degree of vacuum: 78 KPa) was used, to evacuate the air inside of the test section, and then argon gas is inserted into the test section from argon gas cylinder by mean of pipe up to atmospheric pressure makes it possible to reduce corrosion and prevent chemical reaction. However, when the sealed container is heated, there is a

possibility that the argon gas and the heat storage material in the test-section can expand and a large load is applied to the test portion and sapphire glass. As a countermeasure against this, installed a pressure relief valve in the upper part of the test-section, when a pressure exceeding a certain level is applied to the test-section, the argon gas in the test-section will escape outside the test-section. When this pressure relief valve was installed, since the heat resistance temperature of the O-ring used for this valve was 200°C, a copper pipe with a high thermal conductivity in a coil shape was attaching between the valve and the test part, the copper pipe radiates the heat transmitted from the test part and prevents the relief valve from reaching high temperature. Before starting the heating of heat stored (melting) process, the mixture of heat storage material NaOH: LiOH (70:30) mol% inserted into the test-section. And then attached the thermocouple and cover all test-section with rock wool, and heated by using main and guard heaters until the temperature of bottom plate reaches to 400°C to mix the heat storage material of NaOH and LiOH. For the melting process, the temperature of the bottom plate of test-section raises to 280°C by using the main and guard heater. The histories of temperature measured by thermocouples were recorded by the data logger and the behaviors of solidification of heat storage material were captured by the digital camera at every 15 min. The experiment was stopped when the temperature of the heat storage material that shown in data logger at constant.

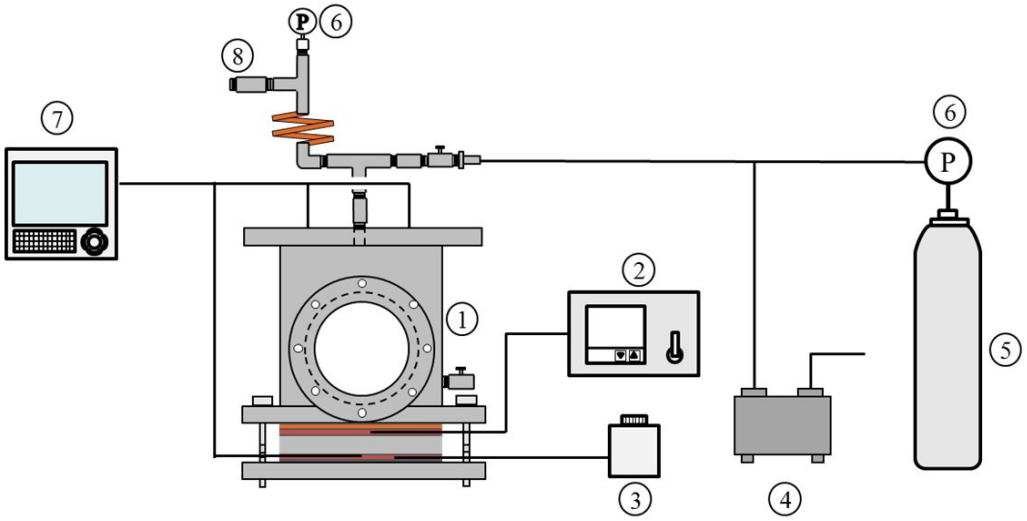

Figure 4.15: Test section with heating system.

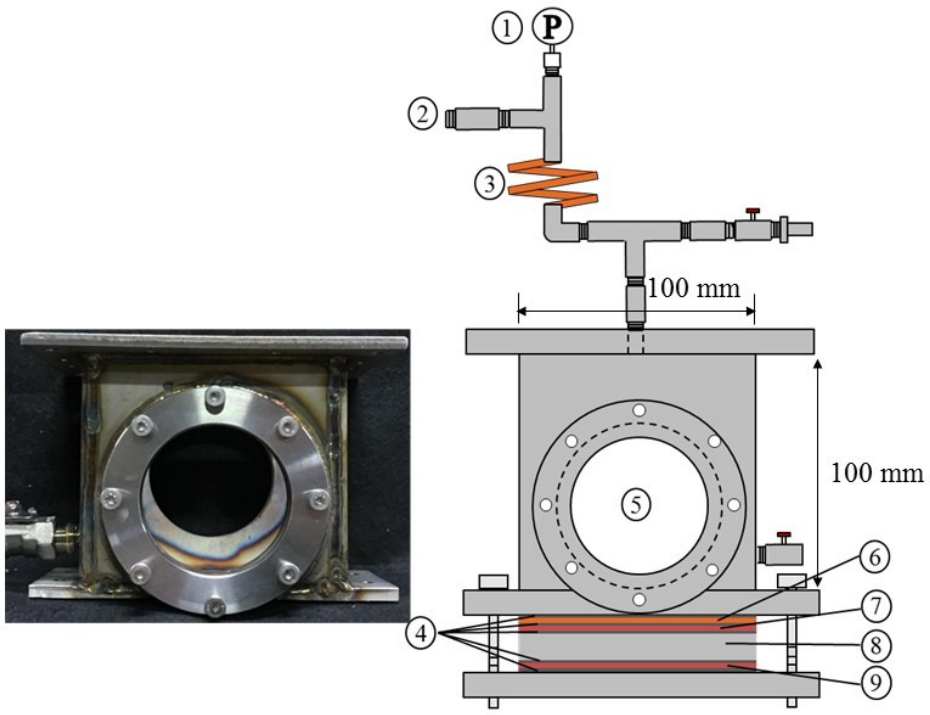

Figure 4.16: Detail of test section.

4.4.2 Test Section and Cooling System

The cooling system of heat released consists of an oil bath (Thomas Scientific Instruments, T 205), a heat exchanger, a pump, a cooling part and a test part, and silicone oil (TSF 458, manufactured by Momentive Co.) was used as a heat medium. Figure 4.17 shows the test-section with the cooling system. Test-section, Heat exchanger, Oil bath, Argon gas cylinder, Pump, Cooling chamber, and Data Logger were shown as 1∼7,respectively. Detail of cooling chamber is shown in Figure 4.18 . Inside of the cooling chamber, the partition with stainless steel plates were installed as shown in Figure 4.18 to get the oil flow near the upper cover of the cooling chamber and slightly heighten the oil outlet pipe over the cooling chamber for touching the oil to upper cover of the cooling chamber.

After finishing the heating of heat stored (melting) process, the test-section and heat storage material is heated to 300°C and kept constant at this temperature. In preparation for cooling of heat released process, before starting the solidification process, the temperature of the oil inside of the oil bath keep the constant temperature of 36°C and run the pump at

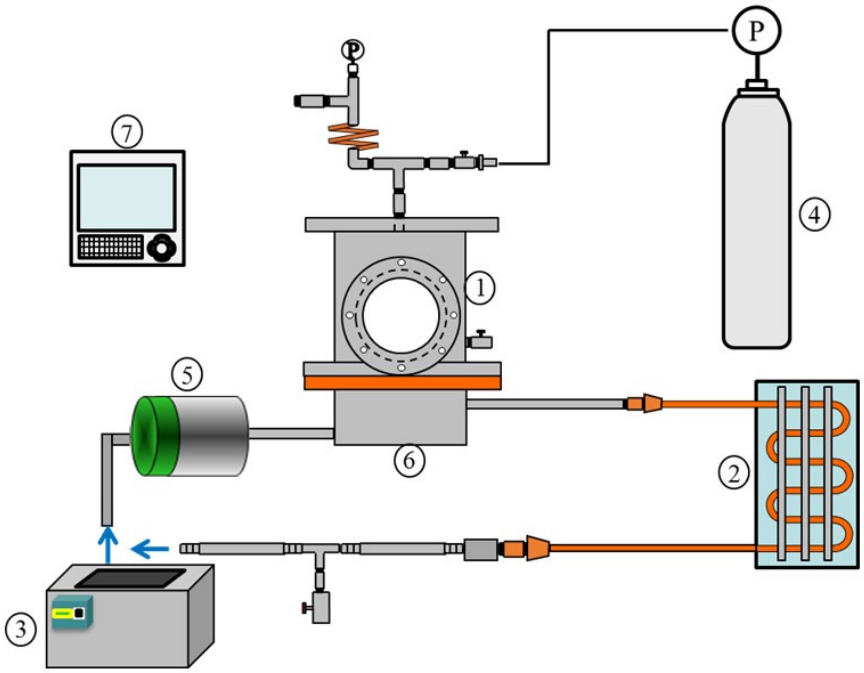

Figure 4.17: Test section with cooling system.

the constant oil flow rate of 0.05 kg/min. After the temperature of the heat storage material reaches 300°C, heating is stopped. After that, remove the all insulation cover rock wool from the test-section and remove the heaters installed in the lower part of the test section and test-section is attached to the cooling chamber of the cooling system. The test-section and the cooling chamber are covered with rock wool, and the cooling of heat release (solidification) process is started when the heat storage material temperature reaches 250°C. The histories of temperature that measured with thermocouples were recorded by the data logger and the behaviors of solidification of heat storage material was taken by the digital camera at every 15 min. The end of the experiment of data collection with data logger was taken when the temperature of heat storage material reaches to 160°C.

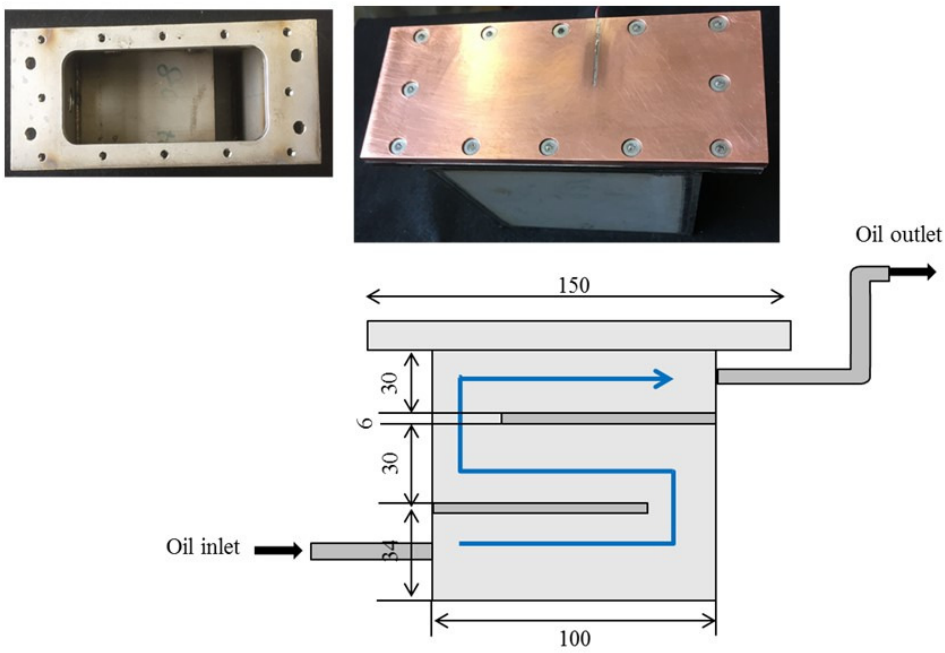

Figure 4.18: Detail of cooling section.

4.5 Experimental Result and Consideration

4.5.1 Melting process

For the melting process, the temperature of the bottom plate of test-section raises to 280°C by using the main and guard heater. The histories of temperature measured by thermocouples were recorded to the data logger and the behaviors of solidification of heat storage material were taken by the digital camera at every 15 min. The experiment was stopped when the temperature of the heat storage material at constant.

Figure 4.19 shows the temperature histories of phase change material during the melting process. At the start of the melting process, the temperature increases quickly because of heating by the main and guard heater to 280°C. After reaching to this temperature, the temperature of heater is controlled by controller at constant value. The melting temperature is about 220°C. Figure 4.20 shows visualization of PCM melting during the melting process. PCM melts at the bottom of the test section at 3600 s and the melted PCM increase to top section according the heating time. All of the PCM melt about 9500 s.

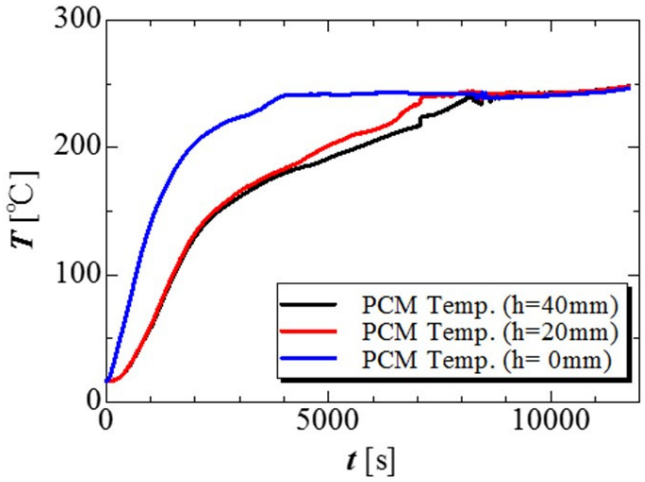

Figure 4.19: Temperature histories during melting process.

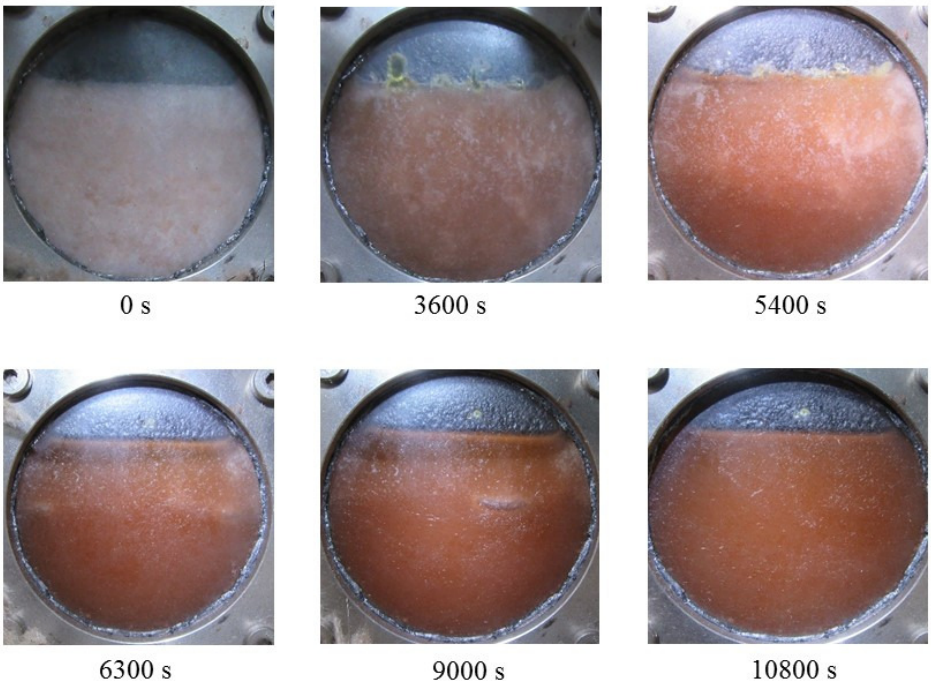

Figure 4.20: Visualization of PCM melting during the melting process.

The amount of heat stored during the melting process Q_m is calculate from the watt meter which connected to the plate heater. Figure 4.21 shows the amount of heat stored during the melting process in Watt. Figure 4.22 shows the total amount of heat stored during the melting process. This graph shows the experimental value and the theoretical value by the time during the melting process. At the end of the experiment, the experimental value is higher than the theoretical value. It means that the heater need to give more amount of

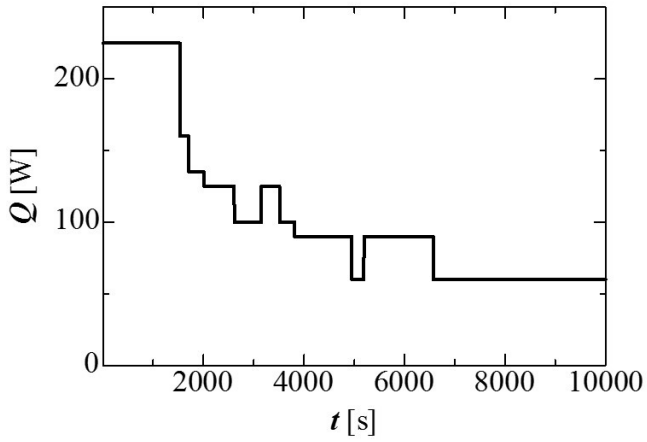

Figure 4.21: The amount of heat storage by watt meter.

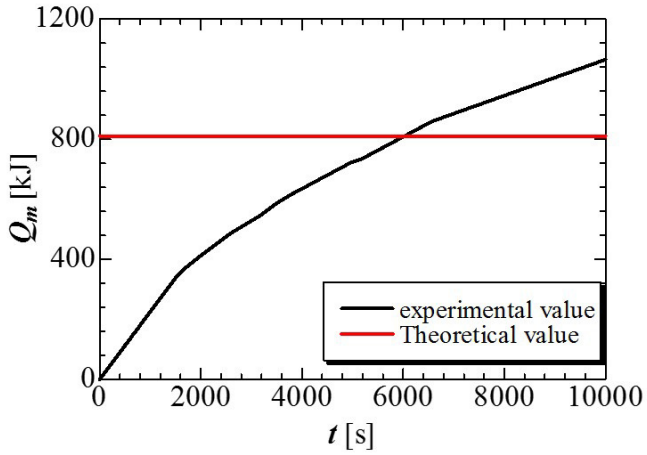

Figure 4.22: Total amount of heat storage.

heat to test section and PCM because some heat is lost to surrounding.

4.5.2 Solidification process

After finishing the heating of heat stored (melting) process, the test-section and heat storage material is heated to 300°C and kept constant at this temperature. In preparation for cooling process, the temperature of the oil inside of the oil bath keep the constant temperature of 36°C and run the pump at the constant oil flow rate of 0.05 kg/min. After the temperature of the heat storage material reaches 300°C, heating by the heater is stopped. After that, remove the all heat insulation rock wool covered to the test-section and remove the heaters installed in the lower part of the test section and test-section is attached to

the cooling chamber of the cooling system. The test-section and the cooling chamber are covered with rock wool, and the cooling of heat release (solidification) process is started. The histories of temperature are that measured with thermocouples were recorded by the data logger and the behaviors of solidification of heat storage material was taken by the digital camera every 15 min.

Figure 4.23 shows the temperature histories of PCM during the solidification process at the different height in 0 mm, 20 mm, and 40 mm inside the test section. In this figure, phase change temperature is not clear at the 0mm and 40 mm. At the height of 20 mm,solidification process start about 1000 s and it finish about 7000 s. Figure 4.24 shows the visualized result of PCM condition during the solidification process. Surface corrosion appears to the construction material after so many repeating cycles of experiment. The PCM color has changed and the solidification condition of PCM cannot be seen clearly in this photo.

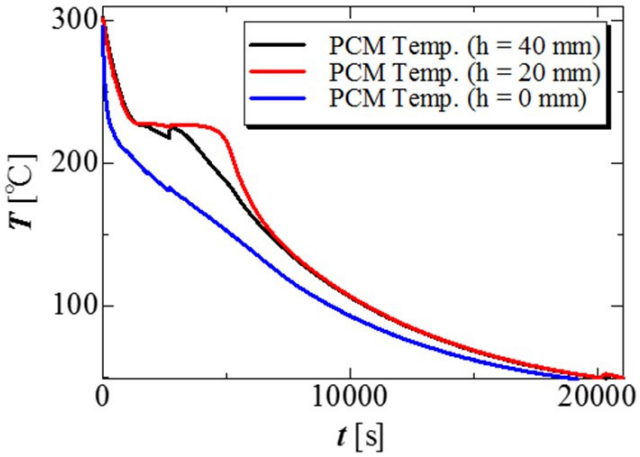

Figure 4.23: Temperature histories during the solidification process.

The amount of heat release during the solidification process Q_s was calculated from the temperature difference between the inlet and the outlet of the cooling chamber was measured by thermocouples installed at the inlet and the outlet of the cooling chamber. At this time, the heat release amount Q_s [kJ] is calculated from the Equation 4.1, and the temperature difference between the inlet and outlet of the cooling chamber, the mass flow rate of oil f_{oil} [kg/min] and the specific heat of oil $C_{P_{oil}}$[kJ/(kgK)]. Figure 4.25 shows the total amount of heat release during the solidification process. The total amount of heat release

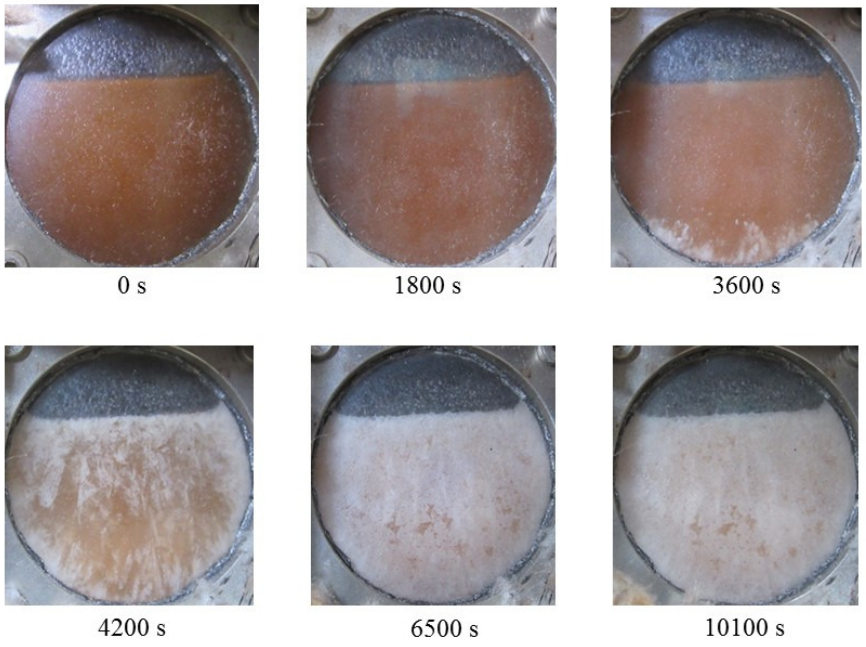

Figure 4.24: Visualization of PCM during the solidification process.

by experimental value is 500 kJ and the theoretical value is about 800 kJ. The difference is large because difference between the operating temperature and at room temperature is high and there has a lot of heat loss to surroundings.

$$Q_s = \int_{t_e}^{t_b} \{\frac{1}{60} \times f_{oil} \times C_{P_{oil}} (T_{out} - T_{in})\} dt \tag{4.1}$$

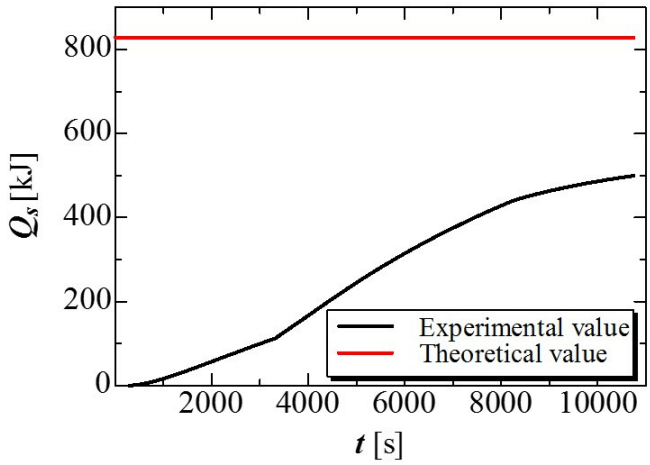

Figure 4.25: The total amount of heat release during the solidification.

4.5.3 Summary

In this Chapter, selection of phase change materials to store the waste heat energy from the factories for the temperature range 200∼300°C was conducted. NaOH:LiOH (70:30)mol% was selected as the heat storage material mixture. For using these mixture, corrosion test with different types of material SS304, SS316, SS316L, copper, and nickel were conducted. According to the result of the corrosiveness test, SS316L was used for construction the experimental device. But argon gas must be inserted inside the test section to decrease the corrosiveness problem. The experimental device contains test section, heating system and cooling system. The melting process is conducted by using the plate heater and solidification process is conducted by the oil heated in oil bath and pump. Using these devices, melting and solidification behavior of PCM was investigated. Device has some surface corrosion and PCM color changed after the repeating cycle. Thus, it is not very clear the PCM condition when taking the photo. And there has some heat transfer losses, because the operating temperature and outside temperature are very different.

Chapter 5

Heat Storage Material Mixture at Temperature Range 100∼200°C

5.1 Selection of Heat Storage Material

Nowadays, a lot of waste heat energies from industrial is discarded to the environment. Thus, global warming is a very important problem. This waste heat energy must be reused effectively to recover both of utilization of waste heat energy and protecting to environmental impact. To reuse this waste heat energy, thermal energy storage technology is a very important role. By using thermal energy storage technology, it can be reduced primary energy consumption, carbon dioxide emissions, and global warming.

Figure 5.1 shows the amount of industrial waste heat energy classified by waste heat temperatures and various sections [80]. A Huge amount of waste heat is being discarded by various industrial sectors, even in the case of Japan only, more than 400 PJ waste heat in the temperature range 100∼150°C have discarded annually. Most of this waste heat is discarded by power plants, followed by chemical and steel companies, as shown in Figure 5.1. In this graph, medium waste heat temperature is about 150°C. Because of this reason, in this research, we would like to select the heat storage material and study the heat transfer characteristics of this material at this temperature of 150°C.

Figure 5.2 shows various heat storage material at the temperature range of 100∼250°C.

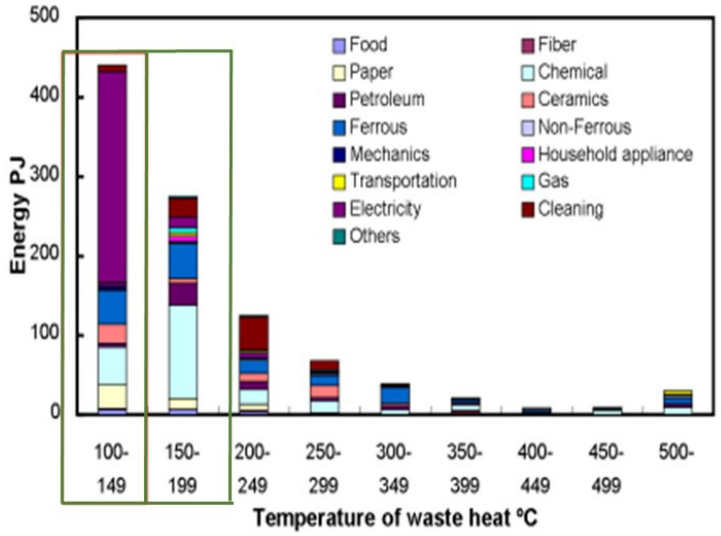

Figure 5.1: Annual discarded waste heat by various industrial sectors in Japan. [80].

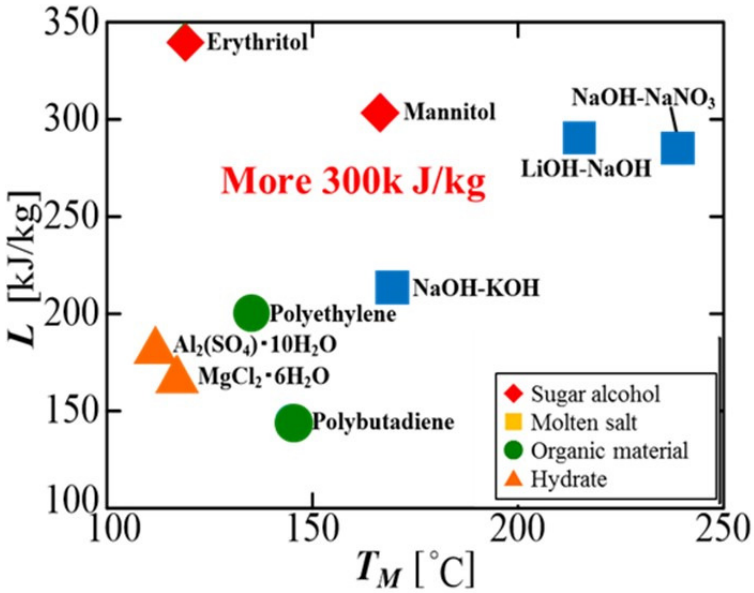

Figure 5.2: Various heat storage material at the temperature range of 100∼250°C[81],[82].

In this Figure also shows the melting point T_M and the latent heat amount L of the main heat storage material [81], [82] in the range of 100∼250°C. It includes main four types of heat storage materials like sugar alcohol, molten salt, organic material, and hydrate. As a feature of each substance, hydrate has a property of low melting temperature and latent heat value. Organic substances such as polyethylene and polybutadiene are relatively expensive and have low latent heat and are not considered to be used for latent heat storage materials.

Molten salt such as lithium hydroxide - sodium hydroxide has a high latent heat value close to 300 kJ/kg, but it causes deliquescence and it has the corrosion problem to construction materials, and it is harmful to the human body. Among them, sugar alcohols such as erythritol and mannitol are both chemically stable in both substances and are extremely harmless to the human body as it is also used in sweeteners. Also, because it has high latent heat and is relatively inexpensive, it is considered to be used as latent heat storage materials. In addition, erythritol and mannitol are environmentally friendly materials, non-toxic and non-flammable. From the above, in this study, sugar alcohols erythritol and mannitol, which have high latent heat and are harmless to people, were selected as heat storage materials.

In most latent heat storage systems, a multi-tube direct contact heat exchanger is used. A direct contact heat exchanger can exchange energy more rapidly than an indirect contact heat exchanger. A spray tower-type direct contact heat exchanger using a phase-change material (PCM) (tetradecane) in low-temperature regions and air has been studied experimentally [83]. The heat transfer characteristics of a direct contact evaporator of a two-phase refrigerant have also been studied [84]. Performance of a direct contact latent heat energy storage system during the discharging process has been investigated using a storage medium of sodium thiosulfate pentahydrate [85].

The development and performance of a direct contact heat exchanger using erythritol with the melting temperature of 119°C as a PCM and heat transfer oil for accelerating heat storage. A nozzle facing vertically downward was placed at the bottom of the heat transfer unit. It was examined the effects of the flow rate and inlet temperature of the heat transfer oil using three characteristic parameters of heat storage: the difference between inlet and outlet heat transfer oil temperatures, temperature effectiveness, and heat storage rate.

The thermal and flow behaviors in a trans-heat (TH) container have been examined, in which the solidification and melting of the PCM were observed directly using a two-dimensional roundly sliced model [86]. The improvement in heat storage performance of a direct contact heat exchanger using the PCM erythritol and heat transfer oil was described. A series of binary systems of palmitic acid (PA) and stearic acid (SA) in different

proportions were prepared from liquid mixtures by slow cooling to room temperature to determine the eutectic mixture ratio. After determining of the eutectic composition ratio of the (PA/SA) binary system, its thermo-physical properties were measured with differential scanning calorimetry (DSC). Next, the phase transition characteristics of the mixture, such as the total melting and solidification temperatures and times, were established [87].

Erythritol-polyalcohol mixtures were prepared as PCM, which may be applicable for heat storage in the temperature range between 80°C and 100°C, for a hot water supply system. The melting and solidification temperature was adjusted by adding polyalcohols, such as trimethylolethane (TME), 2-ethyl-2methyl-1,3-propanediol, 2-amino-methyl-1,3-propanediol-1,4-butanediol,2-amino-1,3-propanediol,and trimethyl-lolpropane (TMP), to erythritol [88]. A eutectic composition with a melting temperature of 363°C was determined as (mol%) LiF (17.4), LiCl (42.0), LiVO−3 (17.4), Li_2SO_4 (11.6), and Li_2MoO_4 (11.6) [89].

A comprehensive analysis of sugar alcohol (SA) relevant properties for TES has been carried out in order to select the most appropriate single SA for mixtures analysis. Sixteen SA-based binary systems have been investigated. Their corresponding phase diagrams have been experimentally and theoretically established. Four eutectic mixtures with potential for long-term TES at a temperature around 80°C have been identified. They are: 1) adonitol-erythritol at 30 mol% of erythritol, with melting temperature of 87°C and latent heat of fusion of 254 J/g; 2) arabitol- erythritol at 40mol% of erythritol, with melting temperature of 86°C and latent heat of fusion of 225 J/g; 3) xylitol-erythritol at 36mol% of erythritol, with melting temperature of 82°C and latent heat of fusion of 270 J/g; and 4) arabitol-xylitol at 56mol% of xylitol, with melting temperature of 77°C and latent heat of fusion of 243 J/g [90]. The direct contact melting and solidification behavior between heat transfer oil and erythritol (PCM) were visualized to investigate the characteristics of heat storage and release at different flow rates of oil (1.0-4.0 kg/min) and the effects of a perforated partition plate [91].

In this study, it was investigated the melting and solidification characteristics of mixtures of mannitol and erythritol ($C_m = 70$ mass%, $C_e = 30$ mass%) for latent heat storage at about

(100∼200°C). The melting point and latent heat of mannitol are T_m = 168°C and L_m = 301.2 kJ/kg, respectively. The melting point and latent heat of erythritol are T_e = 119°C and L_e = 340 kJ/kg, respectively. The mixture of mannitol and erythritol had melting temperatures [latent heat] of T_{m1} = 103°C [$L_1 = 81kJ/kg$], T_{m2} = 151°C [L_2 = 201 kJ/kg]. The melting temperature and latent heat of the mixture were measured using a DSC device [92].

5.2 Characteristics of Erythritol and Mannitol

The photographs and chemical structural formulas of erythritol (manufactured by Mitsubishi Kagaku Foods Co., Ltd., purity: 98% or more) and mannitol (D-mannitol, manufactured by Mitsubishi Shoji Foodtec, purity 99.9%) selected in this study are shown in Figure 5.3. Both of these substances are sugar alcohols of polyhydric alcohols and are harmless to people, as can be seen from the fact that they are used as food additives. As can be seen from Figure 5.3, both substances are solid at normal temperature, erythritol is transparent granular, and mannitol is white powder.

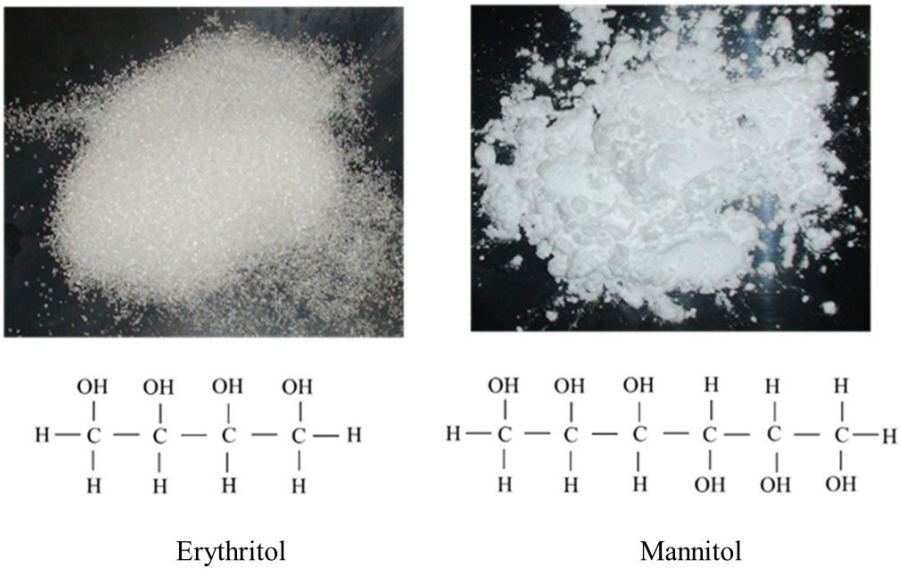

Figure 5.3: Erythritol and Mannitol material.

Physical property values of erythritol and mannitol are shown in Table 5.1 [93][94]. From

Table 5.1, in the published values, the melting point of erythritol is 118 to 119°C, and the mannitol is 166.5°C. In addition, since the density difference between both substances in liquid and solid state is relatively small, separation is difficult even when melting and solidification is repeated, and it is considered that mixing of both substances is effective.

Table 5.1: Properties of Erythritol and Mannitol [93][94].

Properties	Unit	Erythritol		Mannitol
Melting point T_m	°C	118	119	166.5
Latent heat L	kJ/kg	320	340	303.7
Specific heat C_p	kj/kg.K	2.8 (at 140°C)		2.85 (at 180°C)
		1.39 (at 20°C)		1.62 (at 100°C)
Thermal conductivity k	W/m.K	0.338 (at 140°C)		0.415 (at 170°C)
		0.676 (at 20°C))		0.491 (at 73°C))
Density ρ	kg/m^3	1300 (at 140°C)		1386 (at 200°C)
		1480 (at 20°C)		1403 (at 28°C)

5.3 Characteristics of Mixed Latent Heat Storage Material

The melting point and the latent heat at each mixing ratio of erythritol, mannitol mixture selected in this study are measured using differential scanning calorimetry (DSC) and are shown in Figure 5.4. This figure shows the melting temperatures and latent heat of each mixing ratio of erythritol and mannitol mixtures. The latent heat amount represents the total value when there is a plurality of melting points in the mixing ratio. From Figure 5.4, there has one melting peak temperature at a ratio of mannitol content of 10 mass% to 30 mass%, three melting peak temperatures at 50 mass% to 65 mass%, and two melting peak temperatures at other mixing ratios. After the mannitol content of 40 mass%, it shows a plurality of melting peaks on the low-temperature side and the high-temperature side, and on the high-temperature side, there is a tendency to approach the melting point of mannitol as the content increases. Further, when mannitol content is 50 to 65 mass%, there is two low-temperature side melting peaks.

In addition, it can be seen from Figure 5.4 that the melting peak temperature of the

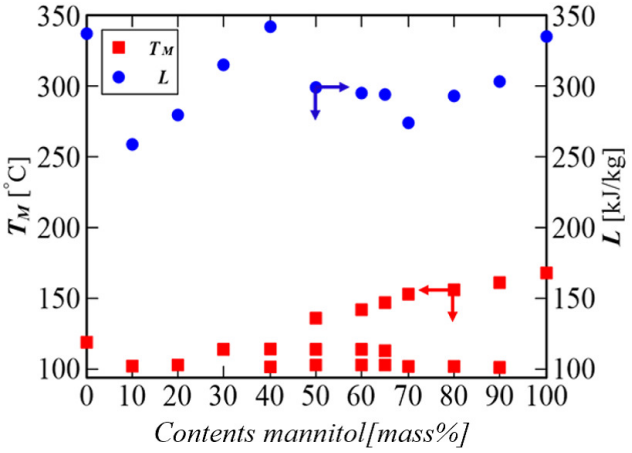

Figure 5.4: DSC measurement results of each mixing ratio of mannitol and erythritol [81].

mixture falls below the melting points of erythritol and mannitol. This suggests that the melting peak temperature of the mixture dropped below the melting point of the pure substance. This phenomenon is explained as follows. In general, it is reported that the adjustment of the melting point can be achieved by disrupting the crystal arrangement and weakening the intermolecular interactions by adding impurities [88]. From Figure 5.4, it can be seen that the mannitol content of 70 mass% mixture has a melting peak temperature around 150°C aiming for this study. Based on this fact, a mixture of mannitol content of 70 mass% was selected as latent heat storage material. Table 5.2 shows the melting peak temperature and latent heat value of pure substance and 70 mass% mixture measured by DSC apparatus [81].

Table 5.2: DSC measurement values and reference values [81], [93],[94].

Properties		Melting point	Latent heat
Measurement value (Reference value)	Mannitol	168°C (166.5°C)	335 kJ/kg (303.7 kJ/kg)
	Erythritol	119°C (119°C)	337 kJ/kg (340 kJ/kg)
	70mass% mixture	103°C / 151°C	81 kJ/kg / 201 kJ/kg

5.4 Experimental Apparatus

In this study, it was investigated the melting and solidification characteristics of mixtures of mannitol and erythritol (C_m = 70 mass%, C_e = 30 mass%) for latent heat storage at the temperature range (100∼200°C). This waste heat energy can get from the factories. To investigate the melting the solidification characteristics of mannitol and erythritol mixture, the experimental apparatus of Figure 5.5 was used. The experimental apparatus consisted of a heat-storage vessel (test section), high- and low-temperature oil baths (heating capacity: 2 kW) (T301, Thomas Kagaku,16 L, 10∼300°C,0.05°C, Japan), a heat exchanger (plate heat exchanger), a coolant water constant temperature control bath (TBF 230DC; ADVANTEC, 21 L, -20∼ -80 °C: ±0.1 °C, 220 W), (cooling capacity: 4.5 kW), pressure gauges (measuring range: −0.1 to 0.3 Mpa), a digital camera, a pump (MMH21, Sanwa, lift 28 m, -20°C-80°C: ±0.1°C, 90 W to 550 W, Japan), pressure gauges, 2.3 mm K-type thermocouples, a digital balance, and a data logger to collect the measured temperature data. The accuracy of temperature measurement was ±0.2°C.

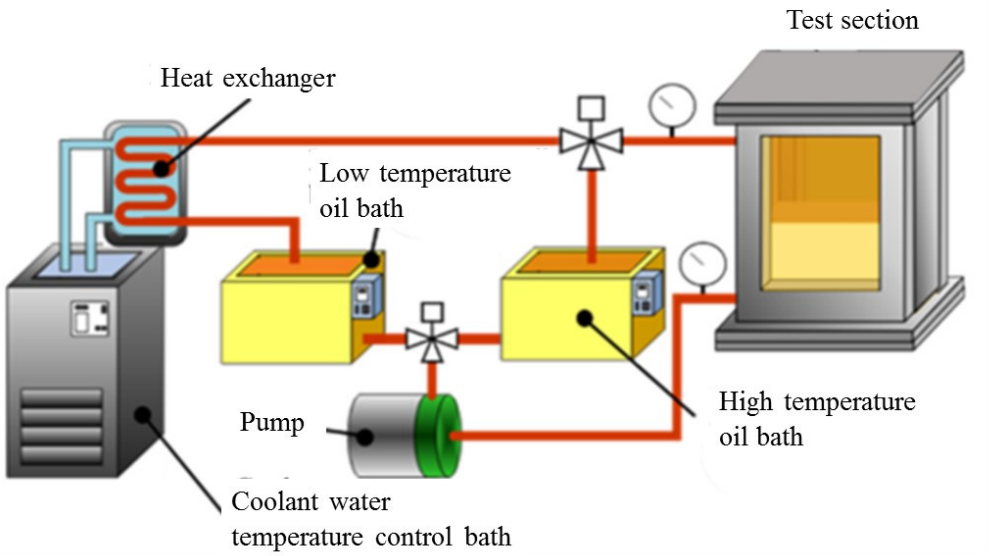

Figure 5.5: Schematic diagram of the experimental apparatus.

The dimensions of the test section were W288 mm x L80 mm x H510 mm and its thickness were 6 mm. Figure 5.6 shows the detail of the test section. The heat-transfer oil flowed

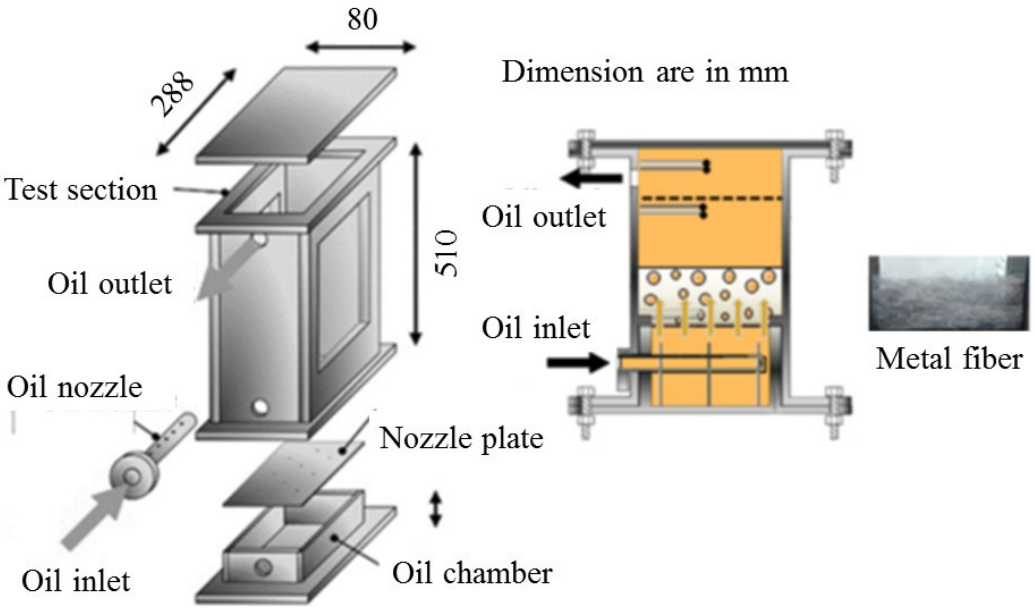

Figure 5.6: Details of the heat storage vessel.

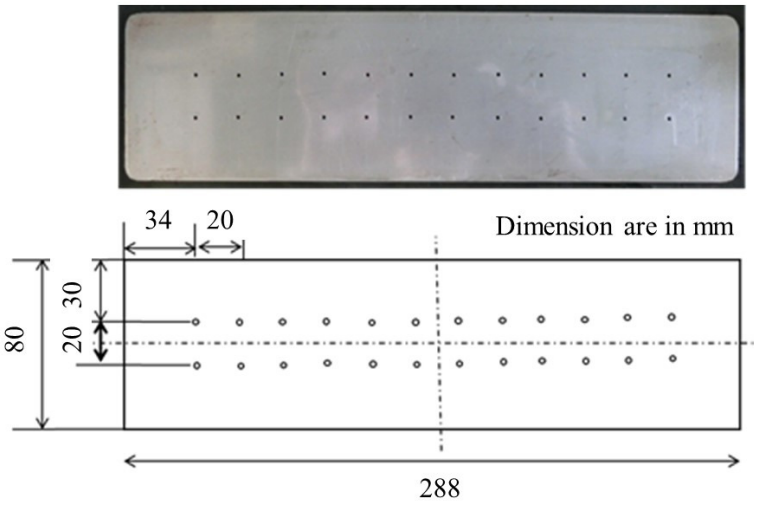

Figure 5.7: Nozzle plate photo and its dimension.

through a nozzle plate at the bottom of the test section and continues upward through the PCM region, where heat was directly exchanged with the PCM. The nozzle plate had 24 holes, each with a diameter of 1.6 mm. By using the nozzle plate, the heat transfer fluid oil can be distributed almost of PCM region inside of heat storage vessel. The nozzle plate and its dimension are shown in Figure 5.7. Pyrex glass wool (thickness of 10 mm) was placed on both sides of the test section to enable photographs to be taken of the PCM under conditions

of melting and solidification. Ten thermocouples were installed in the test section: four at the oil inlet, two in the PCM region, two in the oil region, and two at the outlet. The arrangement of thermocouples is as shown in Figure 5.8. The temperature of inlet oil T_{in} is the average temperature of T1, T2, T3, and T4.

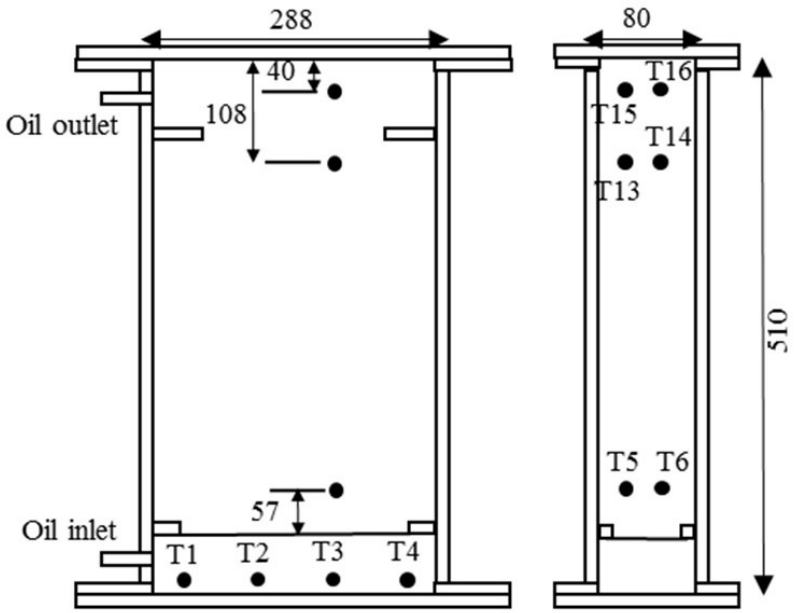

Figure 5.8: The arrangement of thermocouples.

Table 5.3: The properties of heat transfer fluid oil (silicone) [95].

Specific heat (25°C)	0.963
Viscosity (25°C)	100 [mm^2/sec]
Volume expansion coefficient (25°C -250°C)	9.810-4 [1/K]
Flashpoint	325 [°C]
Thermal conductivity	0.16[$W/m.K$]
Specific heat (40°C)	1.55 [kJ/ kg.K]
Specific heat (100°C)	1.63 [kJ/ kg.K]
Specific heat (200°C)	1.76 [kJ/ kg.K]

The temperature of mixture T_{Mix} is the average temperature of T5 and T6. The temperature of outlet oil T_{out} is the average temperature of T15 and T16. The data logger recorded measured temperature data at 15 s intervals. Photographs of melting and solidification of the PCM in the storage vessel were taken using the digital camera. The silicone oil (TSF 458,

manufactured by Momentive) was used as a heat transfer fluid oil. Table 5.3 shows physical property values of heat transfer fluid oil (silicone) [25]. Since the oil bath does not have a cooling function in the solidification process if the return oil from the heat storage vessel, the return oil temperature will be raised and the oil temperature inlet to the heat storage vessel cannot be kept constant. Therefore, before return to the oil bath, the temperature is regulated by exchanging the temperature of the oil and the cooling water by using a heat exchanger. Between the upper cover plate and test section, insert the O-ring seal and a heat-resistant fluorine rubber sheet ($t = 2$ mm) for preventing the oil leakage. When setting the Pyrex glass wool on both sides of the test section, a heat-resistant fluorine rubber sheet also uses for preventing oil leakage and for preventing the cracking of glass by tightening.

5.5 Experimental Method

Before the experiment, the mannitol and erythritol 70 : 30 mass% mixture (weight, 3.0 kg) was inserted in the heat storage vessel. In the initial conditions of the melting process, all the temperatures of the heat storage vessel, the PCM, and the heat transfer fluid oil in the heat storage vessel were maintained at 90°C. To melt the mixture in the test section, silicone oil at 200°C from the high-temperature oil bath was pumped through the inlet of the heat storage vessel. Then, it flowed upward, through the nozzle plate at the bottom of the heat storage vessel and the PCM region, until the temperature of the mixture increased to 190°C. The silicone oil was then returned from the outlet of the heat storage vessel to the high-temperature oil bath.

The solidification process started after completion of melting. First, all the temperatures in the heat storage vessel, mixture, and heat transfer fluid oil in the heat storage vessel were maintained at 190°C. To solidify the mixture, the silicone oil from the low-temperature oil bath at 90°C flowed into the heat storage vessel until the temperature of the mixture decreased to 95°C. The oil that exited from the outlet port of heat storage vessel passed through the heat exchanger. In the heat exchanger, the heat of the oil was exchanged with water from the temperature controlled bath.

In both the melting and solidification processes, oil flowed at a constant mass flow rate. The flow rate of the oil (f_{oil}) was measured with the digital weighing machine. These two processes were repeated at different oil flow rates: 1.0, 1.5, and 2.0 kg/min. Temperature changes during the experiment were recorded with the data logger and the melting and solidification behavior of the latent heat storage mixture were recorded with the digital camera.

5.6 Method of Arranging Experimental Data

In the melting and solidification processes, the amount of heat stored and heat released are as following Equation 5.1 and Equation 5.2.

$$Q_M = \int_{t_b}^{t_e} f_{oil}.C_{P_{oil}} \, (T_{in} - T_{out})dt \tag{5.1}$$

$$Q_S = \int_{t_b}^{t_e} f_{oil}.C_{P_{oil}} \, (T_{out} - T_{in})dt \tag{5.2}$$

Where Q_M is the amount of heat stored (kJ), Q_S is the amount of heat released (kJ), t_b, t_e is the beginning and ending time of experiment (min), f_{oil} is the flow rate of the heat transfer oil (kg/min), C_{Poil} is the specific heat of the heat transfer oil (kJ/kg K), T_{in}; oil inlet temperature, T_{out}; oil outlet temperature (°C).

$$Q_{PCM} = m_{pcm} C_{Pl} \, (T_b - T_m) + L \; m_{pcm} + m_{pcm} \; C_{Ps} \, (T_m - T_e) \tag{5.3}$$

$$Q_{oil} = m_{oil} C_{Poil} \, (T_b - T_e) \tag{5.4}$$

$$Q_{ts} = m_{ts} C_{Pts} \, (T_b - T_e) \tag{5.5}$$

$$Q_{th} = m_{PCM} + Q_{oil} + Q_{ts} \tag{5.6}$$

Where Q_{PCM} is the amount of sensible heat and the amount of latent heat in the PCM (kJ). Q_{oil} is the amount of sensible heat of oil (kJ). Q_{ts} is the amount of sensible heat of test section material (kJ). m_{pcm} is the mass of PCM (kg), $C_{Pl}$is the specific heft of liquid PCM (kJ/kgK), T_b, T_e is the temperature at the begin and end of the experiment (°C), T_m is the melting Temperature of PCM (°C), L is the latent heat of PCM (kJ/kg), C_{Ps} is the specific heat of solid PCM (kJ/kgK), m_{oil} is the mass of oil inside of the heat storage vessel (kg), m_{ts} is the mass of the construction material of heat storage vessel(kg), C_{Pts} is the specific heat of the construction material of heat storage vessel (kJ/kgK).

For calculating the theoretical amount of heat during the solidification process, the temperatures of heat transfer oil at the begin and end of the experiment were 190°C and 95°C respectively. During the melting process, the temperatures of heat transfer oil at the begin and end of the experiment were 90°C and 190°C of oil respectively.

The physical properties used in the empirical formulas described above are oil specific heats C_{Poil} = 1.65, 1.63 [kJ/(kgK)] at melting and solidification, mass m_{ts} = 23.6 [kg] at the test part (stainless steel) The specific heat of stainless steel C_{Pts} = 0.500 [kJ / (kg K)], the heat storage material mass m_{pcm} =3.0 [kg], the latent heat amounts L of the mannitol, erythritol, and 70 mass% mixture L = 303,81, 337, and 201 [kJ/kg] were used. The specific heat of erythritol and mannitol is solid phase: C_{Pl} = 2.85, 2.80 [kJ/(kgK)], liquid phase: (C_{Ps} = 1.62, 1.39 [kJ/(kgK)]).

The ratio of heat stored and released is calculated by the Equation 5.7 and Equation 5.8 by dividing the heat stored and release Q_M, Q_S of the theoretical stored and release heat Q_{th}.

$$\phi_M = \frac{Q_M}{Q_{th}} \tag{5.7}$$

$$\phi_S = \frac{Q_s}{Q_{th}} \tag{5.8}$$

And also, the rate of heat storage and release, P_M and P_S are defined as by dividing the experimental values Q_M and Q_S of the time interval δt [sec] of each experiment.

$$P_M = \frac{Q_M}{\delta t} \tag{5.9}$$

$$P_S = \frac{Q_S}{\delta t} \tag{5.10}$$

The average heat transfer rate can be calculated by dividing the total amount of heat stored and released by the experiment finishing time as follow:

$$P_{M-AVG} = \frac{Q_{TM}}{t_f} \tag{5.11}$$

$$P_{S-AVG} = \frac{Q_{TS}}{t_f} \tag{5.12}$$

5.7 Solidification Behaviors of 70mass% Mixture

The solidification process of 70 mass% mixture was carried out using direct contact latent heat storage tank. The experimental conditions are shown as follow: Latent heat storage material: 70 mass% mixture , Filling amount: 3 kg , Inflow oil temperature: T_{in} = 90°C , Initial temperature: T_b = 190°C , Oil flow rate: f_{oil} = 1.0, 1.5, 2.0 kg/min

Figure 5.9 shows the temperature histories without any insertion of perforated partition plate(lattice) and metal fibers at an oil flow rate of 1.0 kg/min. It indicates the temperatures of the PCM mixture (T_{Mix}), the inlet oil (T_{in}), and the outlet oil (T_{out}) from the heat storage vessel during the solidification process. Average temperatures of the PCM and inlet and outlet temperatures of the oil in the heat storage vessel were measured by installing thermocouples in each part and the temperature histories were recorded with the data logger.

The temperature histories of the mixture showed that the temperature declined from 0 to 10 min with the sensible heat release. The temperature of the mixture in the latent heat part was 150 °C. The solidification process ended at 70 min.

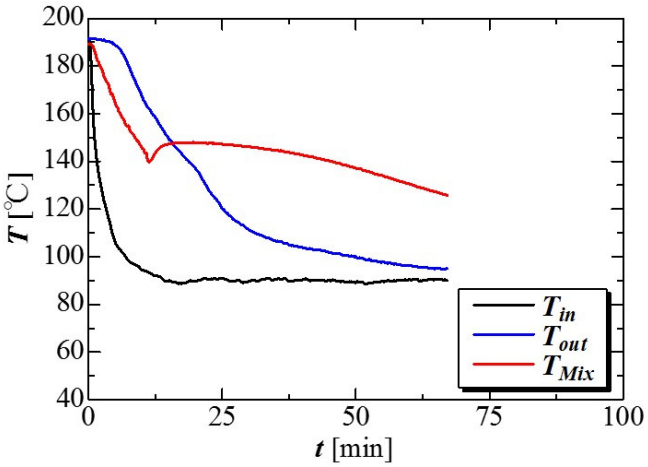

Figure 5.9: Temperature histories of solidification at 1.0 kg/min flow rate.

Figure 5.10 shows visual observation of solidification process at 1.0 kg/min of oil flow rate. The solidification behavior without any inserting of the perforated partition plate and metal fiber was as follow: At the start of the experiment, the liquid of the 70% mannitol mixture in the heat storage vessel at a height of 80 mm. After oil flowed through the nozzle plate, oil droplets became coated by the solidifying PCM as a layer around the oil droplet, and they flowed up to the interface between the PCM and oil. At the interface between the PCM and oil, the oil droplets and the solidified PCM were separated by the density difference between the oil and PCM. At this time, the solidified PCM formed a porous zone, and the solidification height of the PCM increased with time. Furthermore, since the initial solidified layer hinders the flow of the oil, and the new solidified porous layer was deposited under the initial solidified layer, and the porous solidified layer became thicker. It can be confirmed that it is densely solidified in the lower part of the heat storage vessel.

With time, the amount of solidified PCM increased from the interface to the base of the test section, during which it formed a porous zone and the solidification height increased. The solidified porous layer very quickly appeared between 9 min to 15 min. It was also found the latent heat process at the temperature histories of Figure 5.9. Figure 5.11 shows the

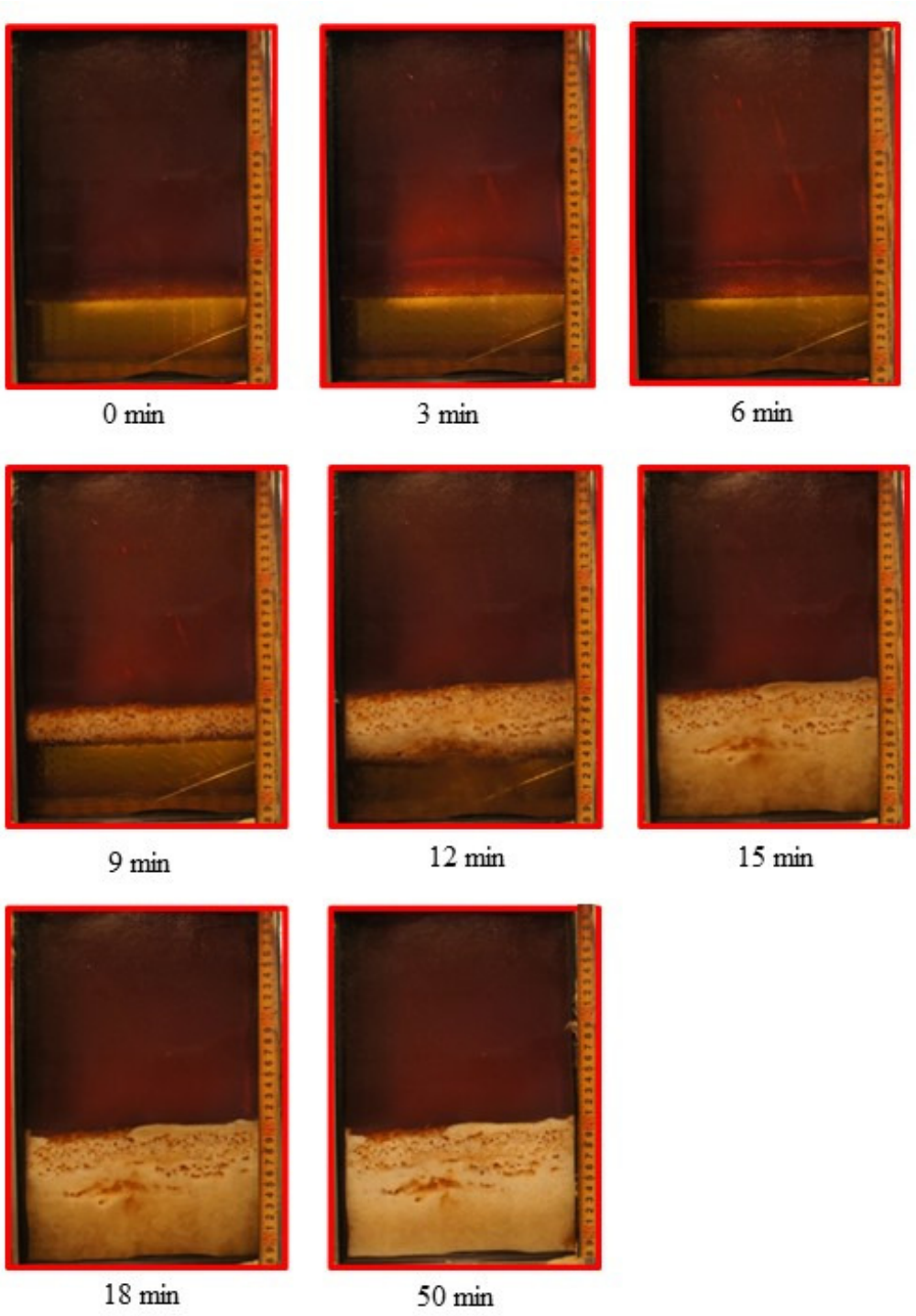

Figure 5.10: Visual observation of solidification process at the flow rate of 1.0 kg/min.

temperature histories of solidification process of 70% mass mixture at the three-different oil flow rate of 1.0,1.5, 2.0 kg/min. As shown in Figure 5.11, the experimental time shortened due to the increase in the oil flow rate.

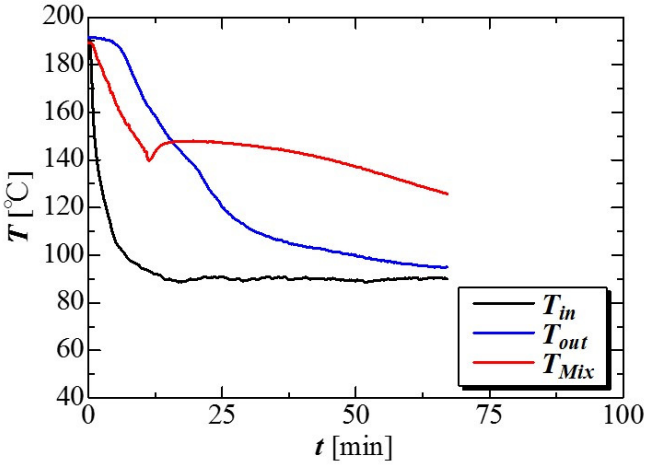

(a) At 1.0 kg/min of oil flow rate

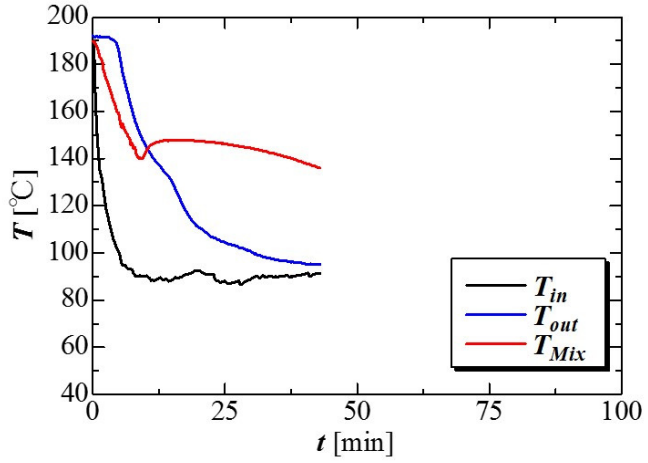

(b) At 1.5 kg/min of oil flow rate

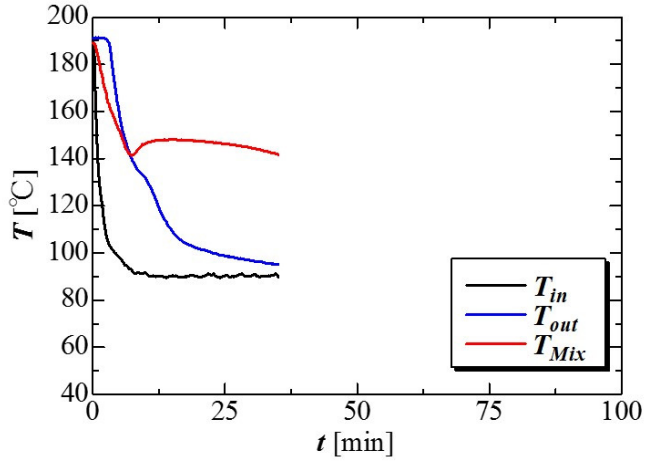

(c) At 2.0 kg/min of oil flow rate

Figure 5.11: Temperature histories with three different oil flow rates.

Figure 5.12 shows the comparison of visual observation of solidification process with three different of oil flow rate 1.0, 1.5, and 2.0 kg/min. From these photographs, the solidified heights of PCM were 120 mm, 190 mm, and 270 mm for these oil flow rates, respectively. By increasing the oil flow rate, solidified PCM at the interface flowed up with the oil from the inlet, the porous area increased, and the solidified height increased. At high oil flow rates, solidified PCM flowed out of the test section with the oil.

Figure 5.13 shows the amount of heat released at oil flow rates of 1.0, 1.5, and 2.0 kg/min, without any inserting such as the perforated partition plate and metal fibers. It is seen that If the flow rate of oil increased, the finishing time of experiment was shortened. The theoretical amount of heat released of the 70 mass% mixture is 3626 kJ, which is shown by the broken line in Figure 5.13. It is about 89% or more when calculating the heat release rate from Equation 5.8. Therefore, in this experiment the latent heat storage system has less of heat loss and this system is effective for heat transfer process. Figure 5.14 shows the rate of heat stored at the three different of oil flow rates. At the start of the experiment, the temperature difference of the inlet oil and the PCM mixture is large, so that the speed of heat transfer is very fast at the start of the experiment. After that, in this Figure 5.14 the change in heat storage rate becomes gentle. This state is phase change process.

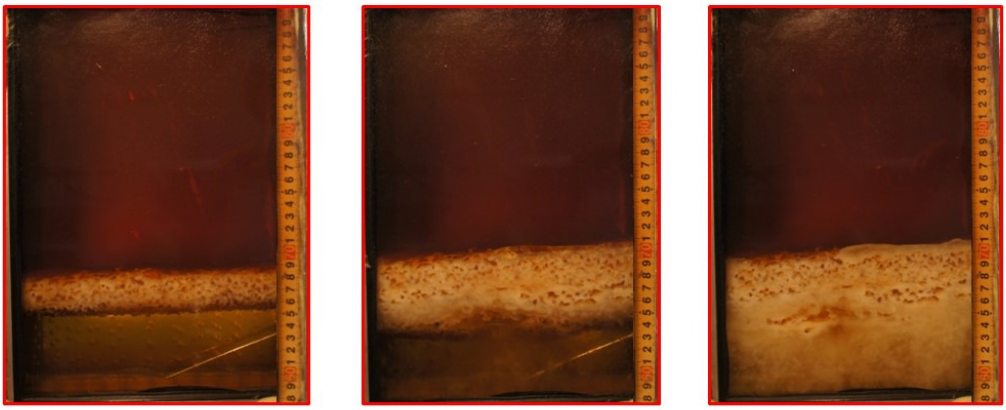

9 min 12 min 15 min

(a) At 1.0 kg/min of oil flow rate

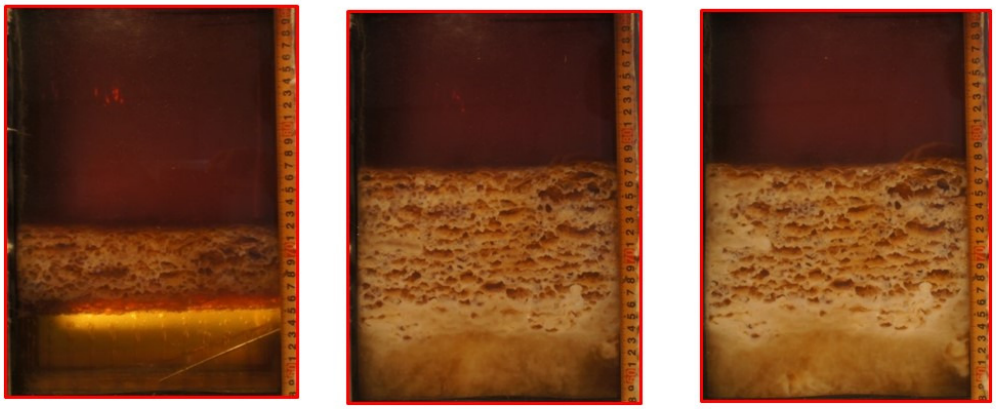

6 min 12 min 15 min

(b) At 1.5 kg/min of oil flow rate

6 min 12 min 15 min

(c) At 2.0 kg/min of oil flow rate

Figure 5.12: Comparison of visual observation of solidification process with three different oil flow rates.

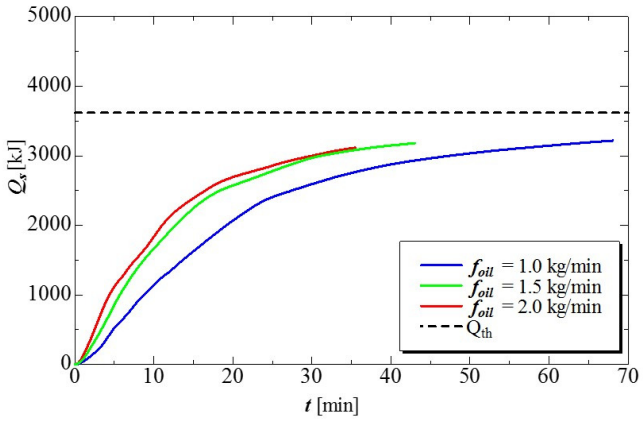

Figure 5.13: The amount of heat released during the solidification process with three different oil flow rates.

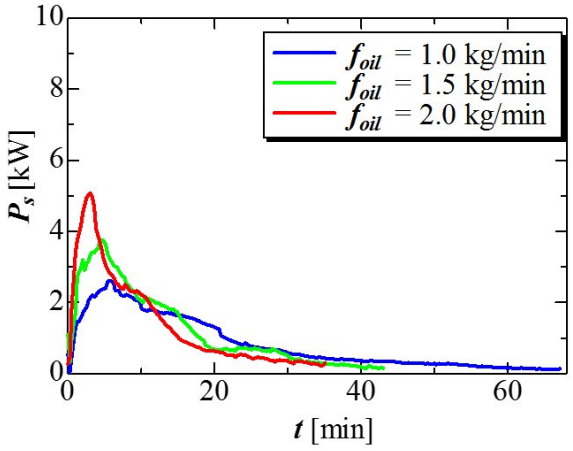

Figure 5.14: The rate of heat released at the three different of oil flow rates.

5.8 Melting Behaviors of 70 mass% Mixture

In this section, the melting behavior of 70mass% mixture was observed and compared the melting characteristic with the three different types of oil flow rate 1.0, 1.5, and 2.0 kg/min. The experimental conditions are as follows; Latent heat storage material: Mannitol: Erythritol 70 : 30 mass% mixture, Filling amount: 3 kg , Inflow oil temperature: T_{in} = 200°C, Initial temperature of PCM: T_b = 90°C, Oil flow rate: f_{oil} = 1.0, 1.5, 2.0 kg/min,

Figure 5.15 shows the temperature histories of the PCM without any insertion of the perforated partition plate and metal fiber in the heat storage vessel with an oil flow rate 1.0 kg/min. It indicates the temperatures of the PCM mixture (T_{Mix}), the inlet oil (T_{in}), and

the outlet oil (T_{out}) from the heat storage vessel in the melting process. Average temperatures of the PCM and inlet and outlet temperatures of the oil were measured by installing thermocouples in each part and the temperature histories were recorded with the data logger. Before starting the melting process, the temperature of the inlet, outlet, PCM and heat storage vessel were maintained at 90°C. To melt the mixture in the test section, silicone oil at 200°C from the high-temperature oil bath was pumped through the inlet of the heat storage vessel.

At the start of the melting process, the temperature of the inlet oil is changed immediately from 90°C to 200°C. Because of this reason, the temperature lines of inlet and outlet oil increased sharply at the start of melting process. The melting process was done at 70 min. As shown in Figure 5.15, the temperature change at this time is not clearly seen and very gentle around 150°C, which is the melting peak on the high-temperature side, it is considered that melting is progressing. In addition, a period where the temperature changed of the heat storage material becomes gentle can be confirmed about 100°C. which is the melting peak on the low-temperature side, but it did not appear of melting in Figure 5.15. It is thought that this was not observed from the visualized surface of the solidified layer adhered to the glass surface because the nozzle hole was placed in the center of the heat storage tank and melted from the inner side around the flow path of the oil. After 40 min,it is able to observe the melting of the heat storage material in the test section. The melting process has finished when the outlet temperature of the oil reaches to 195°C.

Figure 5.16 shows the melting behavior of the latent heat storage mixture PCM with an oil flow rate of 1.0 kg/min. After finishing the solidification process, it is found that the PCM solidified porous layer at the upper portion and dense layer at the lower portion. During the melting process, oil flows through the formed paths from the porous zone of the solidified PCM. The PCM starts to melt from the upper part of the solidified PCM. After that, the amount of melting PCM increases with time from top to bottom in the heat storage vessel. The porous solidified layer has a large surface area per unit volume and is easy to heat exchange from oil even though the oil was flow from the bottom of heat storage vessel.

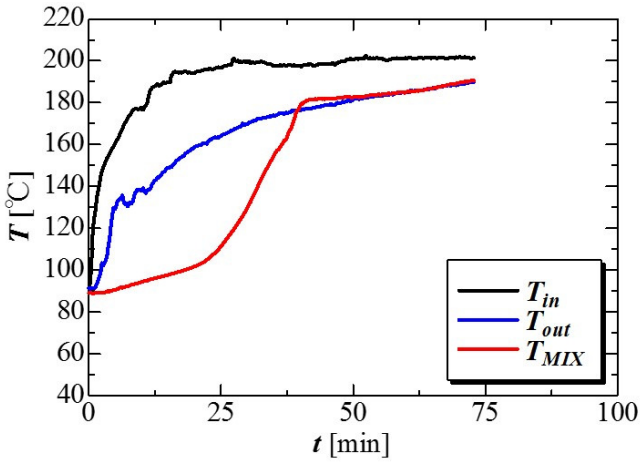

Figure 5.15: Temperature histories of melting process at 1.0 kg/min of oil flow rate.

As shown in Figure 5.16, it can be observed that melting started from a porous layer having a large heat transfer area like a photograph of 40 min.

Figure 5.17 shows the temperature histories of 70mass% mannitol heat storage mixture without any inserting of perforated partition plate and metal fiber at the three different oil flow rates of 1.0, 1.5, and 2.0 kg/min. As shown in Figure 5.13, the experimental time shortened due to the increase in the oil flow rate, because the flow rate passing through the liquid phase of the heat storage material is increased due to the increase in the flow rate. The finish time of experiment is shortened by increasing the flow rate of oil. Figure 5.18 shows the comparison of visual observation of melting process with three different of oil flow rates 1.0, 1.5, and 2.0 kg/min. As the rate of oil flow increases, the speed of melting process is also increased. In all type of oil flow rates, the PCM melts from the upper solidified porous area and there was no big difference in behavior of melting a dense solidified layer after melting from a porous layer with a large heat transfer area.

Figure 5.19 shows the amount of heat stored in the melting process with three different types of oil flow rates 1.0, 1.5, and 2.0 kg/min. The broken line in this figure is 3757 kJ which is the theoretical heat storage amount of the 70 mass% mixture. Most of the oil flow rate can store the amount of heat 83% or more of the theoretical amount of heat. Figure 5.20 shows the rate of heat released at the three different of oil flow rates. At any flow rates of oil, the speed of heat storage increases quickly at the start of the experiment because of the

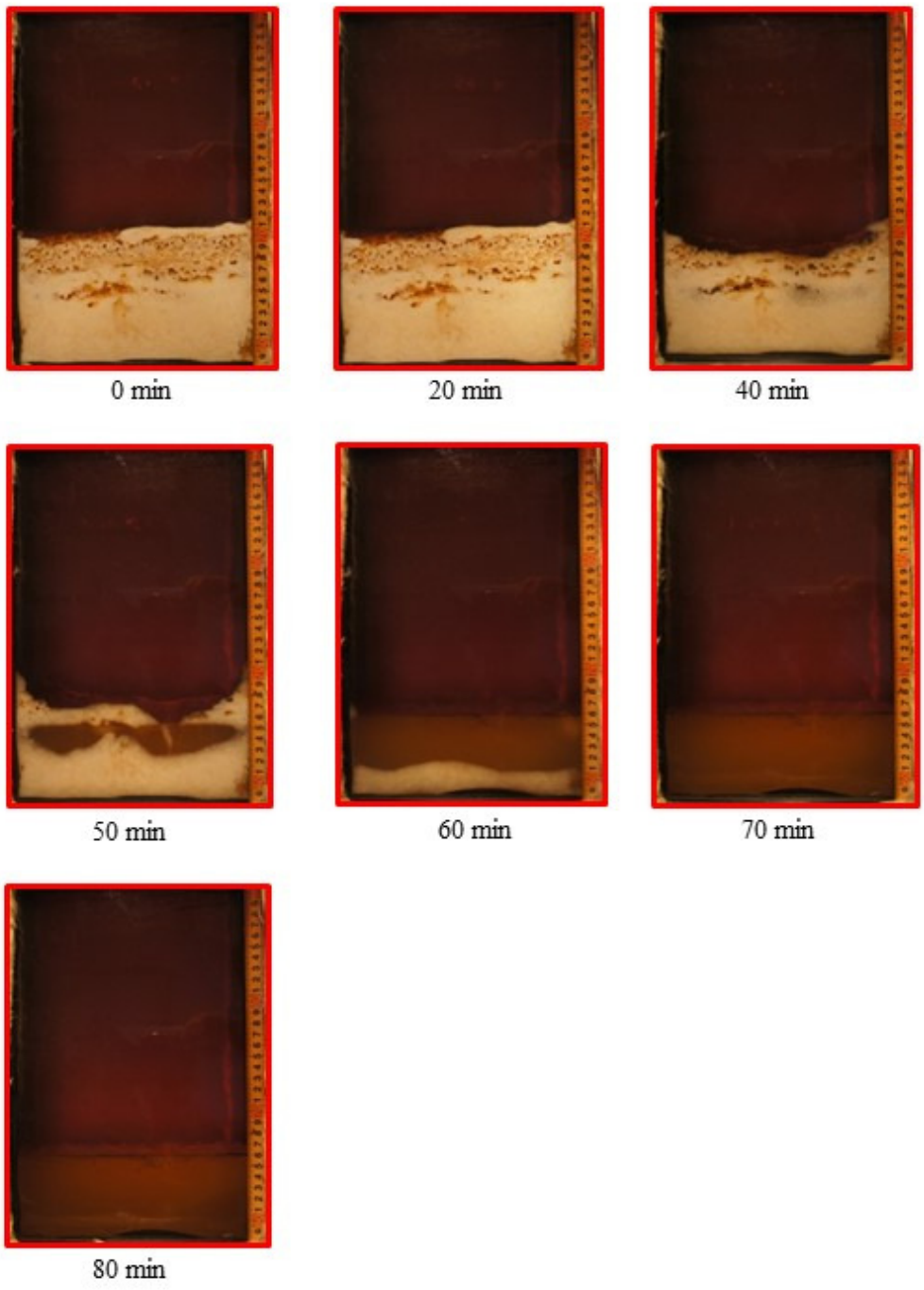

Figure 5.16: Visual observation of melting process at 1.0 kg/min oil flow rate.

large difference between the temperatures of inlet oil and PCM mixture temperature. The speed also increases as the flow rate of oil increase, it will shorten the experimental time.

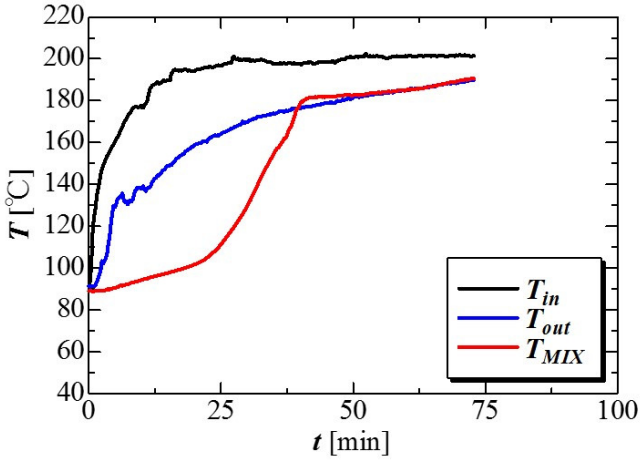

(a) At 1.0 kg/min of oil flow rate

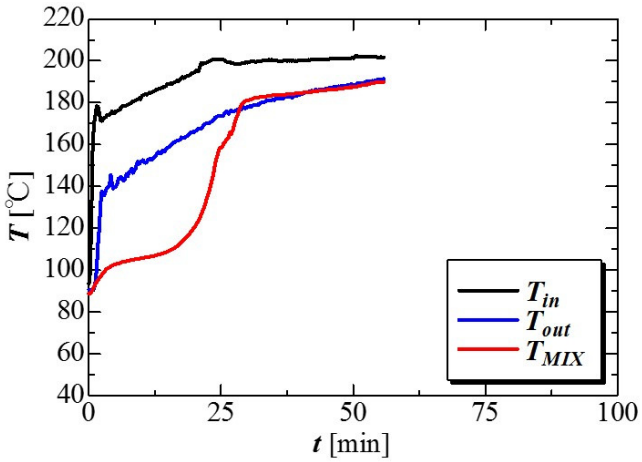

(b) At 1.5 kg/min of oil flow rate

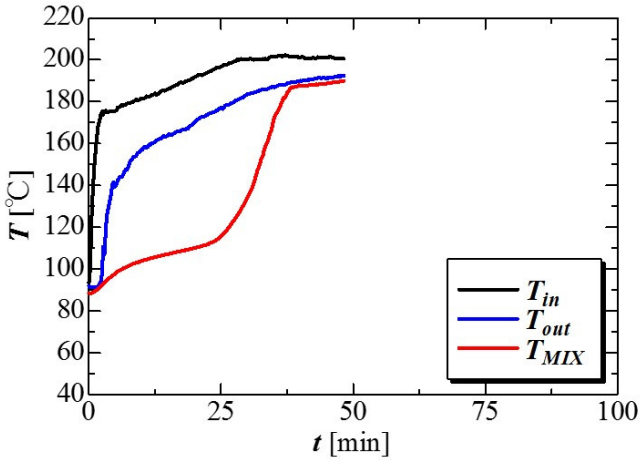

(c) At 2.0 kg/min of oil flow rate

Figure 5.17: Temperature histories of melting process at the three different oil flow rates.

(a) At the flow rate of 1.0 kg/min

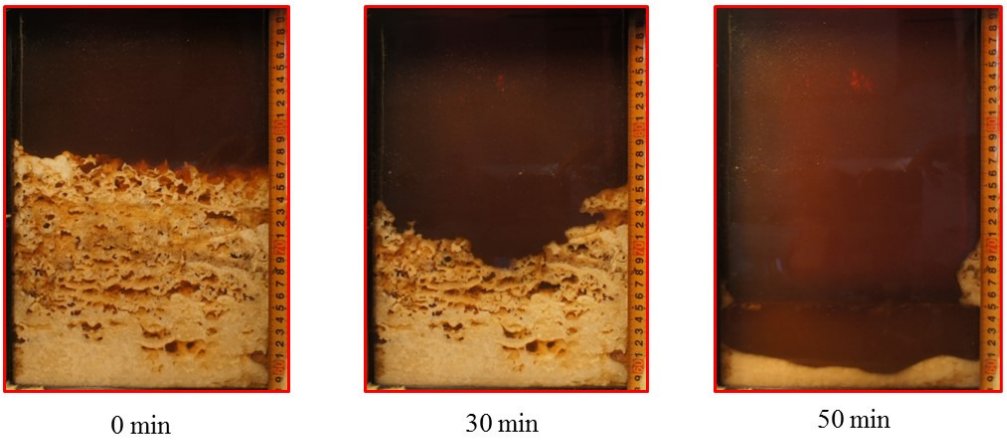

(b) At the flow rate of 1.5 kg/min

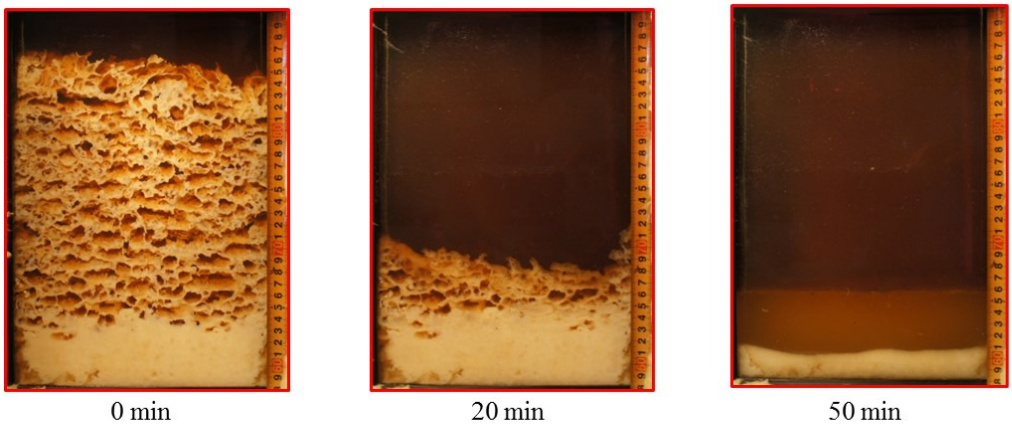

(c) At the flow rate of 2.0 kg/min

Figure 5.18: Comparison of visual observation of melting process with three different of oil flow rate.

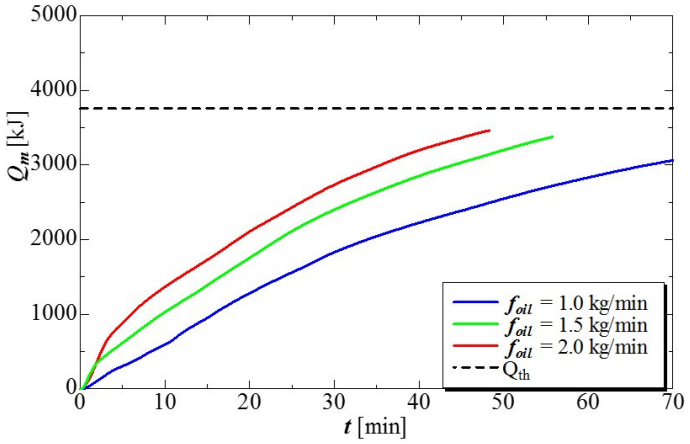

Figure 5.19: The amount of heat stored in the melting process with three different types of oil flow rates.

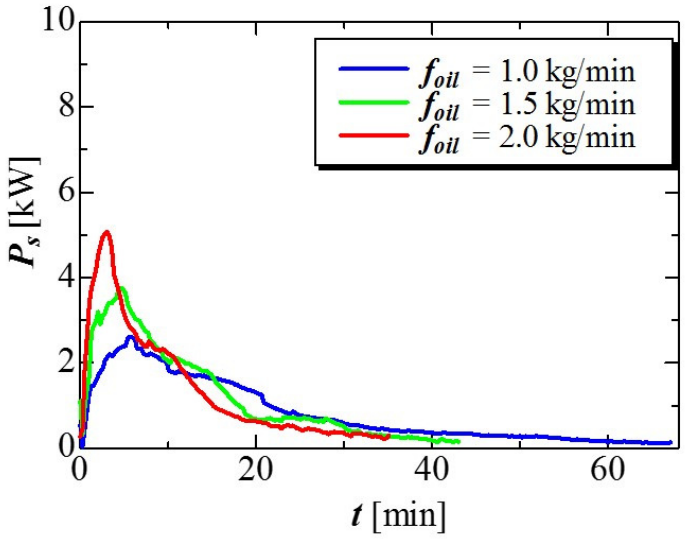

Figure 5.20: The rate of heat released at the three different of oil flow rates.

5.9 Methods of the Reduction of the Solidification Height of Mixture

5.9.1 Using the Perforated Partition Plate

As shown in the previous section, by increasing the oil flow rate, solidified PCM at the interface flowed up with the oil from the inlet, the porous area increased, and the solidified height increased. At high oil flow rates, solidified PCM flowed out of the test section with the oil. To prevent this, it will be shown the various methods of preventing in this chapter. In this section, the aluminum perforated partition plate(lattice) was inserted inside the heat storage vessel. Figure 5.21 shows the aluminum perforated partition plate (lattice). There is 8 rooms and each room has 3 holes of the nozzle plate. Each room has the dimension of 20×60×200 mm. The width of this is 250 mm. The arrangement of perforated holes and each dimension are shown in Figure 5.21(b).

Figure 5.22 shows the temperature histories of PCM with perforated partition plate at the oil flow rate of 1.0 kg/min. In this figure, shows the temperature histories of inlet oil, out oil, and PCM that are recorded by the thermocouples. The temperature rises at about 150°C, which is near the melting peak, and the rapid solidification occurs. The behaviors of temperature histories are nearly same with and without perforated partition plate.Figure 5.23 shows the solidification behaviors of PCM with and without the perforated partition plate at the oil flow rate of 1.0 kg/min. It is understood that a porous layer is formed at the interface between the oil layer and the liquid phase of the heat storage material at 9 min regardless of the presence or absence of the aluminum lattice. After that, from the visualized photographs of 12 min and 15 min, no change due to the aluminum lattice could be observed even in the behavior of forming a dense solidified layer under the porous layer.

Figure 5.24 shows the comparison of solidification behaviors with and without perforated partition plate at three different types of oil flow rates. It can be seen that the effect of suppression of the rise in solidified surface height increases as the oil flow rate increases.

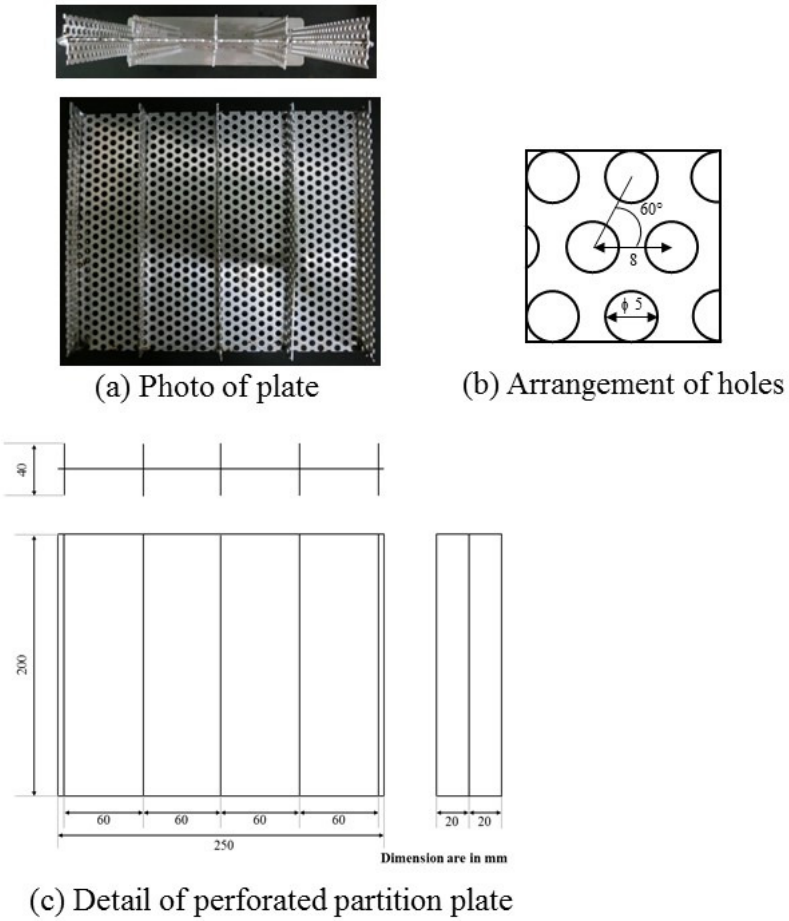

Figure 5.21: Details of perforated partition plate.

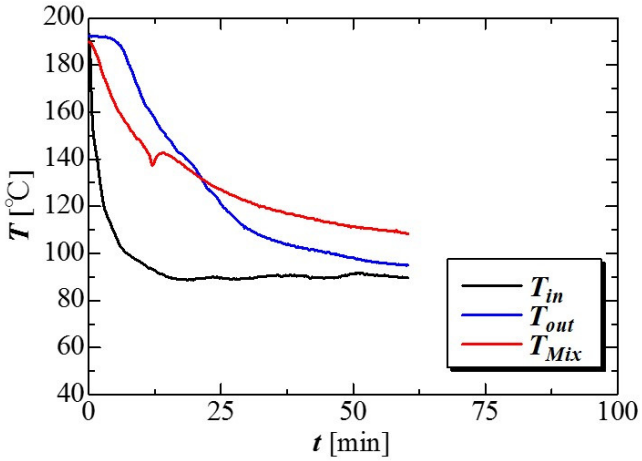

Figure 5.22: Temperature histories of PCM with perforated partition plate at the oil flow rate of 1.0 kg/min.

When the aluminum perforated partition plate is not inserted, the higher the oil flow rate generates, the higher the solidification height, but it became almost the same level by in-

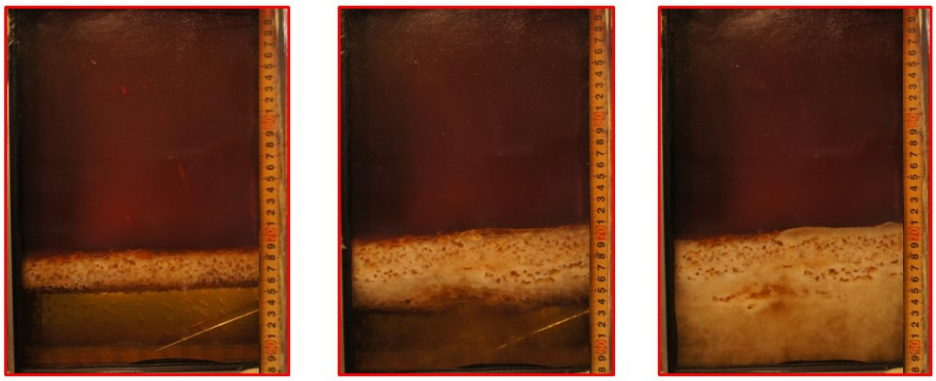

9 min 12 min 15 min

(a) Without perforated partition plate

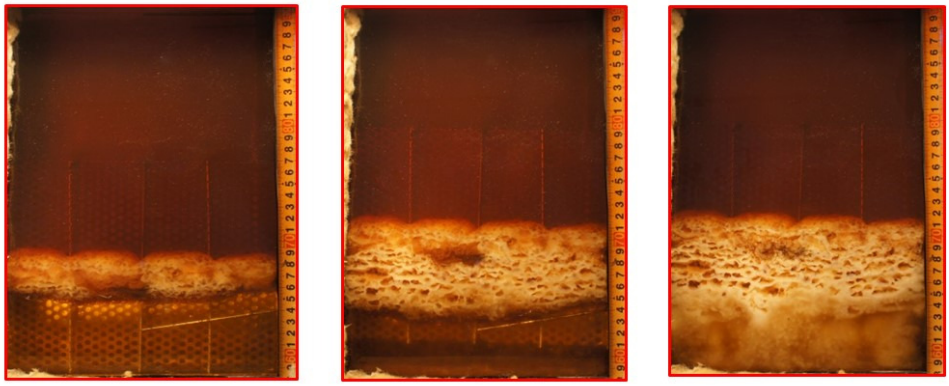

9 min 12 min 15 min

(b) With perforated partition plate

Figure 5.23: Solidification behaviors of PCM with and without the perforated partition plate at the oil flow rate of 1.0 kg/min.

serting the plate. Solidification process started from the interface of the liquid PCM and oil and it proceeded to the bottom of the heat storage vessel both conditions of the with and without perforated partition plate. By using the perforated partition plate, PCM coated oil droplets float on the interface between the oil and PCM, and these oil droplets are pushed next to the other floating oil droplets because of continuous flowing of oil from the bottom of heat storage vessel. And then, the pushed oil droplets will collide to the surface of the perforated partition plate and it will be broken. Because of this mechanism, it could prevent to increase the solidified height of the PCM.

Figure 5.25 shows the comparison of the amount of heat released with and without perforated partition plate at the three types of oil flow rates 1.0, 1.5, and 2.0 kg/min. Even when the aluminum lattice is inserted, the change in the amount of heat released shows

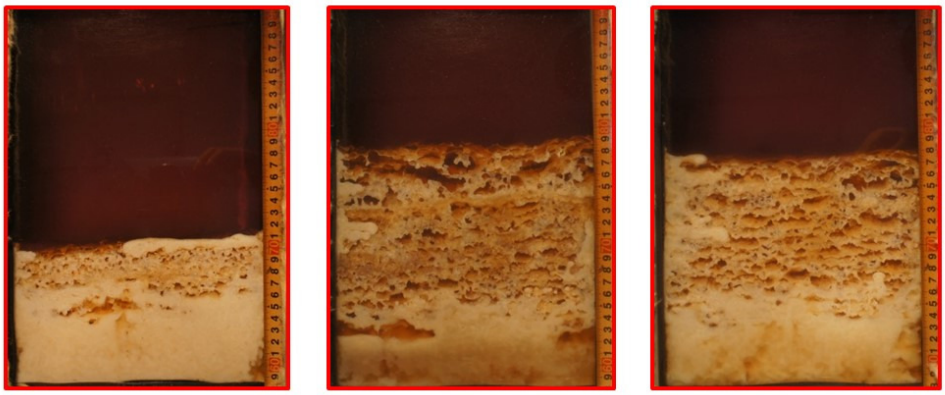

f_{oil}=1.0 kg/min f_{oil}=1.5 kg/min f_{oil}=2.0 kg/min

(a) Without perforated partition plate

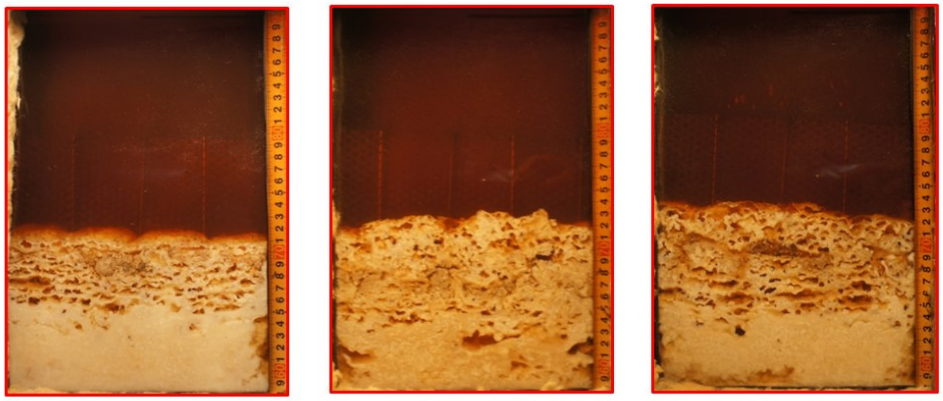

f_{oil}=1.0 kg/min f_{oil}=1.5 kg/min f_{oil}=2.0 kg/min

(b) With perforated partition plate

Figure 5.24: Comparison of solidification behaviors with and without perforated partition plate at three different types of oil flow rates.

almost the same tendency, and the total amount of heat and the experiment finishing time have the same value.

Figure 5.26 shows the comparison of the speed of heat released with and without perforated partition plate at the three types of oil flow rates. The speed of heat released with and without perforated partition plate also almost nearly same. Based on the above results, it is found that the influence on the heat released by the aluminum lattice is small in the 70 mass% mixture, and since it has the effect of suppression the height of the solidified surface, it is considered to be effective as a method of suppression the solidification surface height.

Figure 5.27 shows melting behaviors of PCM with the perforated partition plate at the three types of oil flow rates. The PCM melts from the upper porous part of the solidified PCM

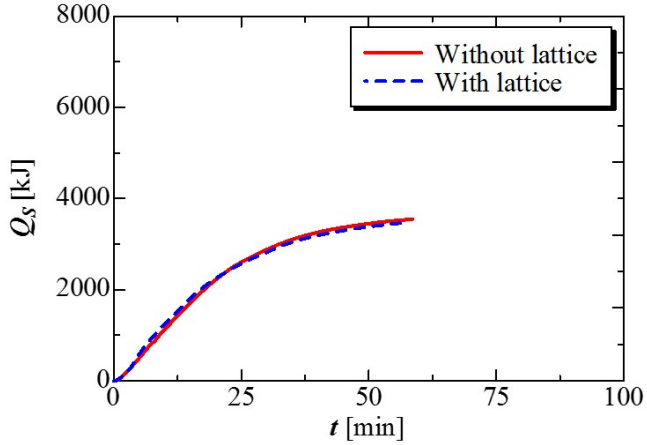

(a) f_{oil} = 1.0 kg/min

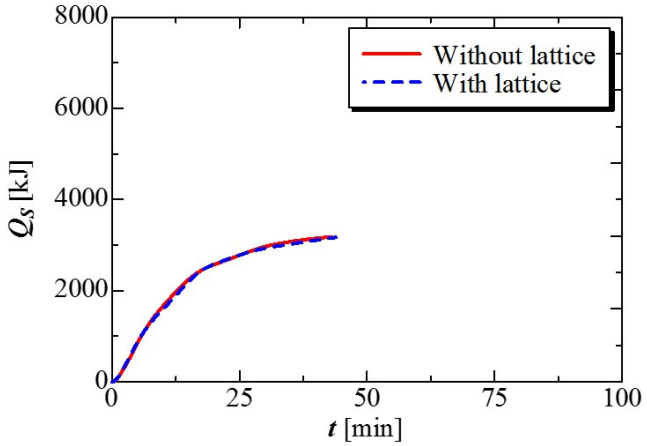

(b) f_{oil} = 1.5 kg/min

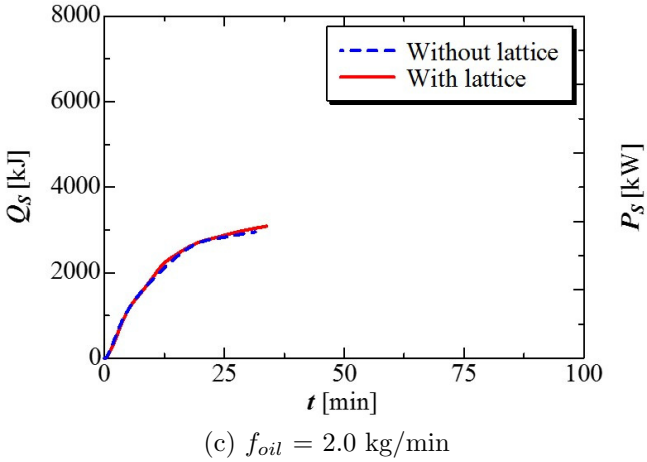

(c) f_{oil} = 2.0 kg/min

Figure 5.25: Comparison of the amount of heat released with and without perforated partition plate at the three types of oil flow rates.

as without perforated partition lattice. With the perforated partition plate, the starting time of the melting process is fast and the melting process finishing time is shortened as the flow

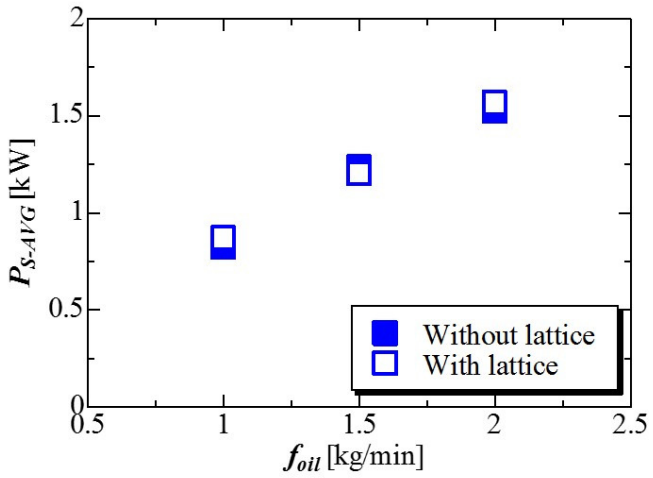

Figure 5.26: Comparison of the speed of heat released with and without perforated partition plate.

rate of oil increases.

Figure 5.28 shows the comparison of the amount of heat stored with and without perforated partition plate at the three types of oil flow rates. It shows the same tendency even when aluminum perforated partition plate is inserted. Figure 5.29 shows the comparison of the rate of heat stored with and without perforated partition plate at the three types of oil flow rates,and the average heat storage rate of all conditions are nearly same. From this, it is considered that the influence on the melting behavior and heat storage performance due to the insertion of the aluminum perforated partition plate in the 70 mass% mixture are small except the solidification height of PCM after the solidification process.

5.9.2 Using the Metal Fiber

5.9.2.1 Using the Metal Fiber diameter 0.4 mm

In this section, aluminum metal fibers are used to prevent the increase of the solidified height problem. At previous section, aluminum perforated partition plate was used. But it cannot distribute all PCM region to break the PCM coated oil droplets. If aluminum metal fibers are used, it can easily distribute all PCM region and it may break the PCM coated oil droplets. As a result, it may more efficient than perforated partition plate. Figure 5.30

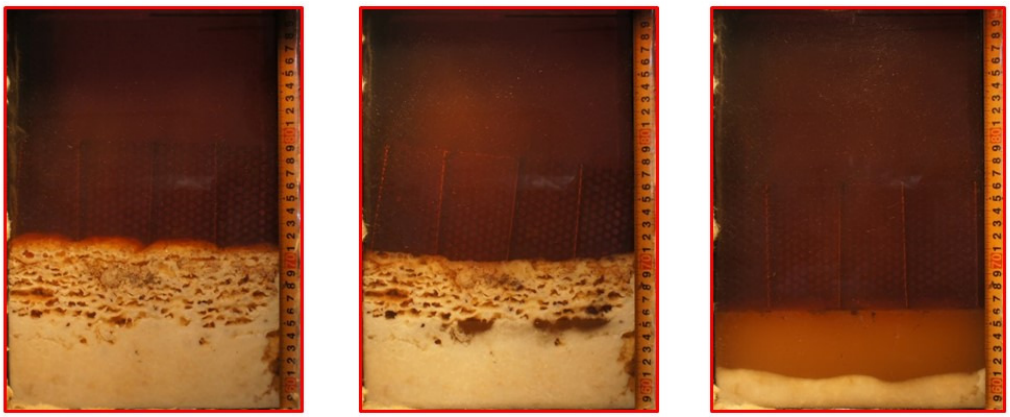

0 min 40 min 60 min

(a) f_{oil} = 1.0 kg/min

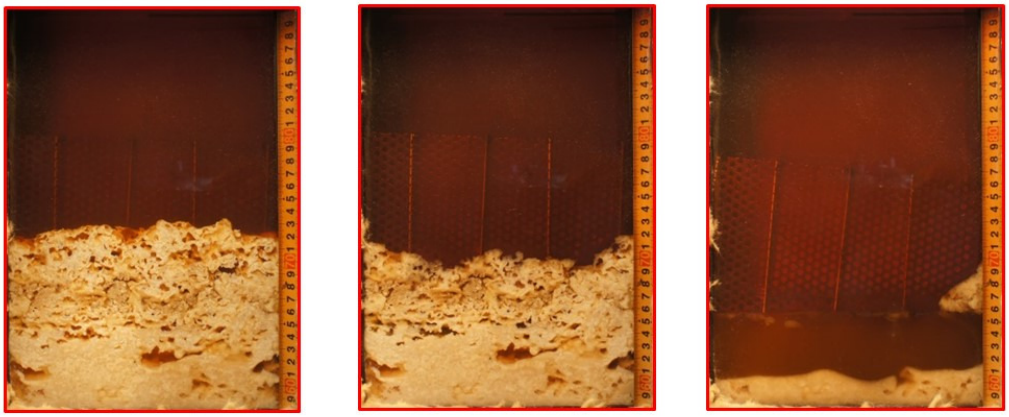

0 min 30 min 50 min

(b) f_{oil} = 1.5 kg/min

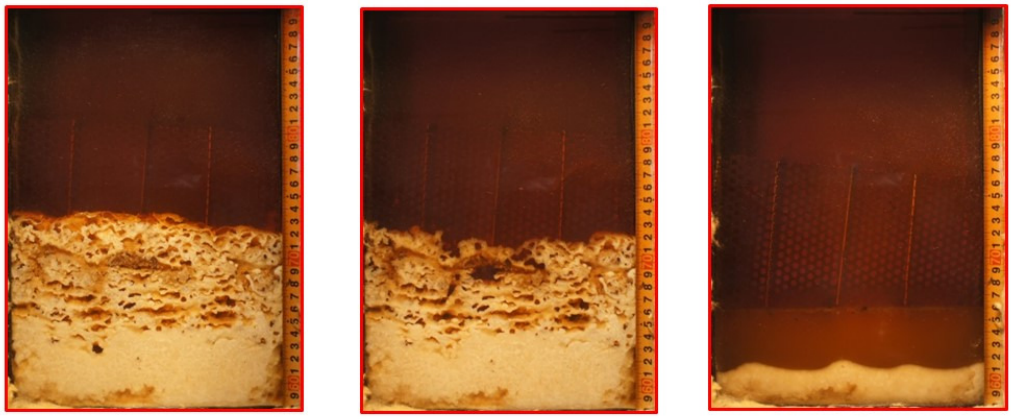

0 min 20 min 40 min

(c) f_{oil} = 2.0 kg/min

Figure 5.27: Melting behaviors of PCM with the perforated partition plate at the three types of oil flow rates.

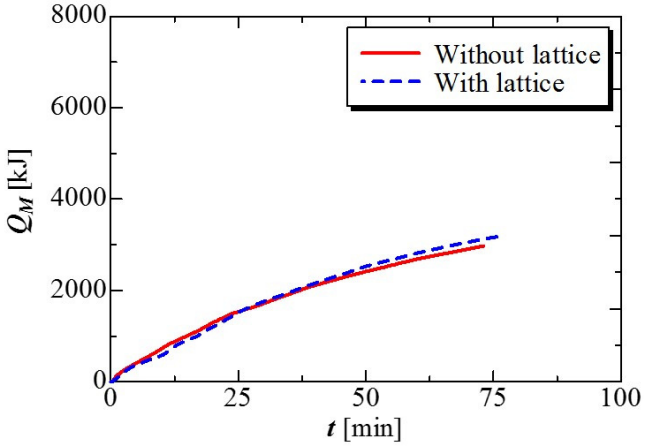

(a) f_{oil} = 1.0 kg/min

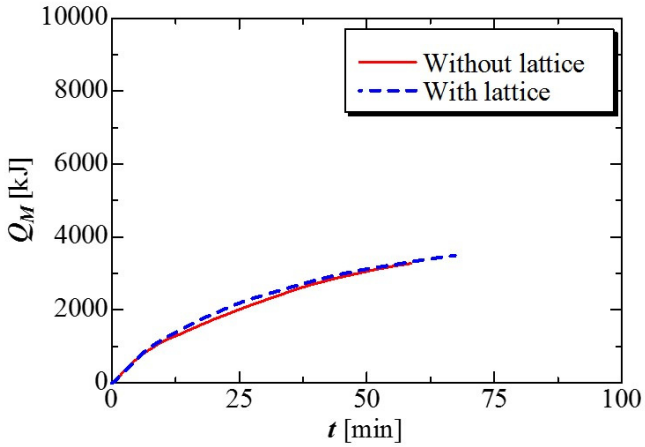

(b) f_{oil} = 1.5 kg/min

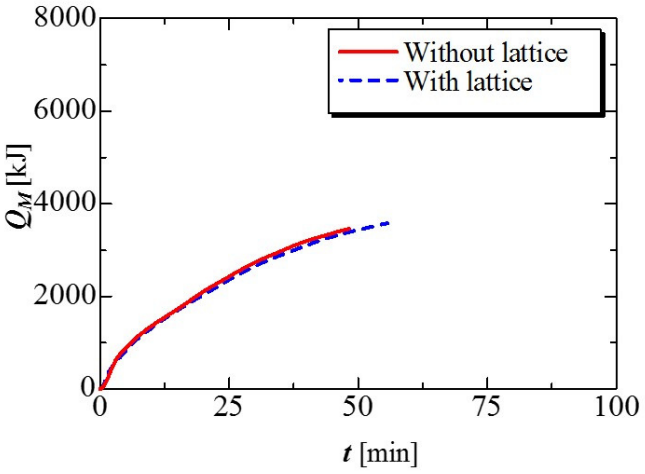

(c) f_{oil} = 2.0 kg/min

Figure 5.28: Comparison of the amount of heat stored with and without perforated partition plate at the three types of oil flow rates.

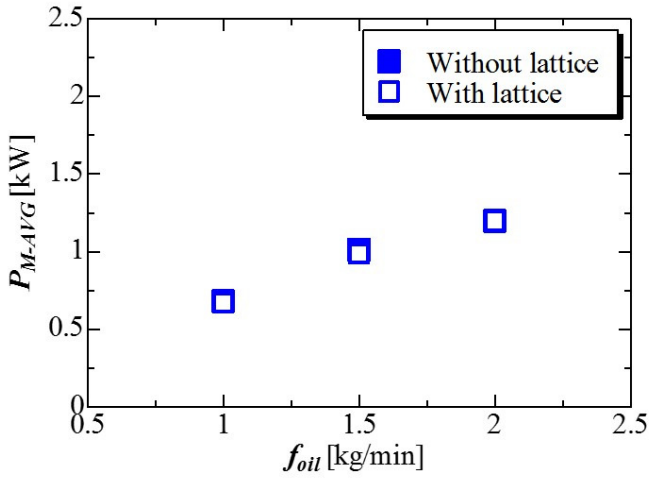

Figure 5.29: Comparison of the rate of heat stored with and without perforated partition plate at the three types of oil flow rates.

shows the aluminum metal fiber with the diameter of 0.4 mm and 0.2 mm. It is inserted the liquid PCM region as Figure 5.31.

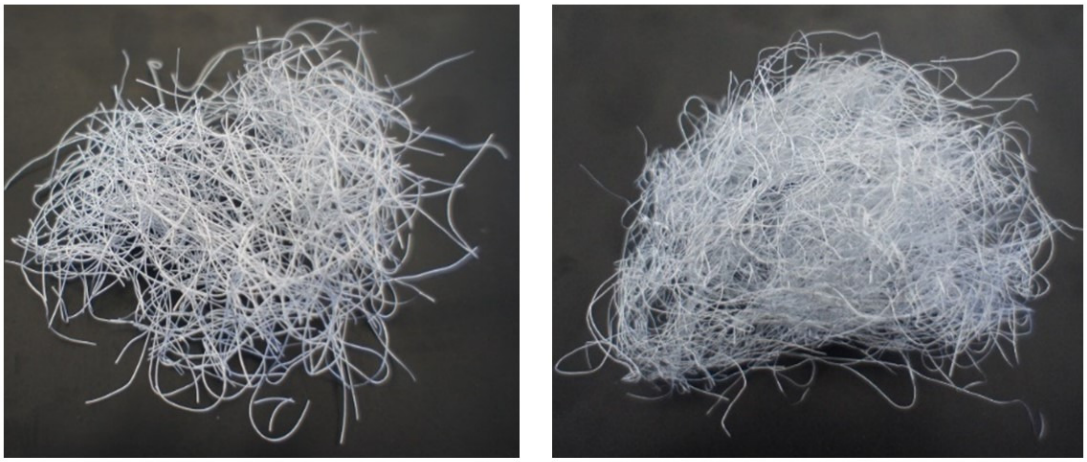

Figure 5.30: Aluminum metal fiber.

Firstly, the metal fiber with diameter of 0.4 mm was used. In this section, metal fiber material ratio was set as $\phi = 1.5\%$. It means the metal fiber volume is 1.5% of the liquid PCM volume. The mass of the inserted metal fiber is 90 g. If this ratio of the metal fiber is too high, it will block the oil flow rate and it may cause oil pressure increase and the oil pump damage. Aluminum is used because it has so many advantages. It has low density, non toxicity, high thermal conductivity, excellent corrosion resistance and can be easily cast,

Figure 5.31: Metal fiber position.

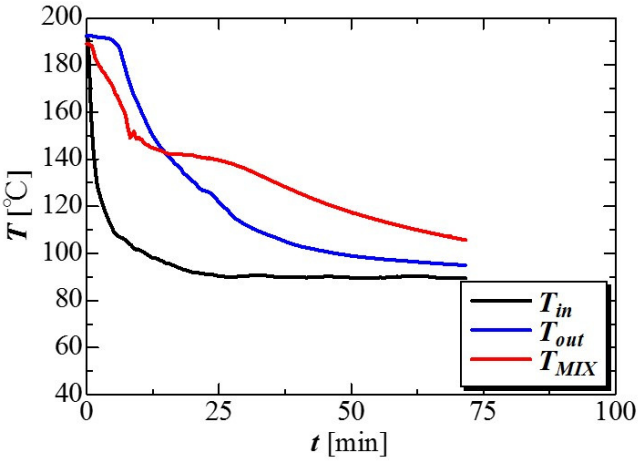

Figure 5.32: Temperature histories of PCM with metal fiber at the oil flow rate of 1.0 kg/min.

machined and formed. It is cheaper than copper and less weight.

Figure 5.32 shows the temperature histories of PCM with metal fiber at the oil flow rate of 1.0 kg/min. In this figure shows the temperature histories of inlet oil, out oil, and PCM temperatures. At the solidification process of with and without aluminum perforated partition plate, the temperature changed of melting peak process is quickly because of solidification process progress is a little fast. With the metal fiber, the temperature changed of melting peak process is gradually because of solidification process progress is a little slow. This condition of temperature histories is different from the with and without perforated partition plate.

Figure 5.33 shows the solidification behaviors of PCM with and without inserting the

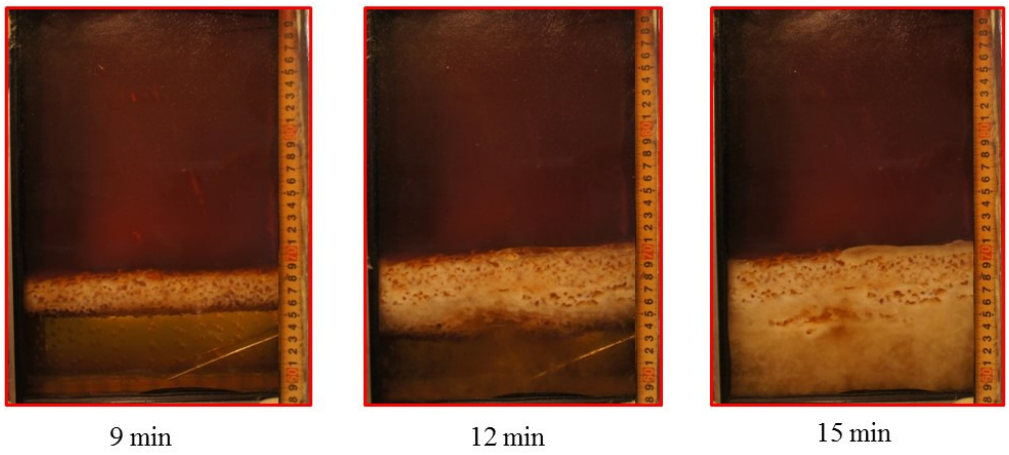

(a) Without metal fiber

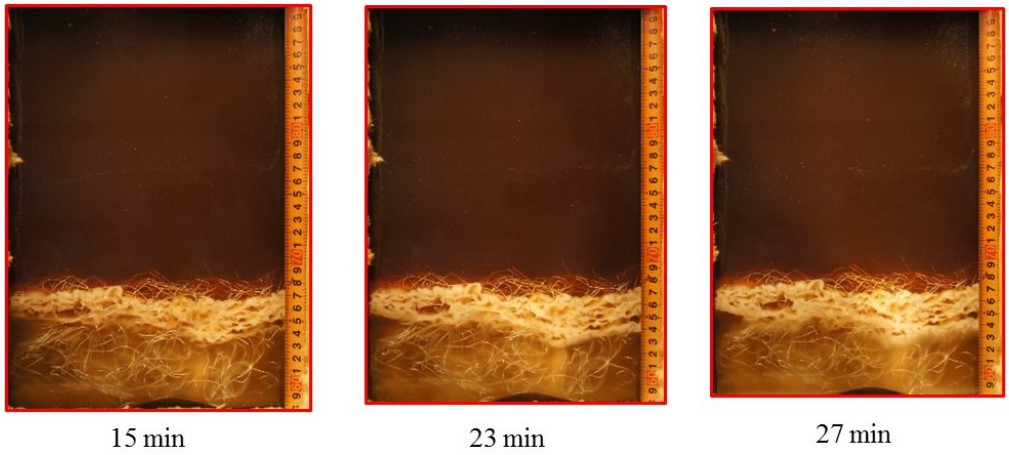

(b) With metal fiber

Figure 5.33: Solidification behaviors of PCM with and without inserting of the metal fiber at the oil flow rate of 1.0 kg/min.

metal fiber at the oil flow rate of 1.0 kg/min. A porous initial solidified layer is formed at the interface between the oil and the heat storage material liquid phase under both conditions, but after that, by mixing the metal fiber material, it can be seen that a gently solidified layer is formed. It is found that by mixing the metal fiber material, convection in the liquid phase is suppressed and a dense solidified layer is formed. Because the phase change progressed gradually rather than rapid solidification.

Figure 5.34 shows the comparison of solidification behaviors with and without inserting of metal fiber at three different types of oil flow rates. Without inserting of metal fiber, the solidified height of PCM increases as the increase in oil flow rate. On the other hand, with

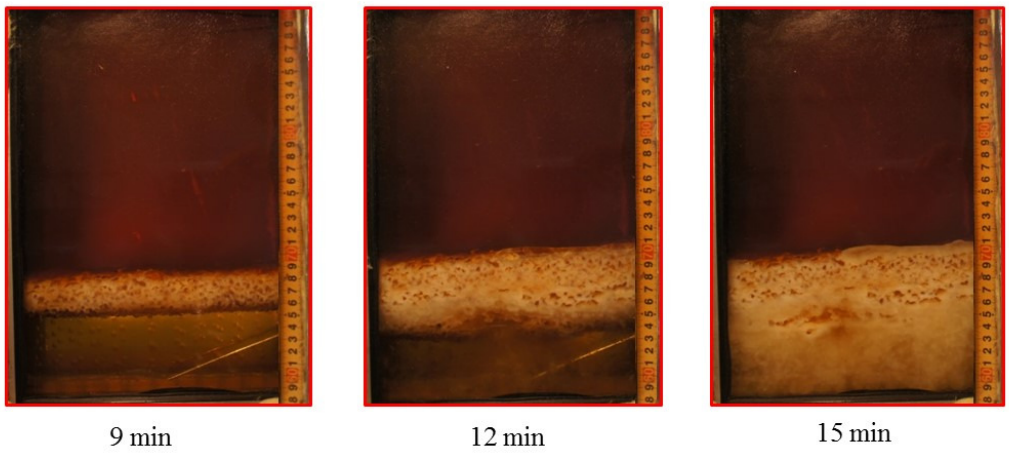

9 min 12 min 15 min

(a) Without metal fiber

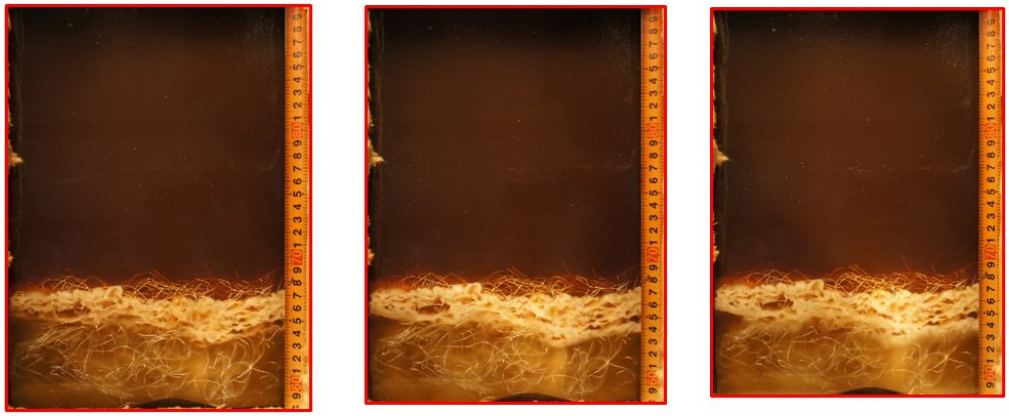

15 min 23 min 27 min

(b) With metal fiber

Figure 5.34: Comparison of solidification behaviors with and without inserting of metal fiber into three different types of oil flow rates.

inserting of metal fiber, the solidified height of PCM nearly same although the flow rate of oil increases.

The fundamental principle of this phenomenon is that PCM-coated oil droplets were broken by the metal fibers. During the solidification process, when the heat-transfer oil flows pass through the liquid PCM region, a solid PCM layer is formed on the surface of the oil droplets because the oil temperature is less than the PCM melting temperature. In the absence of metal fibers, the PCM-coated oil droplets separate at the interface of the liquid PCM and oil regions based on their different densities. If the oil flow rate increases, this interface rises because of the increasing oil volume, which causes the solidified height of the

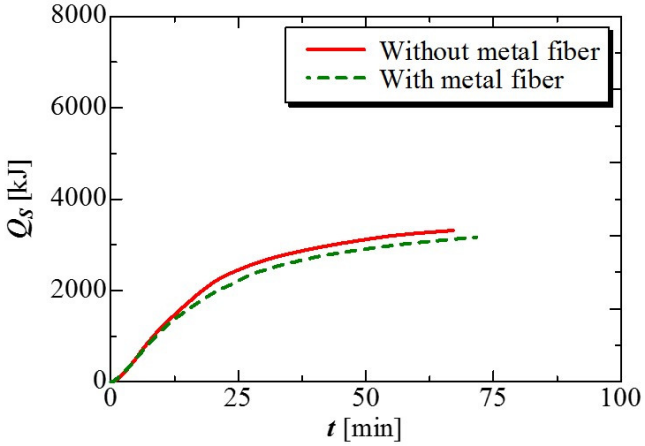

(a) f_{oil} = 1.0 kg/min

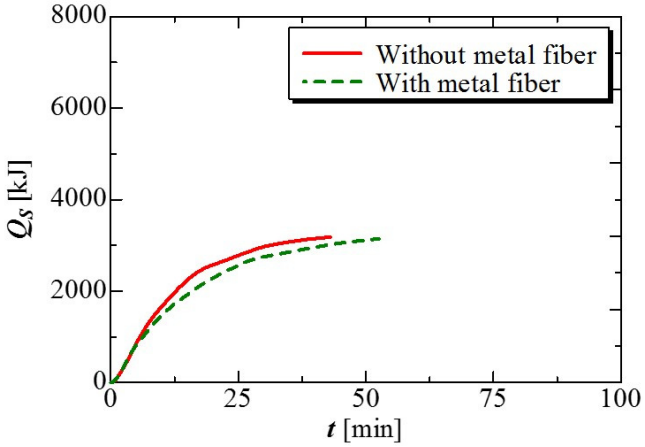

(b) f_{oil} = 1.5 kg/min

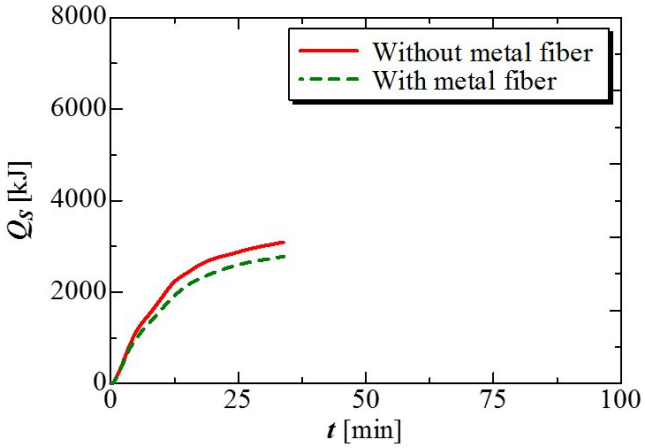

(c) f_{oil} = 2.0 kg/min

Figure 5.35: Comparison of the amount of heat released with and without inserting of metal fiber at the three types of oil flow rates.

PCM to increase.

When metal fibers are placed in the PCM region, PCM-coated oil droplets are broken by

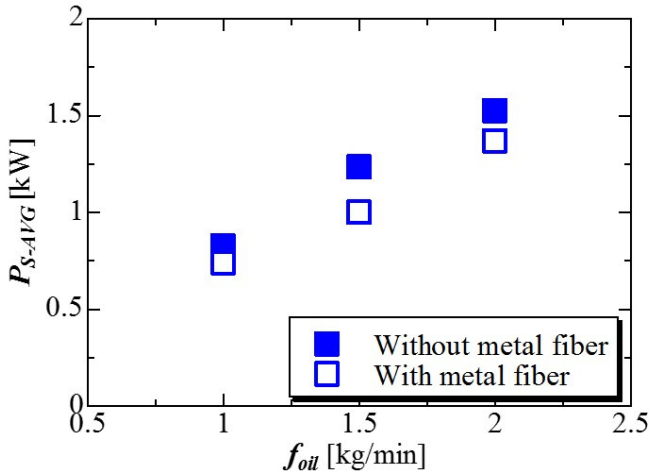

Figure 5.36: Comparison of the speed of heat released with and without inserting of metal fiber at the three types of oil flow rates.

the fibers, thereby decreasing the solidified height. This is an effective method of preventing an increase in the PCM solidified height. It is found that the solidified height of the PCM with inserting the metal fiber more decreases than with inserting of perforated partition plate. Because of the metal fiber distributed all of the PCM region and it has more frequent chance to break the PCM coated oil droplets than with inserting the perforated partition plate.

Figure 5.35 shows the comparison of the amount of heat released with and without inserting of metal fiber at the three types of oil flow rates. And Figure 5.36 shows the comparison of the speed of heat released with and without inserting of metal fiber at the three types of oil flow rates. At all of the oil flow rates, the amount of heat released in the solidification process using the metal fiber was less than that in the without inserting of it. The speed of heat released with inserting the metal fiber also some little decreases at all three types of oil flow rates. Thus, using the metal fibers, may prevent convection heat transfer and decrease the heat transfer area because of the decreased height of solidified PCM on solidification. To determine the possibility of increasing the amount and rate of heat release, the effect of metal fiber diameter, the extent of addition, and position of fiber addition will be examined in the next section.

Figure 5.37 shows the melting behaviors of PCM with the metal fiber at the three types

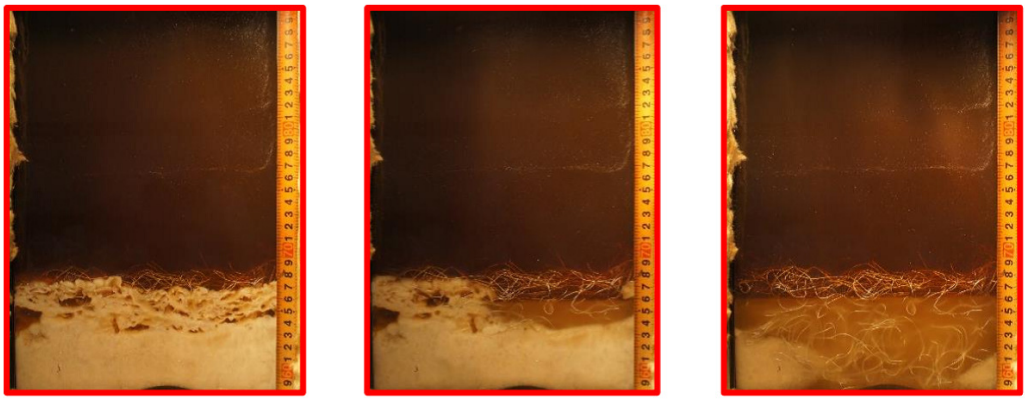

(a) f_{oil} = 1.0 kg/min

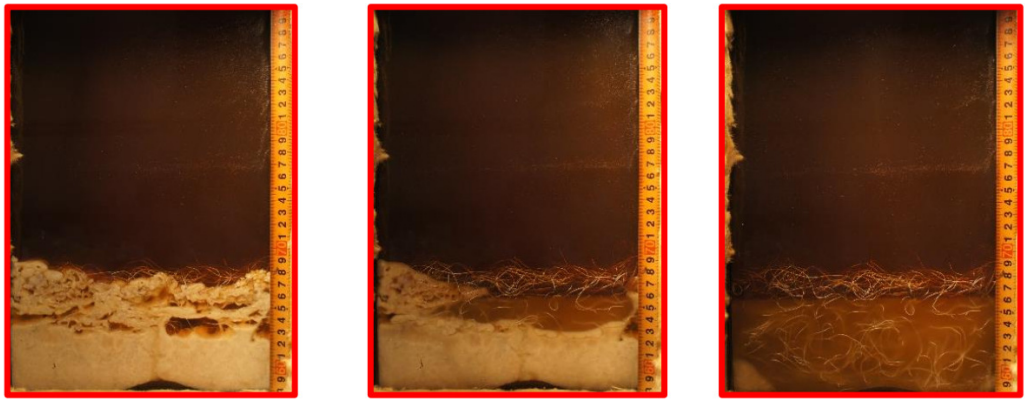

(b) f_{oil} = 1.5 kg/min

(c) f_{oil} = 2.0 kg/min

Figure 5.37: Melting behaviors of PCM with the metal fiber at the three types of oil flow rates.

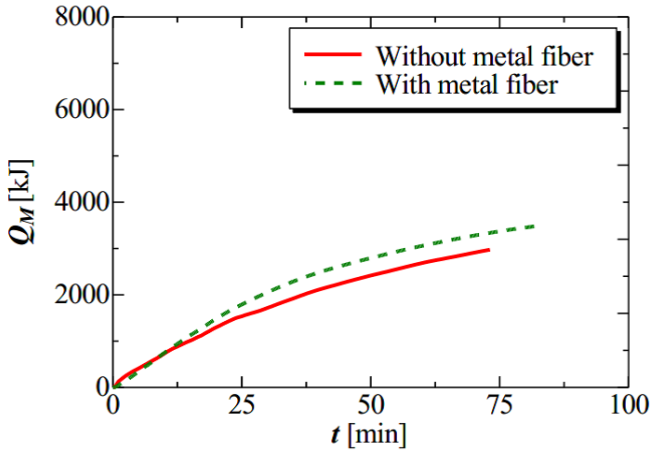

(a) f_{oil} = 1.0 kg/min

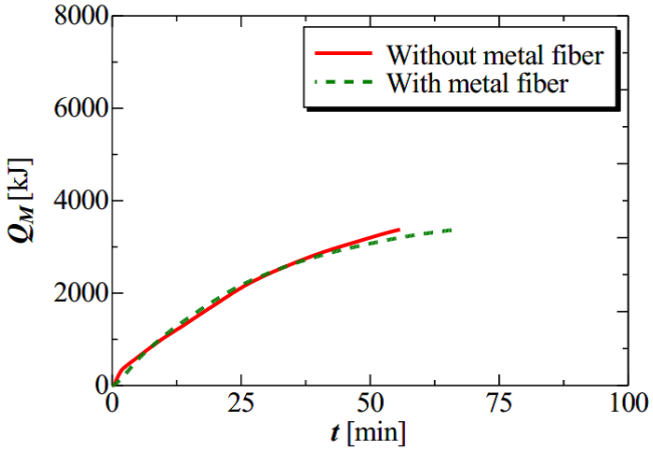

(b) f_{oil} = 1.5 kg/min

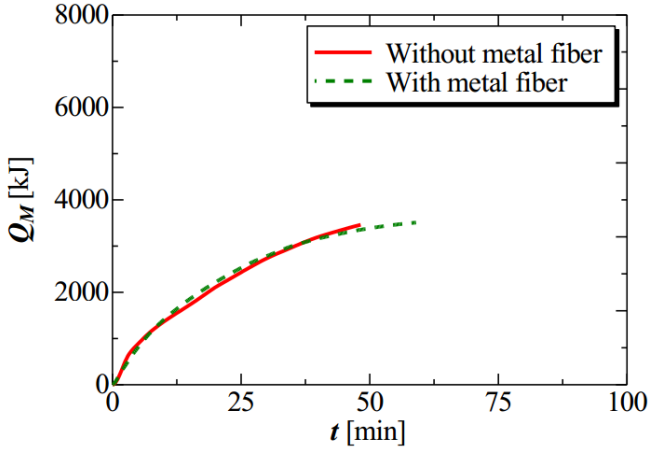

(c) f_{oil} = 2.0 kg/min

Figure 5.38: Comparison of the amount of heat stored with and without inserting of the metal fiber at the three types of oil flow rates.

of oil flow rates. The melting starts from the porous layer and it proceeds to the downward direction of heat storage vessel at any oil flow rate, showing the same tendency as the melting

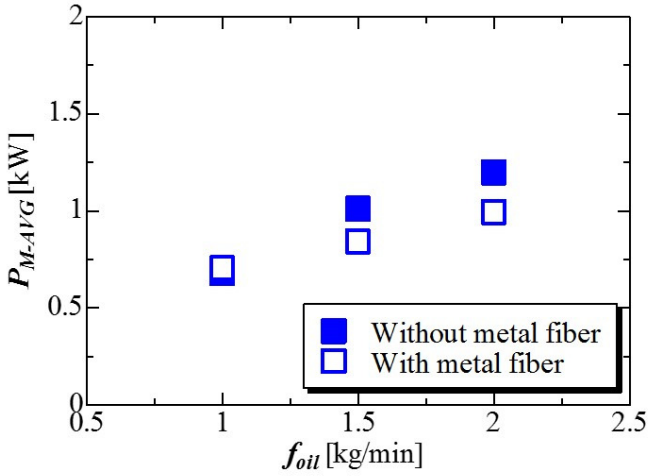

Figure 5.39: Comparison of the rate of heat stored with and without inserting of the metal fiber at the three types of oil flow rates.

process without any inserting and with the inserting of the perforated partition plate. As the flow rate of oil increases, the melting progresses faster and so that the experimental time becomes shorter.

Figure 5.38 shows the comparison of the amount of heat stored with and without inserting of the metal fiber at the three types of oil flow rates. The total amounts of heat storage in the melting process without and by inserting of the aluminum metal fiber were nearly the same. The completion times using the metal fiber was longer than without of it. This is likely because they reduced convective heat transfer in the melting process. Figure 5.39 shows the comparison of the amount of heat stored with and without inserting of the metal fiber at the three types of oil flow rates. The speed of heat storage decreases with the metal fiber. They prevent convective heat transfer and the solidified height of the PCM decreases as does the heat transfer area.

5.9.2.2 Effect of changing the proportion of metal fiber

When inserting the aluminum metal fiber, the speed of heat storage and released shown a little decrease. To increase the speed of heat transfer rate, in this section, the influence of filling ratio of metal fiber material in the mixture was investigated. The fill rate of metal fiber was changed from $\phi = 1.5\%$ to the $\phi = 0.5\%$. Initial tests used 90 g of fiber, representing

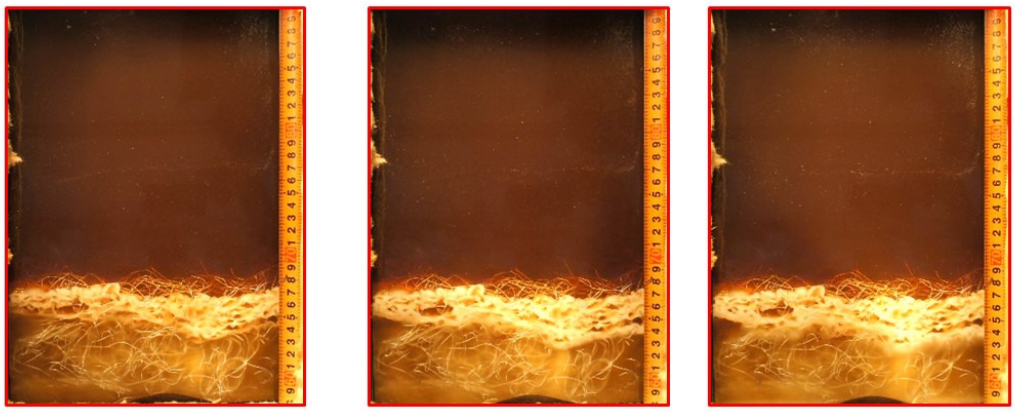

15 min　　21 min　　27 min

(a) With metal fiber $\phi = 1.5\%$

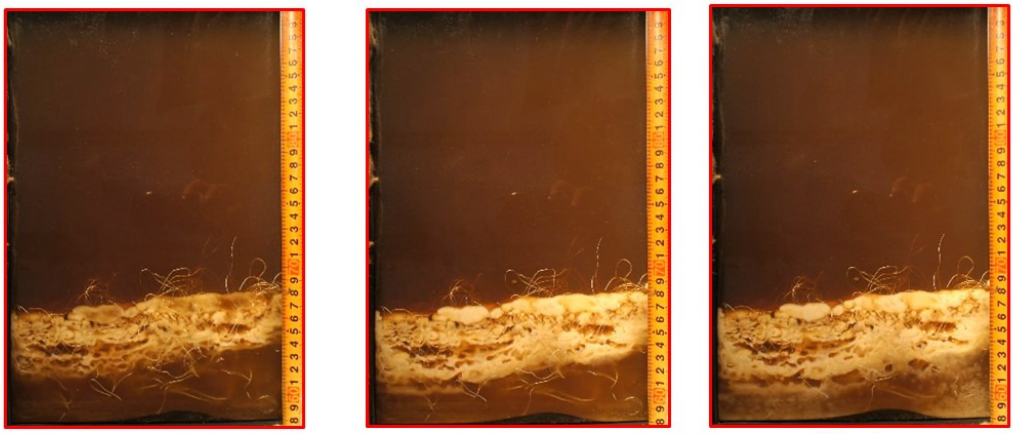

15 min　　21 min　　27 min

(b) With metal fiber $\phi = 0.5\%$

Figure 5.40: Comparison of solidification behaviors with the metal fiber of $\phi = 1.5\%$ and $\phi = 0.5\%$.

1.5 % of the volume of liquid PCM. The mass of metal fiber reduced to 30 g, representing 0.5% of the PCM volume.

From the other point of view, in the case of an actual machine, the filling amount of the heat storage material decreases due to the mixing of the metal fiber material, and the heat storage density per unit volume/unit mass becomes small. Also, when considering the transportation system of the thermal storage tank, the mass increase of the heat storage unit by the metal fiber material causes the increase of transportation cost. Therefore, the influence of filling ratio on heat transfer performance for the purpose of reducing the weight of the thermal storage system is investigated with consideration of the effect of filling ratio

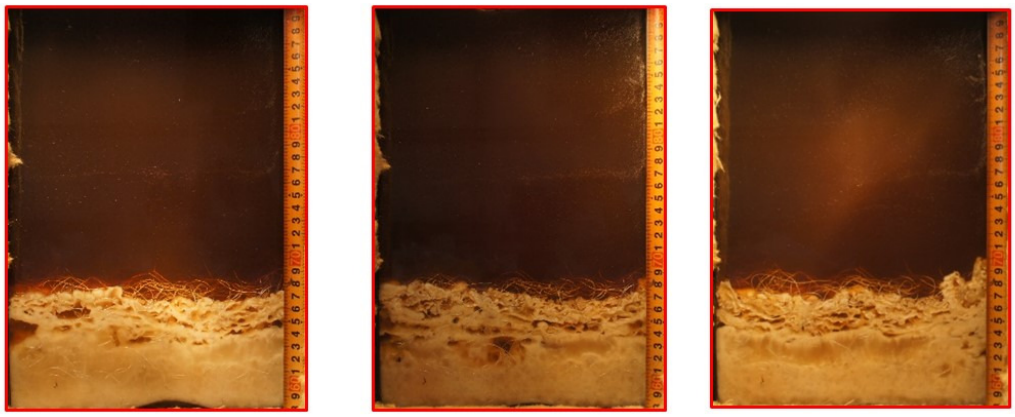

f_{oil}=1.0 kg/min f_{oil}=1.5 kg/min f_{oil}=2.0 kg/min

(a) With metal fiber $\phi = 1.5\%$

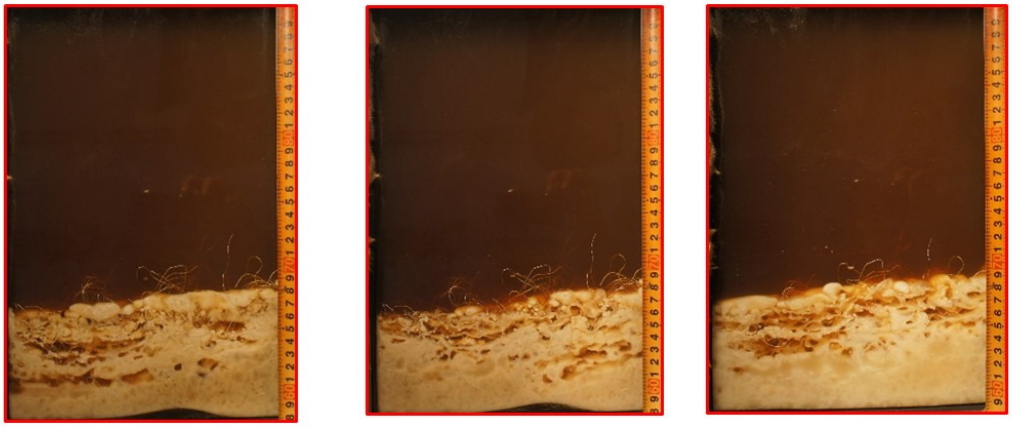

f_{oil}=1.0 kg/min f_{oil}=1.5 kg/min f_{oil}=2.0 kg/min

(b) With metal fiber $\phi = 0.5\%$

Figure 5.41: Comparison of solidification behaviors with the metal fiber of $\phi = 1.5\%$ and $\phi = 0.5\%$ at three different flow rates of oil.

of metal fiber on the suppression of the rise in solidified surface height. Figure 5.40 shows the comparison of solidification behaviors with the metal fiber of $\phi = 1.5\%$ and $\phi = 0.5\%$. A porous solidified layer was also formed from the interface between the oil layer and the heat storage material liquid phase in a photograph of 15 min when filling rate of both conditions. Figure 5.41 shows the comparison of solidification behaviors with the metal fiber of $\phi = 1.5\%$ and $\phi = 0.5\%$ at three different flow rates of oil.

When comparing the solidification surface height of each oil flow rate, almost the same solidification surface height is obtained at all oil flow rates. The negligible effect was found because the heat-transfer area of PCM does not change significantly when changing the

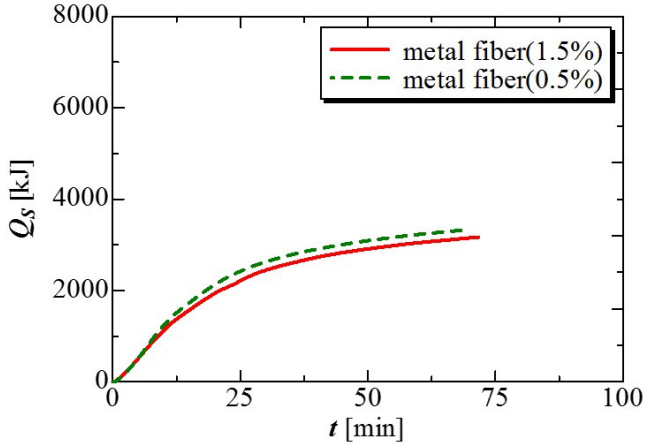

(a) f_{oil} = 1.0 kg/min

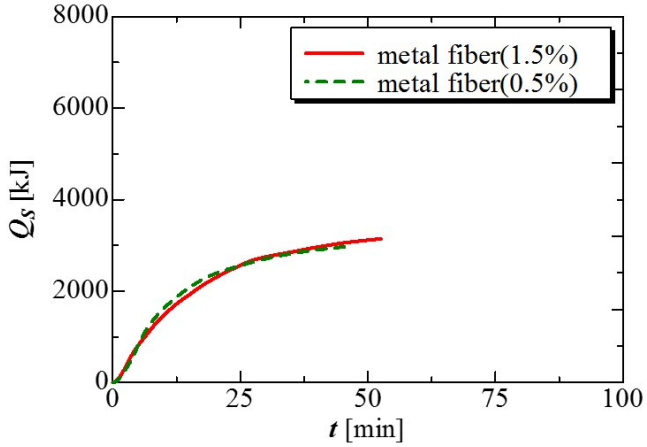

(b) f_{oil} = 1.5 kg/min

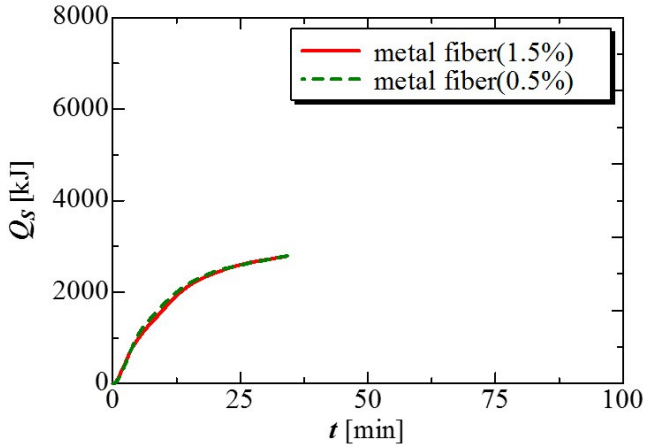

(c) f_{oil} = 2.0 kg/min

Figure 5.42: Comparison of the amount of heat released with the metal fiber of $\phi = 1.5\%$ and $\phi = 0.5\%$.

proportion of fiber. The fiber diameter was very small and so it was distributed throughout the PCM region, even when lower quantities were added. Reducing the proportion of fiber

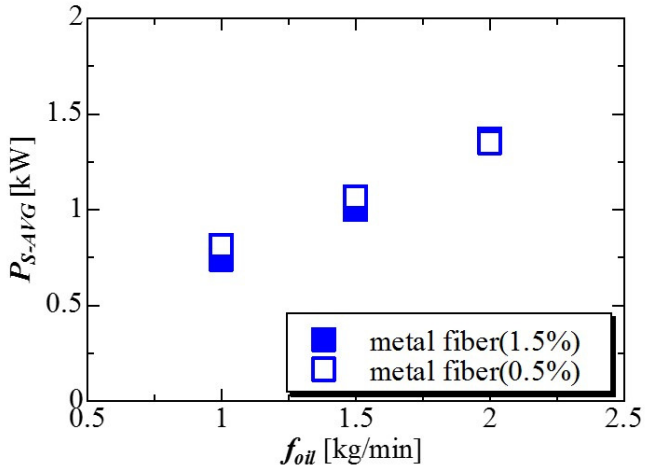

Figure 5.43: The rate of heat released with the metal fiber of $\phi = 1.5\%$ and $\phi = 0.5\%$.

reduces the chance of contact with oil droplets and reduces the height-suppression effect; however, it can be considered that a similar restraining effect is obtained, because, even at a proportion of 0.5%, sufficient fibers contacted the oil droplets to effectively break the PCM-coated oil droplets.

Figure 5.42 shows the comparison of the amount of heat released with the metal fiber of $\phi = 1.5\%$ and $\phi = 0.5\%$. The tendency is almost the same even when the filling ratio of the metal fiber material is changed.

Figure 5.43 shows the rate of heat release with the metal fiber of $\phi = 1.5\%$ and $\phi = 0.5\%$. There was no change in the solidified height of PCM or rate of heat release when decreasing the proportion of fiber added. From the above results, it is considered effective from the viewpoint of transportation cost and heat storage material charge amount, since almost the same effect can be expected even when the filling ratio of metal fiber material is reduced.

Figure 5.44 shows the melting behaviors of PCM with the metal fiber $\phi = 0.5\%$ at the three types of oil flow rates. The melting started from the porous layer even when the filling ratio of the metal fiber material is changed, and the importance of the heat transfer area can also be understood from the experiment under this condition.

Figure 5.45 shows the comparison of the amount of heat stored with the metal fiber $\phi = 0.5\%$ at the three types of oil flow rates and the comparison of the rate of heat stored with the metal fiber $\phi = 1.5\%$ and $\phi = 0.5\%$ is shown in Figure 5.46. There was no

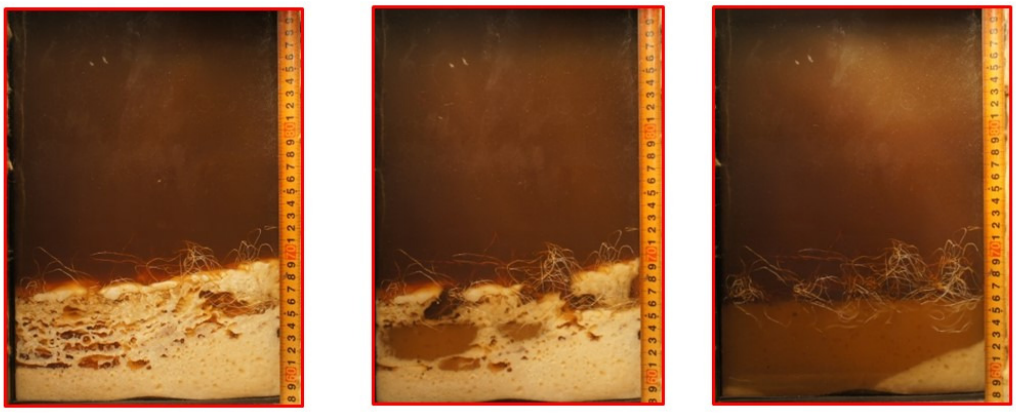

0 min　　30 min　　60 min

(a) f_{oil} = 1.0 kg/min

0 min　　30 min　　60 min

(b) f_{oil} = 1.5 kg/min

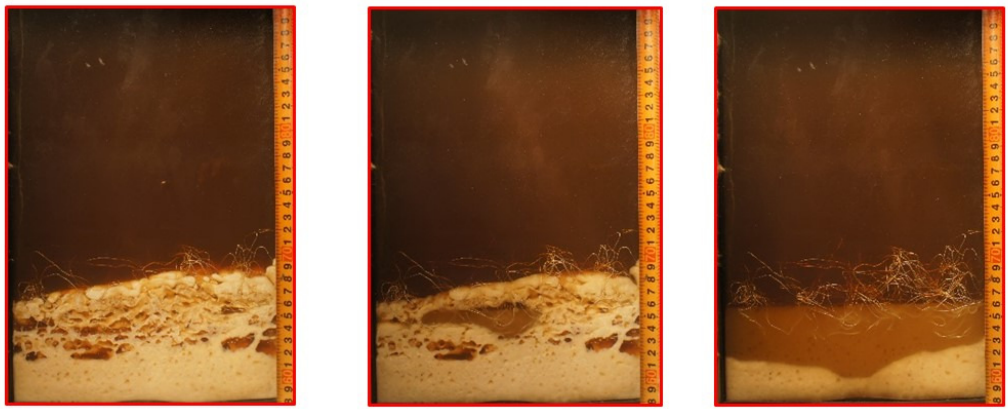

0 min　　30 min　　50 min

(c) f_{oil} = 2.0 kg/min

Figure 5.44: Melting behaviors of PCM with the metal fiber $\phi = 0.5\%$ at the three types of oil flow rates.

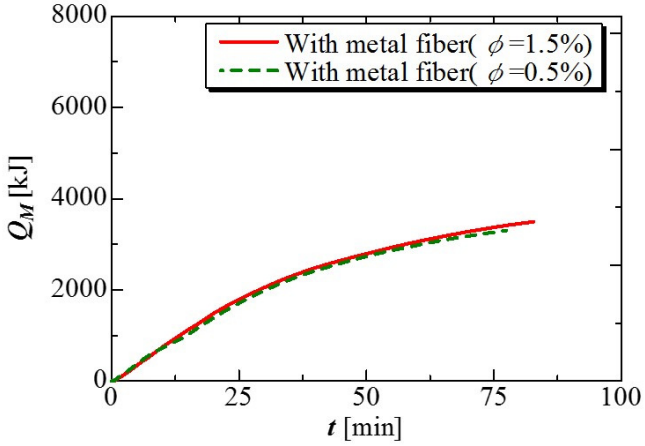

(a) f_{oil} = 1.0 kg/min

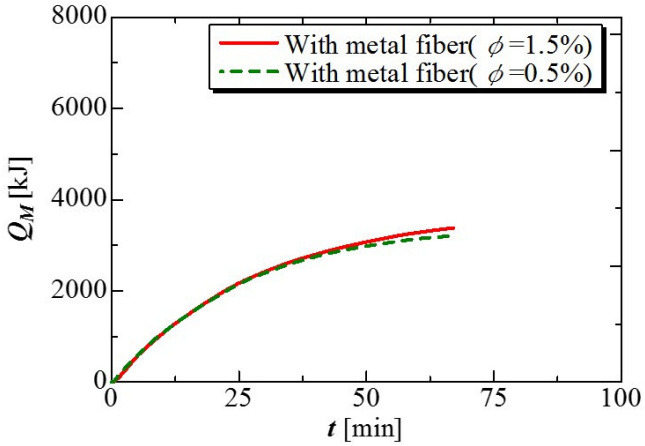

(b) f_{oil} = 1.5 kg/min

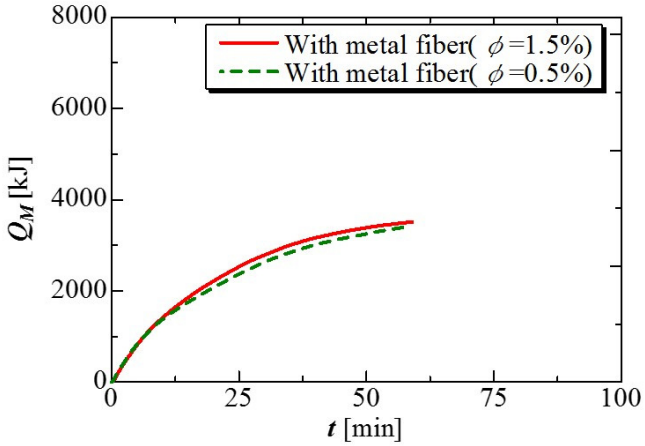

(c) f_{oil} = 2.0 kg/min

Figure 5.45: Comparison of the amount of heat stored with the metal fiber $\phi = 0.5\%$ at the three types of oil flow rates.

large difference between both of the amount of heat storage and the rate of heat storage although the filling ratio of metal fiber was changed. The same tendency was observed

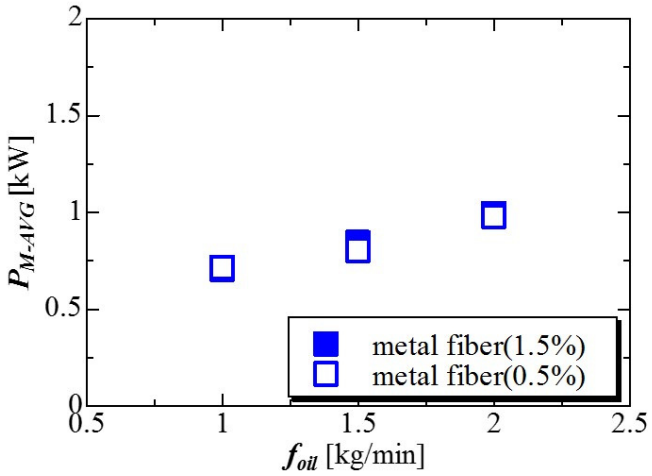

Figure 5.46: Comparison of the rate of heat stored with the metal fiber $\phi = 1.5\%$ and $\phi = 0.5\%$.

even in the case of changing the filling ratio in the melting process, because of the height of the solidified surface was about the same. In both solidification and melting processes, the filling ratio $\phi = 1.5\%$ and the suppression effect of the solidified surface height and the performance on the heat transfer were almost the same as the filling ratio of both $\phi = 1.5\%$ and 0.5%. Therefore, when using the metal fiber material, reduction of PCM solidification height is sufficiently useful for weight reduction and increase in filling amount of heat storage material.

5.9.2.3 Effect of changing metal fiber diameter

Changing the wire diameter of the metal fiber may change the size and the number of the gaps between the fiber materials and may affect to the behavior of solidification and melting processes of PCM mixture. Therefore, the influence on the solidification and melting behavior was investigated by changing the wire diameter $d = 0.4$ mm and $d = 0.2$ mm. The relative volume and mass of the fiber remained constant at 1.5% and 90 g, respectively at both diameters of the metal fiber.

Figure 5.47 shows a comparison of PCM height after solidification as the fiber diameter was changed from 0.4 mm to 0.2 mm at an oil flow rate of 1.0 kg/min. Even when the wire diameter of the metal fiber material was changed as shown in Figure 5.47, it was not seen

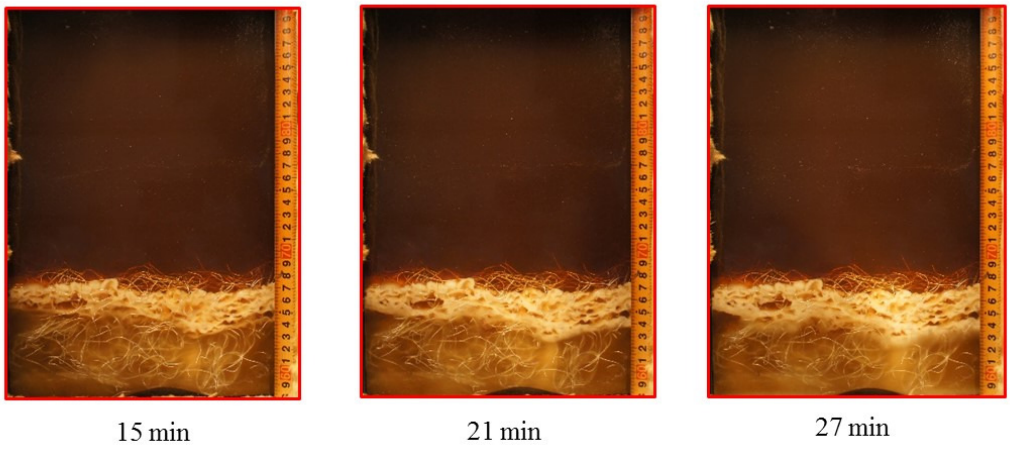

(a) With metal fiber $d = 0.4$ mm

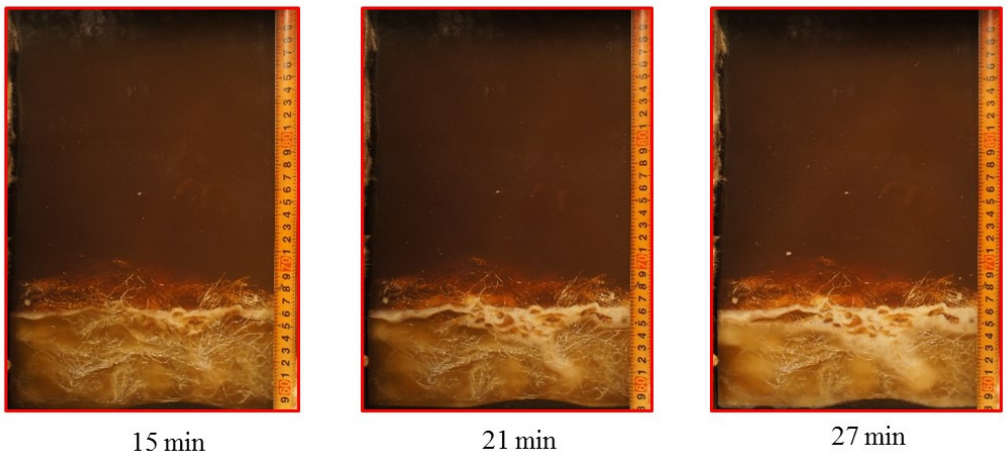

(b) With metal fiber $d = 0.2$ mm

Figure 5.47: Comparison of solidification behaviors with the metal fiber of $d = 0.4$ mm and $d = 0.2$ mm at the oil flow rate of 1.0 kg/min.

the large difference in the behavior of solidification from the interface between the oil layer and the liquid phase of the heat storage material and thereafter solidified densely.

Figure 5.48 shows the comparison of solidification behaviors with the metal fiber of $d =$ 0.4 mm and $d = 0.2$ mm at three different flow rates of oil. The PCM solidified height when using fibers of 0.4 mm diameter was 95 mm, while that of 0.2 mm diameter was 85 mm. It means that 10 mm of height of PCM was reduced. As the fiber diameter decreased, the sizes of the gaps between individual fibers decreased, thereby increasing their distribution density in the PCM region. PCM-coated oil droplets, therefore, had a higher probability to be broken by fibers of smaller diameter, which resulted in a corresponding decrease in the

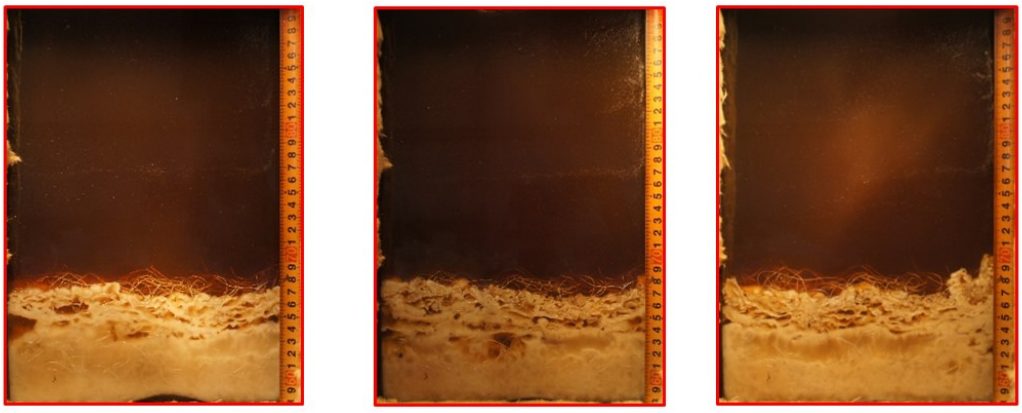

f_{oil}=1.0 kg/min f_{oil}=1.5 kg/min f_{oil}=2.0 kg/min

(a) With metal fiber $d = 0.4$ mm

f_{oil}=1.0 kg/min f_{oil}=1.5 kg/min f_{oil}=2.0 kg/min

(b) With metal fiber $d = 0.2$ mm

Figure 5.48: Comparison of solidification behaviors with the metal fiber of $d = 0.4$ mm and $d = 0.2$ mm at three different flow rates of oil.

height of the solidified PCM.

Figure 5.49 shows the comparison of the amount of heat released with the metal fiber of $d = 0.4$ mm and $d = 0.2$ mm and Figure 5.50 shows the rate of heat released with the metal fiber of $d = 0.4$ mm and $d = 0.2$ mm. The change on the amount of heat released with the metal fiber of both diameter was very small and the rate of heat release with the smaller fiber diameter was only slightly higher, with other conditions held constant. Changing the fiber diameter, there was no effect on the solidification behavior while the rates of heat release was slightly higher, but the effect was very small with changing the diameter of metal fiber except the solidification height of PCM.

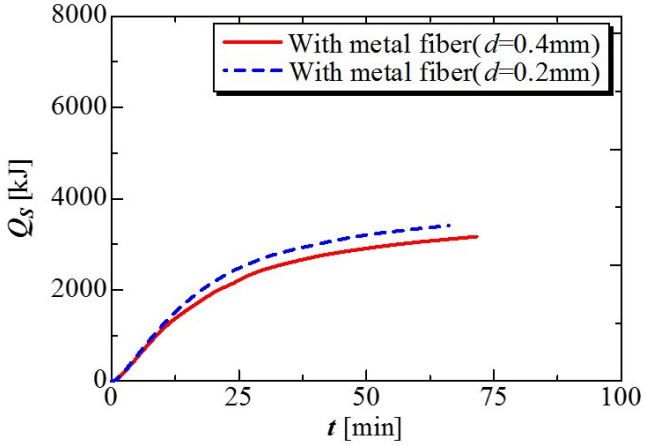

(a) f_{oil} = 1.0 kg/min

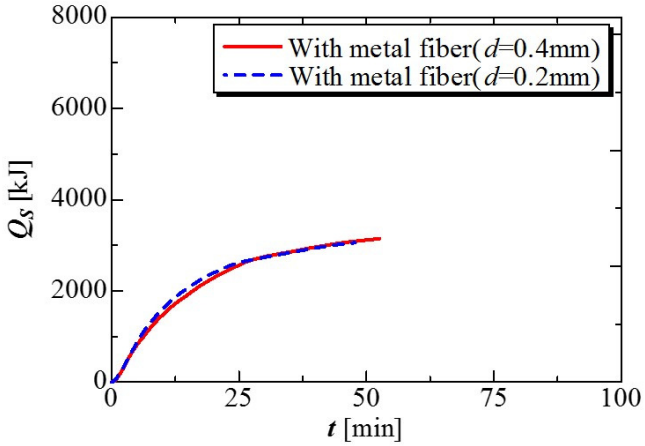

(b) f_{oil} = 1.5 kg/min

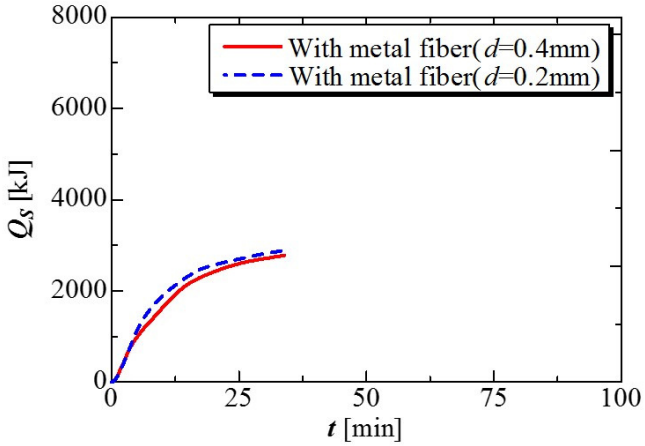

(c) f_{oil} = 2.0 kg/min

Figure 5.49: Comparison of the amount of heat released with the metal fiber of d = 0.4 mm and d = 0.2 mm.

Figure 5.51 shows the melting behaviors of PCM with the metal fiber d = 0.2 mm at the three types of oil flow rates. As shown in this figure, melting started from a porous layer

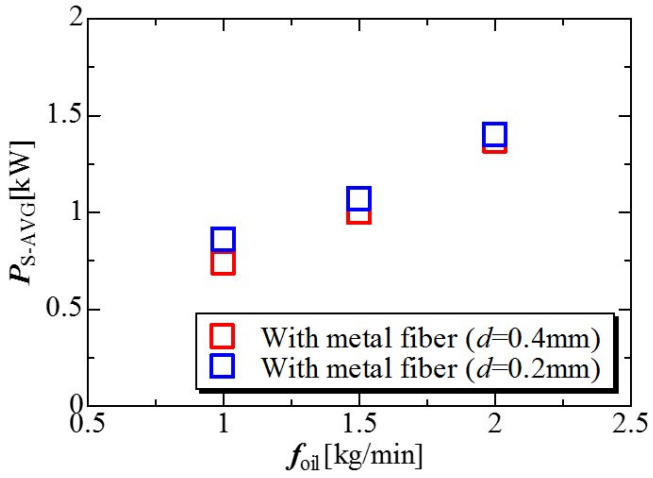

Figure 5.50: The rate of heat released with the metal fiber of $d = 0.4$ mm and $d = 0.2$ mm.

with a large heat transfer area at all oil flow rates, and then the dense solidified layer melts out. The speed of the melting process was increased, and the completion time was shortened by increasing the oil flow rate even though changing the diameter of the metal fiber.

Figure 5.52 shows the comparison of the amount of heat stored with the metal fiber $d = 0.2$ mm at the three types of oil flow rates and Figure 5.53 shows the comparison of the rate of heat stored with the metal fiber $d = 0.4$ mm and $d = 0.2$ mm. The change of the heat storage amount with time is almost same trend, and it is understood that there is no large difference in the average heat storage speed value. From the above results, it can be considered that the influence of the melting process due to the changing of the wire diameter of the metal fiber material is small.

5.9.2.4 Effect of changing the position of metal fibers

Figure 5.54 shows the changing the position at which the metal fibers are placed from throughout the entire PCM region to the top one-third only. When the fibers were placed throughout the PCM region, 90 g of fiber (1.5%) was used; when only placing fibers into the top one-third of the PCM region, the fiber proportion was held at 1.5%, so only 30 g was required. It means only changing position and mass of the metal fiber and the filling ratio remain the same.

Figure 5.55 shows the comparison of solidification behaviors with the metal fiber of

0 min　　40 min　　60 min

(a) f_{oil} = 1.0 kg/min

0 min　　40 min　　60 min

(b) f_{oil} = 1.5 kg/min

0 min　　30 min　　50 min

(c) f_{oil} = 2.0 kg/min

Figure 5.51: Melting behaviors of PCM with the metal fiber d = 0.2 mm at the three types of oil flow rates.

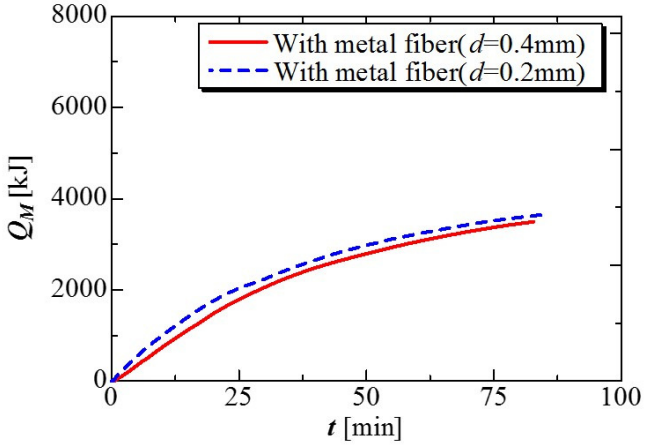

(a) f_{oil} = 1.0 kg/min

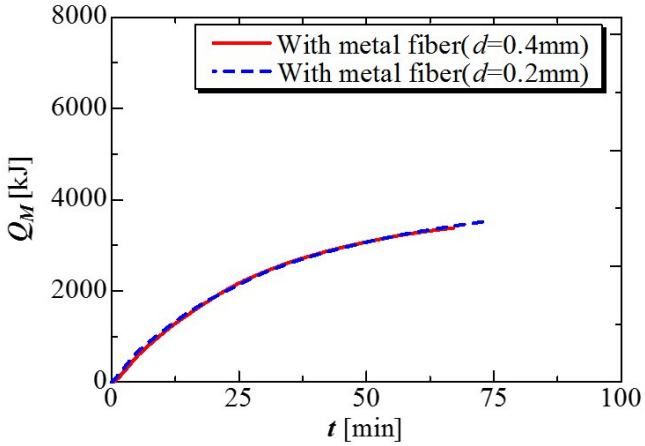

(b) f_{oil} = 1.5 kg/min

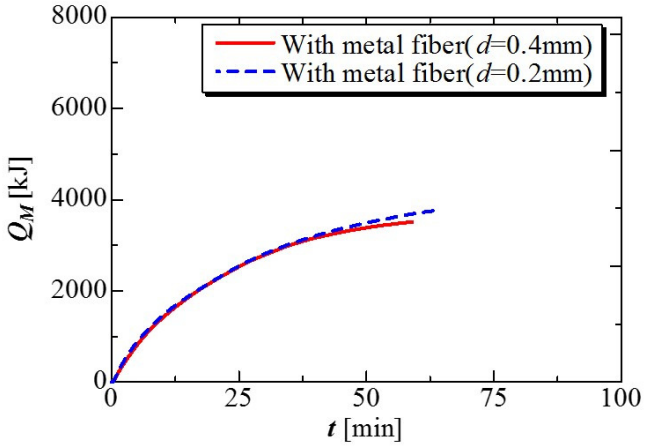

(c) f_{oil} = 2.0 kg/min

Figure 5.52: Comparison of the amount of heat stored with the metal fiber d = 0.2 mm at the three types of oil flow rates.

different positions at the oil flow rate of 1.0 kg/min and Figure 5.56 shows the comparison of solidification behaviors with the metal fiber of different position at a different type of oil

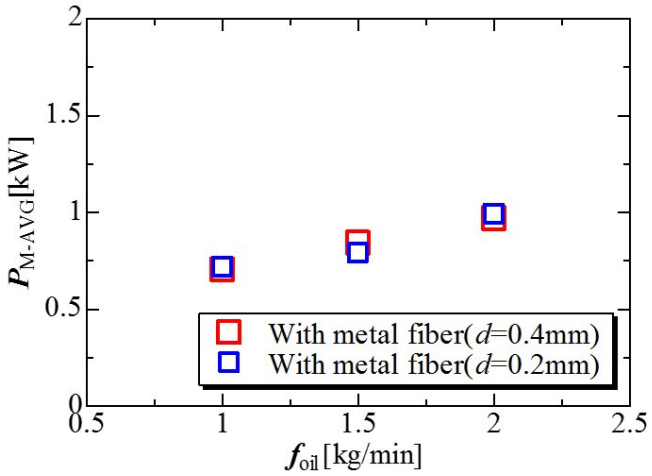

Figure 5.53: Comparison of the rate of heat stored with the metal fiber d = 0.4 mm and d = 0.2 mm.

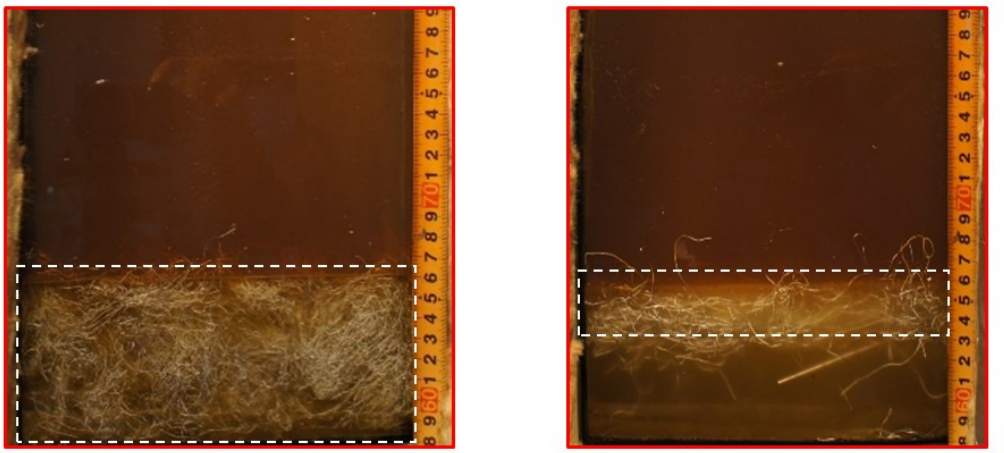

Figure 5.54: The different positions of metal fiber at the PCM region.

flow rates. It is seen that the solidification progress with the metal fiber at the top one-third region is faster than the entire PCM region, but the finishing time of the solidification was shortened at the metal fiber of the entire PCM region. The reason for this condition will be explained later at Figure 5.59. In Figure 5.56, the height of the solidified PCM slightly higher at the metal fiber of the top one-third region than the metal fiber at the all entire PCM region. But the effect was very small.

Figure 5.57 shows the comparison of the amount of heat released with the metal fiber of different position and Figure 5.58 shows the comparison of the rate of heat released with the

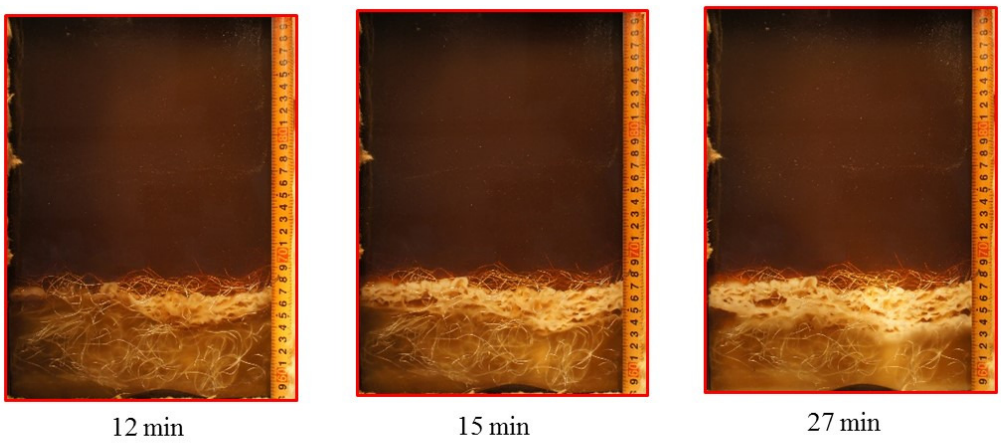

(a) with metal fiber at all PCM region

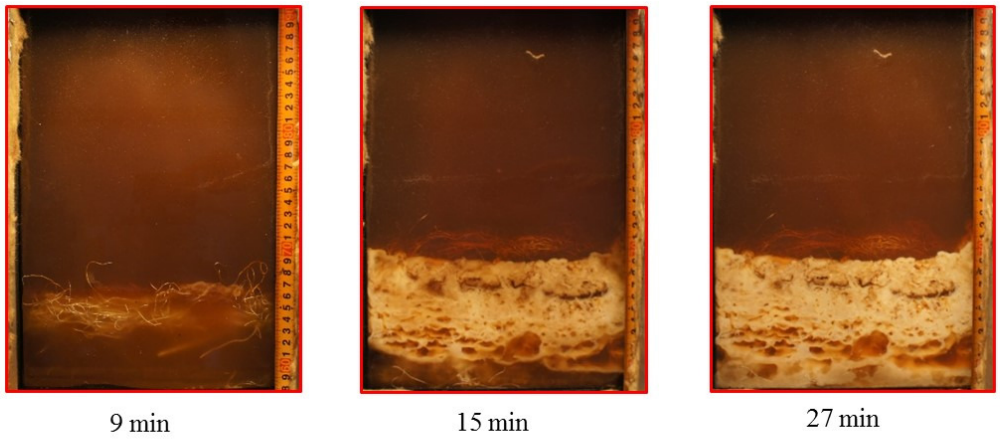

(b) with metal fiber at one-third of PCM region

Figure 5.55: Comparison of solidification behaviors with the metal fiber of different position at the oil flow rate of 1.0 kg/min.

metal fiber of different position.

The amount of heat release with the metal fiber of the top one-third region was increased than the metal fiber at the all entire PCM region. But the finishing time of process was shortened at the top one-third condition. The cause of this reason, the rate of the heat released was nearly same. To discuss the above results, Figure 5.59 shows the solidification behaviors when metal fibers were filled throughout the PCM region and only in the top one-third of this region. Different processes occurred under these two conditions. In the latter, solidification started from the interface and proceeded toward the bottom of the test section; when fibers occupied the entire PCM region, solidification proceeded from near the flow path of the heat-transfer oil and the fibers prevented a convection current. The amount

f_{oil}=1.0 kg/min f_{oil}=1.5 kg/min f_{oil}=2.0 kg/min

(a) with metal fiber at all PCM region

f_{oil}=1.0 kg/min f_{oil}=1.5 kg/min f_{oil}=2.0 kg/min

(b) with metal fiber at one-third of PCM region

Figure 5.56: Comparison of solidification behaviors with the metal fiber of different position at different type of oil flow rates.

of heat release with the meat fiber at the all entire PCM region was less than the case of metal fiber of the top one-third region because the heat-transfer area between the oil and PCM was only near the flow path of the oil. When the temperature of the outlet oil reached 95°C (completion of solidification), the PCM temperature far from the oil flow path was still somewhat higher. This accounts for a faster completion time of solidification under these conditions, although the rate of heat released was almost the same.

Figure 5.60 shows the melting behaviors of PCM when metal fibers were filled throughout the PCM region and only in the top one-third of this region at the three types of oil flow rates. As shown in this figure, melting started from a porous layer with a large heat transfer area at all oil flow rates, and then the dense solidified layer melts out. The speed of the

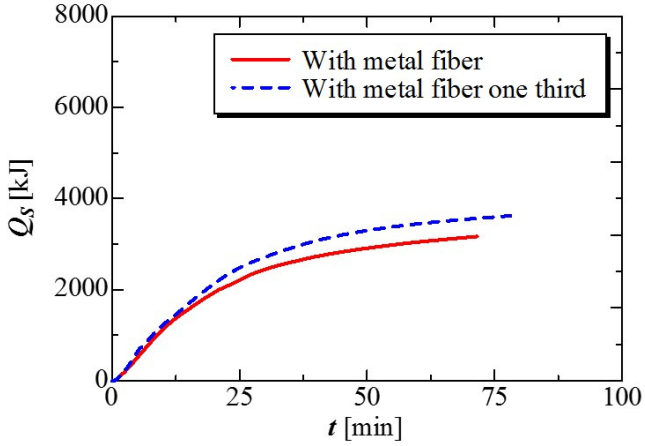

(a) f_{oil} = 1.0 kg/min

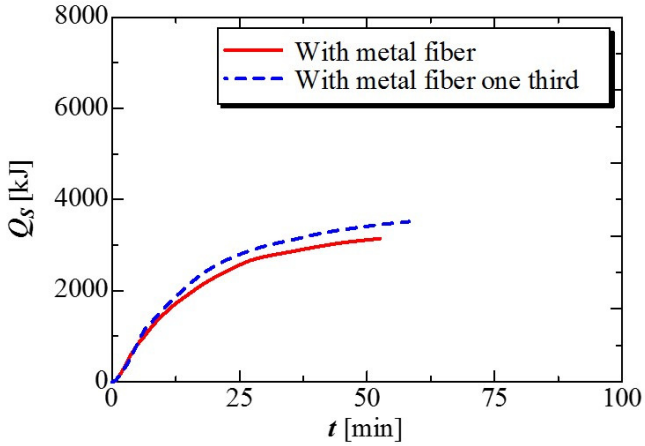

(b) f_{oil} = 1.5 kg/min

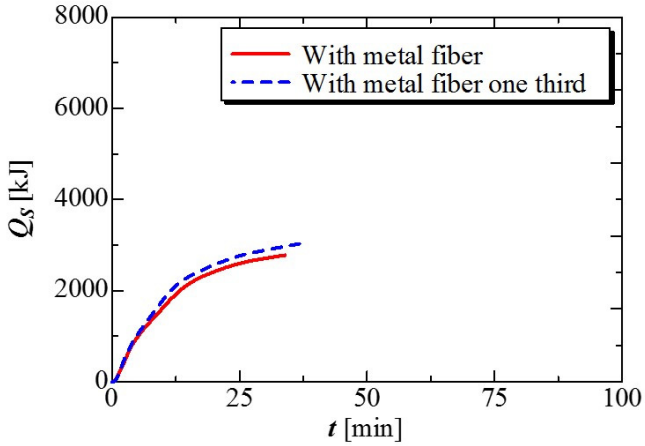

(c) f_{oil} = 2.0 kg/min

Figure 5.57: Comparison of the amount of heat released with the metal fiber of different position.

melting process was slightly increased, and the completion time was shortened by increasing the oil flow rate even though changing the diameter of the metal fiber.

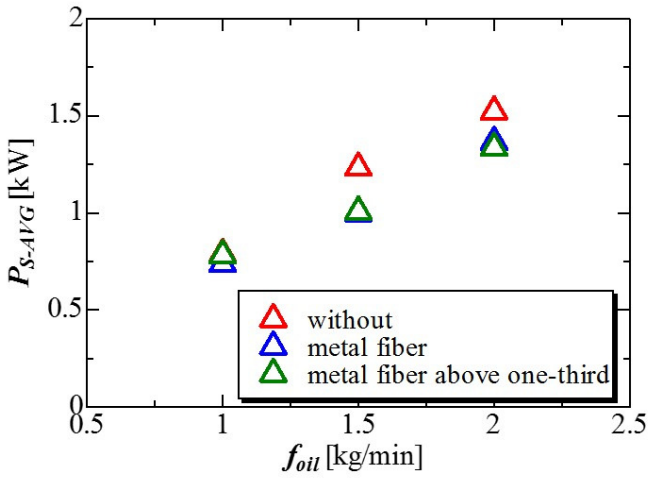

Figure 5.58: Comparison of the rate of heat released with the metal fiber of different position.

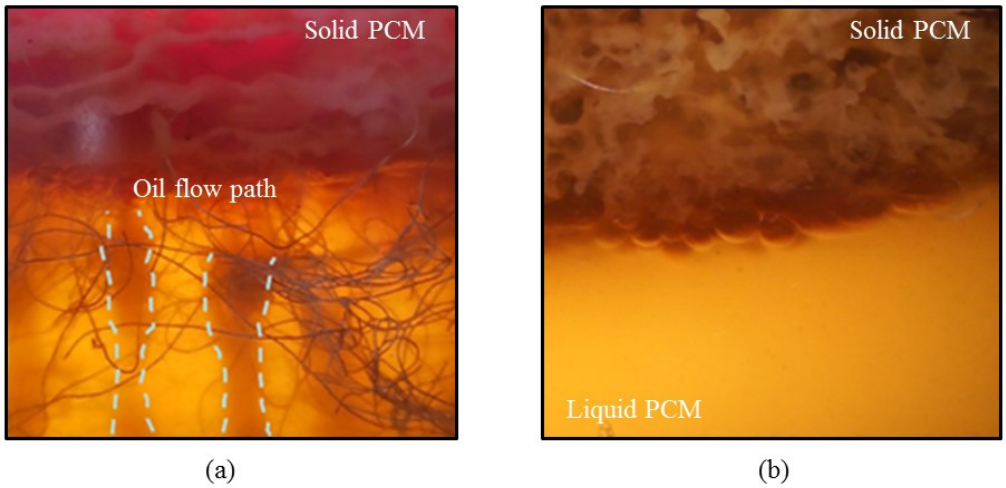

Figure 5.59: Solidification behavior of PCM for (a) fibers filling entire test region and (b) fibers only present in the top third of the test region.

Figure 5.61 shows the comparison of the amount of heat storage when metal fibers were filled throughout the PCM region and only in the top one-third of this region at the three types of oil flow rates and Figure 5.62 shows the comparison of the rate of heat storage when metal fibers were filled throughout the PCM region and only in the top one-third of this region. The change of the heat storage amount with time is almost same trend, and it is understood that there is no large difference in the average heat storage speed value. From these results, it can be considered that the influence of the melting process due to the change of the metal fiber material position is small.

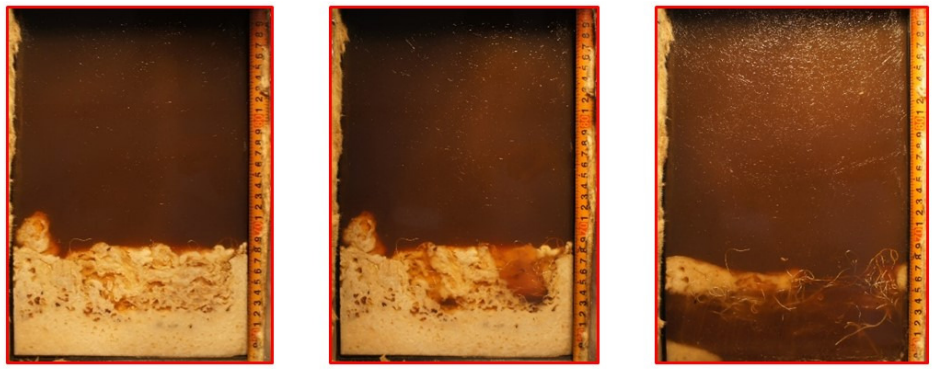

0 min　10 min　60 min

(a) f_{oil} = 1.0 kg/min

0 min　10 min　50 min

(b) f_{oil} = 1.5 kg/min

0 min　10 min　50 min

(c) f_{oil} = 2.0 kg/min

Figure 5.60: Melting behaviors of PCM with the metal fiber at one-third of PCM region at the three types of oil flow rates.

5.9.3 Using the Aluminum Perforated plate

In this section, aluminum perforated plate is used to prevent the flow out problem of PCM. Figure 5.63 shows the photo of it. The design and detail dimension of perforated

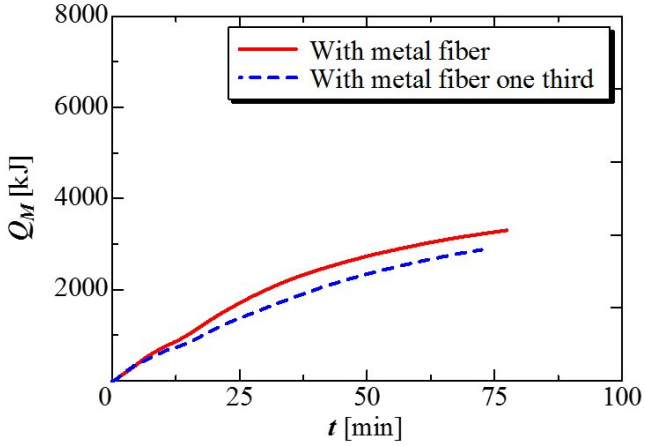

(a) f_{oil} = 1.0 kg/min

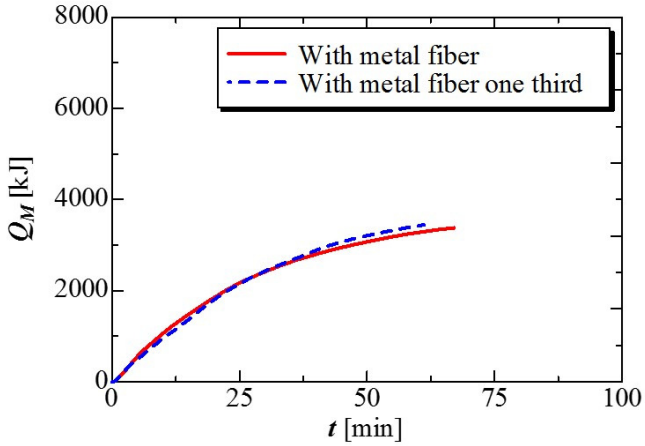

(b) f_{oil} = 1.5 kg/min

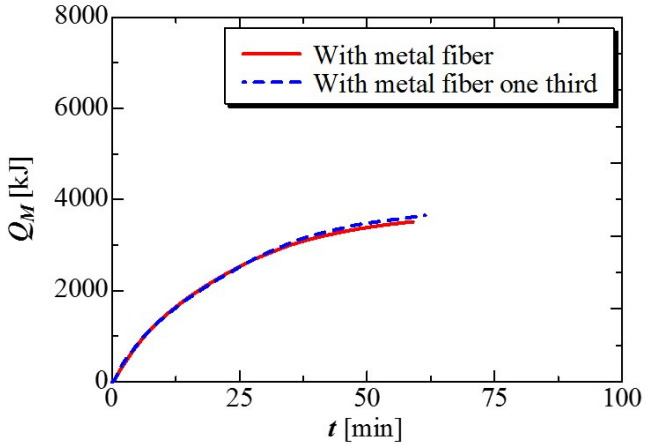

(c) f_{oil} = 2.0 kg/min

Figure 5.61: Comparison of the amount of heat stored with the metal fiber at different positions at the three types of oil flow rates.

holes as like the Figure 5.1(b). The thickness of plate was 2 mm. It inserted inside of the heat storage vessel at the high of 80 mm, 100 mm, and 120 mm respectively and compare their

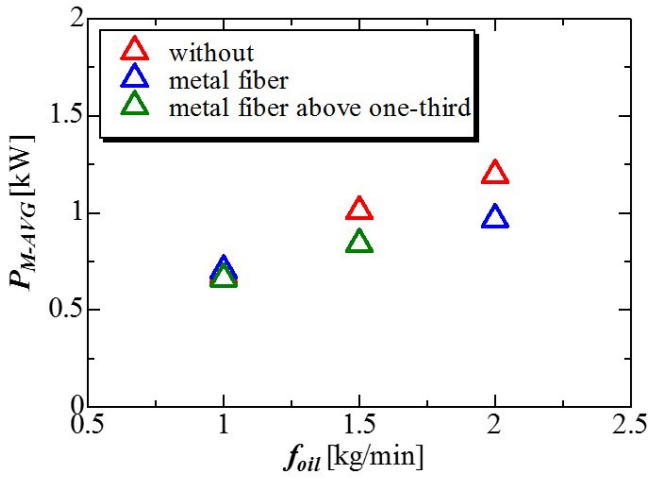

Figure 5.62: Comparison of the rate of heat stored with the metal fiber at the different positions.

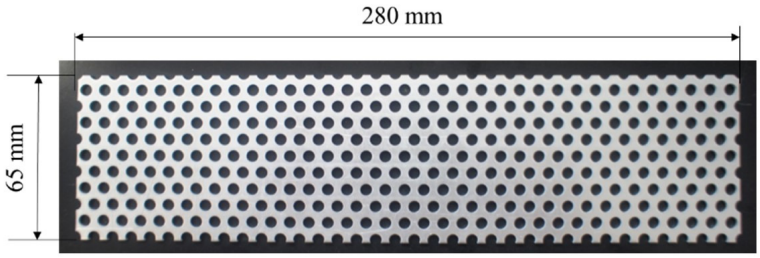

Figure 5.63: Aluminum Perforated plate.

height to the solidified PCM after finishing the solidification process as shown in Figure 5.64. It was found that the solidified heights increase except at the $h = 80$ mm. The rate of heat release is nearly same without any inserting condition as shown in Figure 5.65. It is the better condition than perforated partition plate and metal fiber. But there was a problem of increasing the pressure of oil during the experiment. The pressure of oil increase to 0.03 Mpa at $h = 120$ mm and 0.05 Mpa at $h = 80$ mm and $h = 100$ mm respectively. It can be damage to the oil pump. This method is not effective for reduction of the solidified height of PCM.

5.9.4 Using Mesh

In this section, two different sizes of the mesh is inserted at a height of 120 mm inside the heat storage vessel to prevent the increasing the solidified height of PCM mixture.

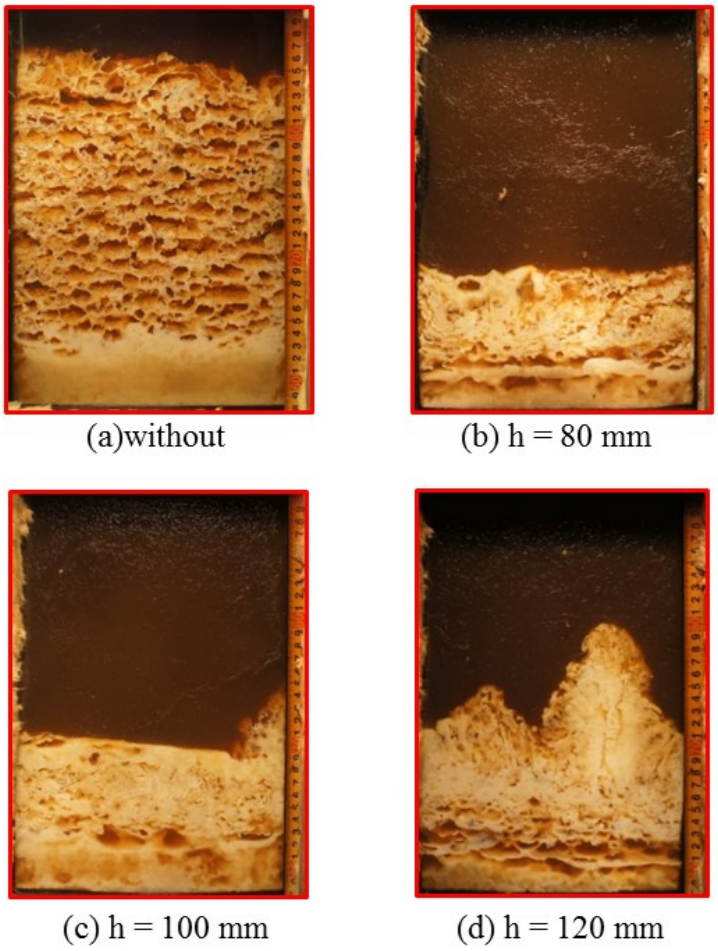

Figure 5.64: Solidification process with the perforated plate.

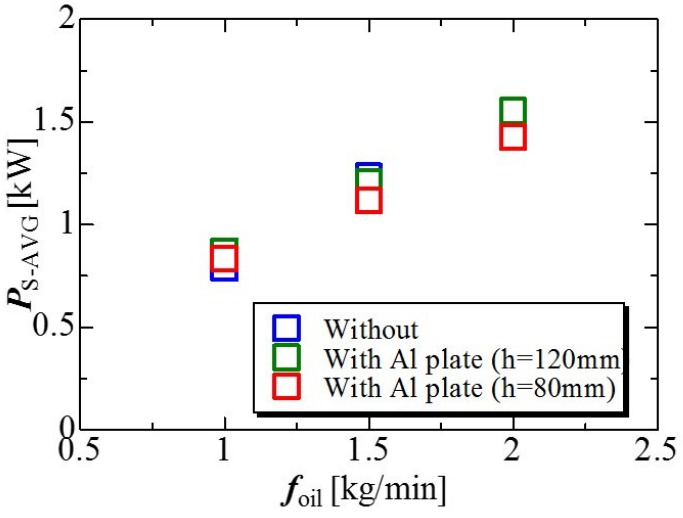

Figure 5.65: The rate of heat released with the perforated plate.

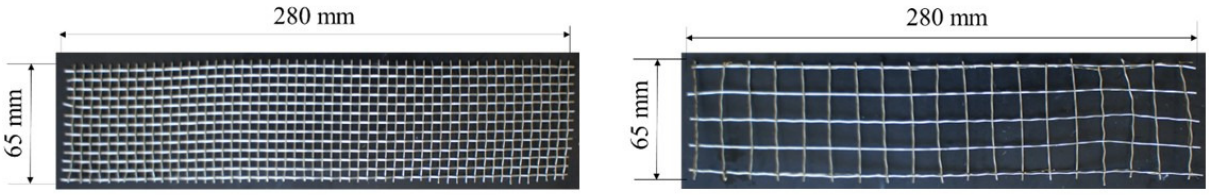

(a) 10×10 mm² mesh (b) 30×30 mm² mesh

Figure 5.66: Two types of mesh.

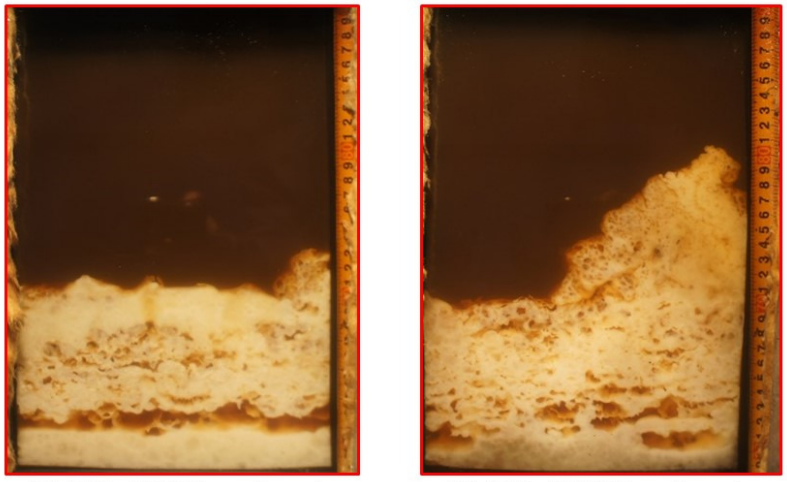

(a) With 10×10 mm² mesh (b) With 30×30 mm² mesh

Figure 5.67: Visualization of solidification process with mesh.

Figure 5.66 shows the two types of mesh, one has 10×10 mm^2 and other has 30×30 mm^2 respectively. Figure 5.67 shows the visualization of solidification process with mesh at the oil flow rate of 2.0 kg/min after finishing the solidification process. While using the 10×10 mm^2 mesh, the solidified height decreases but the solidified height of PCM cannot suppress while using the 30×30 mm^2 mesh. Both of two have the other problem that the pressure of oil increase like using the aluminum perforated plate. This method also cannot be used to prevent the solidification height of PCM mixture.

5.9.5 Calculation for PCM temperature

Calculation for PCM temperature was carried out to predict the temperature of PCM while oil droplet supplied from a nozzle hole pass to the PCM region and to compare with the experimental results. Figure 5.68 shows the schematic diagram of the test section.

To solidify the mixture, the silicone oil from the low-temperature oil bath at 90°C flowed into the heat storage vessel until the temperature of the outlet oil decreased to 95°C. The heat of the oil was exchanged with the mixture at the PCM region while passing the heat transfer oil through this region. The PCM mixture solidified when reaching the solidification temperature of the mixture.

For calculating the PCM temperature, some assumptions are as follow:

The temperature of the PCM is uniform in the test section. The test section is well insulated, and heat lost to surrounding will be ignored. The temperature of the test section is assumed to be the same as that of the PCM mixture inside.

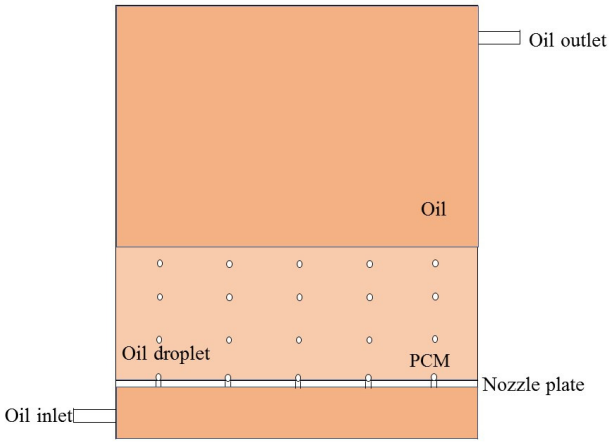

Figure 5.68: Schematic of the test-section.

The energy balance of the direct contact heat transfer of mixture and heat transfer oil can be written as Equation 5.13[84]. The left-hand terms of the Equation 5.13 are the rate of enthalpy changes of the mixture and test section material, respectively. The first right-hand term is the rate of enthalpy change of the heat transfer oil and the final term is the external heat loss to the surroundings. When the test section is well insulated, the heat loss can be neglected. Table 5.4 shows the specific heat of mixture at different temperature range. Equation 5.13 can be rewritten in numerical form as Equation 5.14 and Equation 5.15.

$$\frac{d(m_{mix}h_{mix})}{dt} + m_{ts}C_{pts}\frac{dT_{mix}}{dt} = m_{oil}(h_{out} - h_{in}) + (UA)(T_a - T_{mix}) \tag{5.13}$$

$$T_{mix}^{t+\Delta t} = T_{mix}^{t} + \frac{m_{oil}(h_{out} - h_{in})}{m_{ts}C_{pts} + m_{mix}C_{pmix}} \tag{5.14}$$

$$T_{mix}^{t+\Delta t} = T_{mix}^{t} + \frac{m_{oil}C_{poil}(T_{out} - T_{in})}{m_{ts}C_{pts} + m_{mix}C_{pmix}} \tag{5.15}$$

Table 5.4: The specific heat of mixture at different temperature range [96].

Temperature Range(°C)		Specific Heat (J/kgK)
Solid State T < 99.9°C		1554
Phase Change Region	$99.9°C<T<103°C$	$9331 \times T - (9306 \times 10^2)$
	$103°C<T<105.5°C$	$-11571 \times T + (1222 \times 10^2)$
	105.5°C<T< 152°C	$0.191 \times (T - 105.5)^3 + 1554$
	$152°C<T<156.5°C$	$-3973 \times T + (6246 \times 10^2)$
Liquid State 156.5°C < T		2835

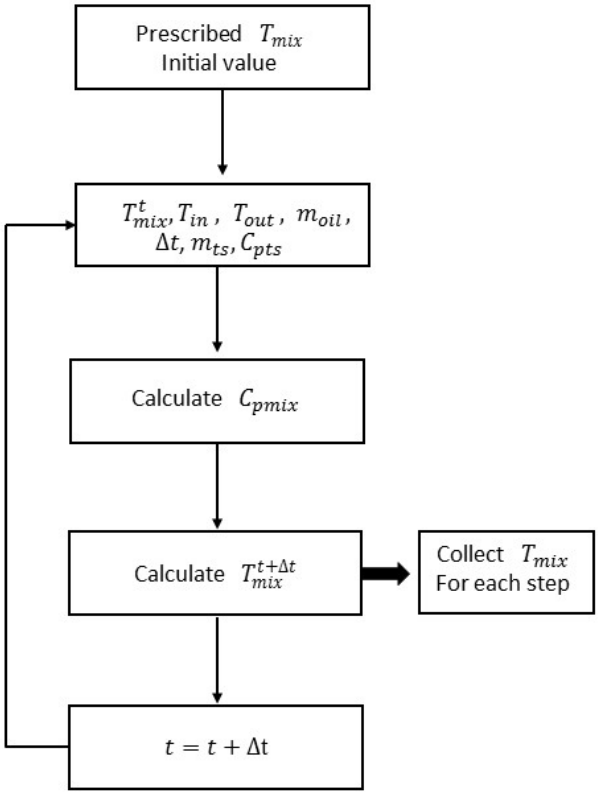

Figure 5.69: Calculation steps for the temperature histories of PCM.

Figure 5.69 shows the calculation steps to predict the temperature histories of PCM. Before starting the experiment of the solidification process, the temperature of test-section,

PCM, and heat transfer oil maintained at 190°C. Thus, the start of the numerical analysis prescribes the temperature of the mixture to 190°C. After that, take the temperature of heat transfer oil inlet and outlet, the flow rate of oil at the same time step from the experiment, and the mass of test section material, and the specific heat of test section. The time step for each step takes 15 s as data collection time of data logger. And then calculate the specific heat of mixture according to the previous step temperature of mixture and data from Table 5.4. Next, the temperature of the mixture was calculated by Equation 5.15 and collect this temperature of the mixture for this time step. Finally, take the new time step and looping again from step two. This calculation for the oil flow rate of 1.0 kg/min and numerical analysis repeats again as previous for the oil flow rate of 1.5kg/min, and 2.0 kg/min.

Figure 5.70, Figure 5.71 and Figure 5.72 show the results of the temperature histories of numerical analysis and experiment for the oil flow rate of 1.0, 1.5, and 2.0 kg/min respectively. In experiment result, the temperature of the mixture is very quickly down after starting the experiment of the solidification process because the difference temperature of the mixture and heat transfer oil is large at this time. And then, the temperature of the mixture increases again because the forming of the solidified mixture is quickly at that time in the experiment. In numerical analysis cannot find this phenomenon. The trend of the temperature histories of mixture quite same with the experiment and numerical analysis method. Thus, this numerical analysis can be used to predict the temperature of the mixture during the solidification. In numerical analysis, the temperature of the mixture is slightly less than that of the experimental result at each time step. The reason for this phenomenon is that the measured thermocouples are not located just pass the PCM region and the outlet temperature is taken the average outlet temperature of the test section. The thermocouples cannot be placed just after the mixture because the solidification heights always change according to the flow rate of oil.

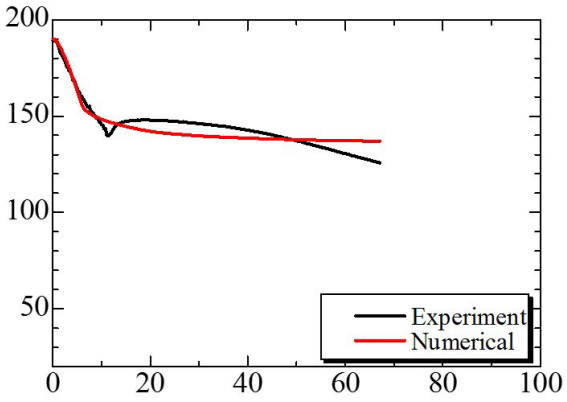

Figure 5.70: Comparison of results for 1.0 kg/min oil flow rate.

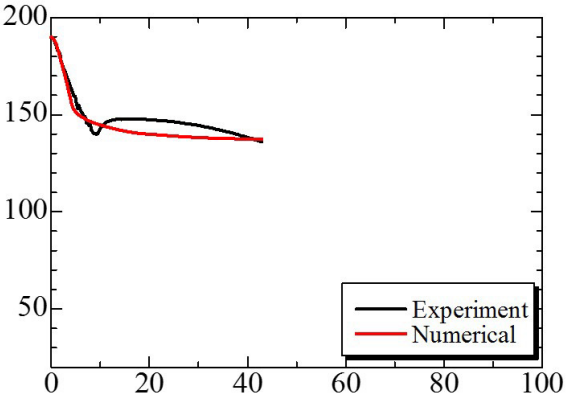

Figure 5.71: Comparison of results for 1.5 kg/min oil flow rate.

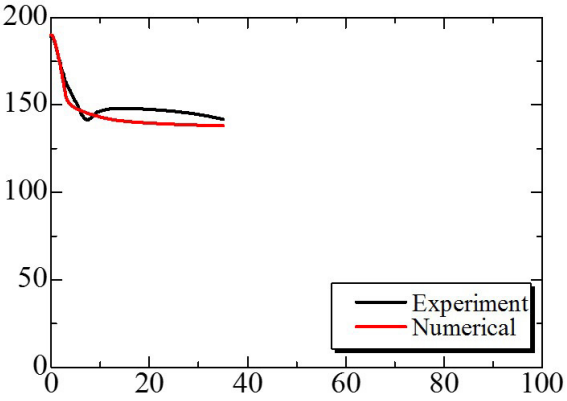

Figure 5.72: Comparison of results for 2.0 kg/min oil flow rate.

5.10 Summary.

An experimental investigation of the characteristics of a direct-contact heat exchanger based on the storage and release of latent heat was undertaken. The characteristics of heat

storage and release of a mannitol and erythritol mixture with various oil flow rates were investigated. By increasing the oil flow rate, solidified PCM at the interface flowed up with the oil from the inlet, the porous area increased, and the solidified height increased. At high oil flow rates, solidified PCM flowed out of the test section with the oil. To prevent this, the various methods were observed in this chapter.

At first, the solidified height was controlled by installing a perforated partition plate in the PCM region in the latent heat storage system. In the solidification process, the solidified height of the PCM was 270 mm without the perforated partition plate and 150 mm with the perforated partition plate. The formed oil droplets were broken by the surface of the perforated partition plate, thus it may have reduced the solidified height of the PCM. An aluminum metal fiber was installed again in the PCM region and the results were compared between experiments without the perforated partition plate, and with the perforated partition plate, and with the metal fiber. Using the metal fiber, the solidified height was 100 mm. The metal fiber was better distributed in the PCM region and PCM-coated oil droplets were broken by the metal fiber.

When inserting the perforated partition plate and metal fiber, although decrease the solidified height of PCM during the solidification process, the amount of heat release is slightly decreased than that of without insertion. To improve the amount of heat release, the effect of changing the diameter of the metal fibers, the filling ratio and the filling position were also investigated. The solidification heights of the addition of metal fibers, changing the metal fiber diameter, changing the filling rate and changing the fill position were 100 cm, 85 cm, 100 cm and 100 cm respectively. The rate of heat release slightly decreased with metal fiber than without metal fibers. But this rate was slightly increased with the metal fiber in diameter 0.2 mm. So, the most effective conditions employed metal fibers with a diameter of 0.2 mm. The aluminum perforated plate and mesh were also used to prevent the flow out problem of PCM. Both of two have the other problem that the pressure of oil increase like using the aluminum perforated plate. This method also cannot use to prevent the solidification height of PCM mixture. The numerical calculation is performed to predict

the temperature of the mixture and compare to the experimental results. As a results, the temperature trend of the calculation is nearly the same with the experimental results.

Chapter 6

Conclusion and Future Work

6.1 Conclusion

In this dissertation, the investigation of three new heat storage material mixtures at the different temperature range of melting temperature were investigated. The waste energy of factories is stored in the latent heat storage material and the energy will be used at the desired place and time. As advantages, it will decrease the usage of fossil fuel, decrease the difference between the energy supply and demand, and can protect the environment impact.

In Chapter 3, phase change materials to store the waste heat energy from the factories for the temperature range 300∼400°C were selected. NaCl:KCl:LiCl (0:54:46)wt% and NaCl:KCl:LiCl (23 : 46 : 31)wt% were selected as heat storage material mixtures. For using these two mixtures, corrosiveness tests were carried out with different types of material SS304, SS316, SS316L, SS310, copper, brass, carbon steel, aluminum, nickel, titanium, and molybdenum. After that also performed tests of the corrosiveness condition of constructive materials by using some corrosion and heat resistance paints and spray. Corrosion can be caused by both of oxygen and heat storage material mixture vapor. Thus, corrosion tests were performed again by inserting the argon gas instead of oxygen inside of the electric furnace. Although the nickel and molybdenum can be used as construction material for the latent heat storage system, they are very expensive and it would not match the economical point of view. Most materials have corrosiveness problem with the heat storage material

because of high temperature operating condition. Electric furnace has some leakage from the upper hole and door while making the corrosiveness test. Thus, corrosiveness test was made again by using small vacuum furnace and argon gas. As results, the corrosiveness of test plate decreased by using argon gas. Further corrosiveness tests are needed to construct the latent heat storage system for this temperature range because of high temperature.

In Chapter 4, phase change materials to store the waste heat energy from the factories for the temperature range 200∼300°C were investigated. NaOH:LiOH (70 : 30)mol% was selected as heat storage material mixtures. For using these two mixtures, make corrosiveness test with different types of material SS304, SS316, SS316L, copper, and nickel. After the corrosiveness test, SS316L was used for construction the experimental device. But argon gas must be inserted inside test section to decrease the corrosiveness problem. The experimental device contains test section, heating system and cooling system separately. The melting process is made by using the plate heater and solidification process is made by the oil heated in oi bath and pump. By using this device, melting and solidification behavior of PCM was investigated. Device has some surface corrosion and PCM color change after the repeating cycle. Thus, The PCM is not in a very clear while taking the photo. And there has some heat transfer losses, because the operating temperature and the outside temperature are very different.

In Chapter 5, an experimental investigation of the characteristics of a direct-contact heat exchanger based on the storage and release of latent heat was undertaken. The characteristics of heat storage and release of a mannitol and erythritol mixture with various oil flow rates were investigated. By increasing the oil flow rate, solidified PCM at the interface flowed up with the oil from the inlet, the porous area increased, and the solidified height increased. At high oil flow rates, solidified PCM flowed out of the test section with the oil. To prevent this, the various methods were observed in this chapter.At first, the solidified height was controlled by installing a perforated partition plate in the PCM region in the latent heat storage system. In the solidification process, the solidified height of the PCM was 270 mm without the perforated partition plate and 150 mm with the perforated partition plate. The

formed oil droplets were broken by the surface of the perforated partition plate, thus may have reduced the solidified height of the PCM. An aluminum fibers were installed in the PCM region and the results were compared between experiments without the perforated partition plate and with the perforated partition plate. Using the metal fiber, the solidified height was 100 mm, representing a further decrease. The metal fiber was better distributed in the PCM region and PCM-coated oil droplets were broken by the metal fiber.

When inserting the perforated partition plate and metal fiber, although decrease the solidified height of PCM during the solidification process, the amount of heat release is slightly decreased than without using of that. To improve the amount of heat release, the effect of changing the diameter of metal fibers, the filling ratio and the fill position were also investigated. The solidification heights of the addition of metal fibers, changing the metal fiber diameter, changing the filling rate and changing the fill position were 100 cm, 85 cm, 100 cm and 100 cm respectively. The rate of heat release slightly decreased with metal fiber than the without metal fiber. But this rate was slightly increased with the metal fiber in diameter 0.2 mm. Thus, the most effective conditions employed metal fibers with a diameter of 0.2 mm. The aluminum perforated plate and mesh were also used to prevent the flow out problem of PCM. Both of two have the other problem that the pressure of oil increase like using the aluminum perforated plate. This method also cannot use to prevent the solidification height of PCM mixture.The numerical analysis is performed to predict the temperature of the mixture and compare to the experimental results . As a results, the temperature trend of the numerical analysis is nearly same with the experimental results.

6.2 Future Work

For the temperature range of 300∼400°C, there has some corrosives problem of construction material to the mixture because of high temperature. New heat storage material will be investigated for this temperature range and make corrosives test of construction material and new heat storage material. For the temperature range of 200∼300°C, the new heat storage material will also be investigated. For the temperature range of 100∼200°C, the new

methods to prevent the problem of the PCM flow out from the test section and the new methods of numerical analysis will be performed as future study.

List of Publications

The research work presented in this thesis has resulted in the following publications.

Journal Paper

1. **Than Tun Naing**, Akihiko Horibe, Naoto Haruki, Yutaka Yamada, "Melting and Solidification Heat Transfer Characteristics of a Phase-Change Material in a Latent Heat Storage Vessel: Effects of a Perforated Partition Plate and Metal Fiber," Journal of Power and Energy Engineering, vol. 5, No. 8, pp. 13-29, 2017.

2. **Than Tun Naing**, Akihiko Horibe, Naoto Haruki, Yutaka Yamada, "Reduction of the solidification Height of Phase-change Material in Direct-contact Latent Heat Storage Vessel," Thermal Science and Engineering Vol. 26, No. 1, pp. 19-27,2018.

International Conferences

1. **Than Tun Naing**, Akihiko Horibe, Naoto Haruki, Yoshitaka Takase , "Direct Contact Heat Storage/Release Characteristics in a Latent Storage Vessel," International student symposium on power and mechanical engineering Okayama, 2016, 8.2016, Okayama, Japan.

2. Akihiko Horibe, **Than Tun Naing**, Naoto Haruki, Yoshitaka Takase, "PCM Solidification Height Control by Using Metal Fiber in a Direct Contact Latent Heat Vessel,"

The 11^{th} Asian Thermo-physical Properties Conference, ATPC2016,10.2016, Yokohama, Japan.

3. **Than Tun Naing**, Akihiko Horibe, Naoto Haruki, Yoshitaka Takase, "Solidification Height of PCM in the Direct Contact Heat Storage Vessel is Controlled by Aluminum Metal Fiber," The 7^{th} International conference on science and engineering, ICSE2016, 12.2016,pp. 467-470, Yangon, Myanmar,

National Conferences

1. Akihiko Horibe, Naoto Haruki, Yoshihiko Sano, **Than Tun Naing**, Yoshitaka Takase,"Effect of Perforated Lattice for Direct Contact Heat Storage with Mixed Sensible-heat Heat Storage Material," The 52^{nd} National Heat Transfer Symposium, 6.2015, Fukuoka, Japan.

2. **Than Tun Naing**, Akihiko Horibe, Naoto Haruki, Yoshitaka Takase, "Study for Solidification Height in Direct Contact Latent Heat Storage Vessel," The 53^{rd} National Heat Transfer Symposium, 5.2016, Osaka, Japan.

3. Akihiko Horibe, Naoto Haruki, Yoshihiko Sano, **Than Tun Naing**, *Masakazu Shinoda, "The Solidification and Melting Behavior in a Direct Contact Latent Heat Storage Vessel, The Effect of Metal Fiber," The 6^{th} Latent Thermal Engineering Symposium, 12.2016, Kyoto, Japan.

4. Akihiko Horibe, Yutaka Yamada, **Than Tun Naing**, *Nobumasa Suzuki and Kazuo Takahashi, "Melting point measurement and corrosion test of mixed molten salt," The 7^{th} Latent Thermal Engineering Symposium, 12. 2017, Okayama, Japan.

Bibliography

Bibliography

[1] Zhengguo Zhang and Xiaoming Fang, "Study on paraffin/expanded graphite composite phase change thermal energy storage material," Energy Conversion and Management Vol. 47, pp. 303310, 2006.

[2] A. Abhat, "Low-Temperature Latent Heat Thermal Energy Storage: Heat Storage Materials," Journal of Solar Energy, Vol. 30 No.40, pp. 313-332, 1983.

[3] K. Pielichowska, K. Pielichowski, Phase change materials for thermal energy storage, Progress in Materials Science, 65, 67-123 (2014)

[4] Mohammed M. Farid et al., "A review on phase change energy storage: materials and applications," Energy Conversion and Management Vol. 45, pp.15971615, 2004.

[5] A. Joseph, M. Kabbara, D. Groulx, P. Allred, M. A. White, "Characterization and real-time testing of phase-change materials for solar thermal energy storage," International Journal of Energy Research, 40, 61-70 (2016).

[6] M. Mazman, L. F. Cabeza, H. Mehling, M. Nogues, H. Evliya, H. . Paksoy, "Utilization of phase change materials in solar domestic hot water systems," Renewable Energy, 34, 1639-1643 (2009).

[7] Nessim Arfaoui, Salwa Bouadila, Amenallah Guizani, "A highly efficient solution of off-sunshine solar air heating using two packed beds of latent storage energy," Solar Energy 155 (2017) 12431253.

[8] Z. Ling, Z. Zhang, G. Shi, X. Fang, L. Wang, X. Gao, Y. Fang, T. Xu, S. Wang, X. Liu, "Review on thermal management systems using phase change materials for electronic components, Li-ion batteries and photovoltaic modules," Renewable and Sustainable Energy Reviews, 31,427-438 (2014).

[9] M. Rastogi, A. Chauhan, R. Vaish, A. Kishan, "Selection and performance assessment of Phase Change Materials for heating, ventilation and air-conditioning applications," Energy Conversion and Management, 89, 260-269 (2015).

[10] M. K. A. Sharif, A. A. Al-Abidi, S. Mat, K. Sopian, M. H. Ruslan, M. Y. Sulaiman, M. A. M. Rosli, "Review of the application of phase change material for heating and domestic hot water systems," Renewable and Sustainable Energy Reviews, 42, 557-568 (2015).

[11] Dan Nchelatebe Nkwetta , Pierre-Edouard Vouillamoz, Fariborz Haghighat Mohamed El-Mankibi , Alain Moreau c, Ahmed Daoud, "Impact of phase change materials types and positioning on hot water tank thermal performance: Using measured water demand profile," Applied Thermal Engineering 67, 460-468 (2014).

[12] Moe Kabbara, Ali Cherom Kheirabadi, Dominic Groulx, "Numerical Modelling of Natural Convection Driven Melting for an Inclined/Finned Rectangular Enclosure," Proceedings of the ASME 2016 Summer Heat Transfer Conference, HT2016,(2016).

[13] Farid, M.M.; Khudhair, A.M.; Razack, S.A.K.; Al-Hallaj, S., "A review on phase change energy storage: Materials and applications," Energy Conv. Manag. 2004, 45, pp. 15971615.

[14] Michal Pomianowski, Per Heiselberg, Yinping Zhang, "Review of thermal energy storage technologies based on PCM application in buildings," Energy and Buildings 67 (2013) pp. 5669.

[15] Sanghoon Baek and Jin Chul Park, "Proposal of a PCM Underfloor Heating System Using a Web Construction Method," International Journal of Polymer Science Volume 2017, Article ID 2693526.

[16] Yinping Zhang, Guobing Zhou, Kunping Lin, Qunli Zhang, Hongfa Di, "Application of latent heat thermal energy storage in buildings: State-of-the-art and outlook," Building and Environment 42 (2007) 21972209.

[17] Kuznik, F.; David, D.; Johannes, K.; Roux, J.J.,"A review on phase change materials integrated into building walls," Renew. Sust. Energy. Rev. 2011, 15, 379391.

[18] Abduljalil A. Al-Abidi n, SohifBinMat, K.Sopian, M.Y.Sulaiman, C.H.Lim, AbdulrahmanTh, .,"Review of thermal energy storage for airconditioning systems," Renewable andSustainableEnergyReviews16(2012)58025819.

[19] Yukitaka Kato, Rui Takahashi, Toshiya Sekiguchi, Naoya Hirao, Junichi Ryu, "Development of chemical heat pump for recovery of waste heat at middle temperatures of 200-400°C," Proceedings of VIII Minsk International Seminar Heat Pipes, Heat Pumps, Refrigerators, Power Sources, (2017).

[20] A. Elefsiniotis, Th. Becker, and U. Schmid, "Thermoelectric Energy Harvesting using Phase Change Materials (PCMs) in High Temperature Environments in Aircraft," Journal of electronic materials, Vol. 43, No. 6, 2014, pp. 1809-1814.

[21] Dakuri Arijun and J.Hayavadana, "Thermal Energy Storage Materials(PCMs) for Textile Application," Journal of textile and apparel, technology and management, Vol.8, Issue 4,2014.pp. 1-11.

[22] Nicholas R. Jankowski, F. Patrick McCluskey, "A review of phase change materials for vehicle component thermal buffering," Applied Energy 113 (2014) pp. 15251561.

[23] Sarada Kuravi, Jamie Trahan, D. Yogi Goswami, Muhammad M. Rahman, Elias K. Stefanakos, "Thermal energy storage technologies and systems for concentrating solar power plants," Progress in Energy and Combustion Science 39 (2013) pp. 285-319.

[24] Atul Sharma, V. V. Tyagi, C. R. Chen and D. Buddhi, "Review on thermal energy storage with phase change materials and applications," Renewable and Sustainable Energy Reviews vol. 13, pp.318345, 2009.

[25] Malek Nofal, Yayue Pan, Said Al-Hallaj, "Selective Laser Sintering of Phase Change Materials for Thermal Energy Storage Applications," Procedia Manufacturing 10 (2017) 851865.

[26] Murray RE, Groulx D., "Experimental study of the phase change and energy characteristics inside a cylindrical latent heat energy storage system: part 2, consecutive charging and discharging," Renewable Energy 2015; 63:724734.

[27] Mohammad Bashar and Kamran Siddiqui, "Investigation of heat transfer during melting of a PCM by a U-shaped heat source,"' Int. J. Energy Res. 2017; 41:20912107.

[28] Zalba, B.; Marin, J.M.; Cabeza, L.F.; Mehling, H., "Review on thermal energy storage with phase change: Materials, heat transfer analysis, and applications.," Appl. Therm. Eng. 2003, 23, 251283.

[29] MM. Sorour, "Performance of a small sensible heat energy storage unit," Energy Convers. Mgmt Vol. 28, No. 3, pp. 211-217, 1988.

[30] Yukitaka Kato, Rui Takahashi, Toshiya Sekiguchi, Junichi Ryu, "Study on medium-temperature chemical heat storage using mixed hydroxides," International Journal of Refrigeration, Volume 32, Issue 4, June 2009, pp. 661-666.

[31] Junichi Ryu, Rui Takahashi, Naoya Hirao, and Yukitak Kato "Effect of Transition Metal Mixing on Reactivities of Magnesium Oxide for Chemical Heat Pump," Journal of Chemical Engineering of Japan, Vol. 40, No. 13, 2007, pp. 1281-1286.

[32] M. A. Boda, R. V. Phand, A. C. Kotali, "Various Applications of Phase Change Materials: Thermal Energy Storing Materials," International Journal of Emerging Research in Management &Technology (Volume-6, Issue-4), 2017, pp. 167-171.

[33] Takahiro Nomura, Masakatsu Tsubota, Teppei Oya, Noriyuki Okinaka, Tomohiro Akiyama, "Heat Storage in Direct-Contact heat exchanger with phase change material," Applied Thermal Engineering 50 (2013), 26-34.

[34] Nomura, T., Tsubota, M., Sagara, A. and Okinaka, N., "Performance Analysis of Heat Storage of Direct-Contact Heat Exchanger with Phase Change Material," Applied Thermal Engineering, 58, 108-113, 2013.

[35] Atul Sharma, V.V. Tyagi, C.R. Chen, D. Buddhi, "Review on thermal energy storage with phase change materials and applications," Renewable and Sustainable Energy Reviews 13 (2009) 318345.

[36] Nitin. D. Patil, S. R. Karale, "Design and Analysis of Phase Change Material based thermal energy storage for active building cooling: a Review," International Journal of Engineering Science and Technology(IJEST), Vol. 4 No. 6 (2012) pp 2502-2509.

[37] MD. Mansoor Ahamed, J.Kannakumar, P.Mallikarjuna reddy, "Design And Fabrication of Cold Storage Plant Using Phase Change Material (PCM)," International Journal of Innovative Research in Science, Engineering and Technology, Vol. 2, Issue 9, September 2013, pp 4277-4286.

[38] Aneesh.V, Gnanadurai Ravikumar Solomon, "Review on heat transfer enhancement during solidification of PCM," IOSR, Journal of Mechanical and Civil Engineering (IOSR-JMCE) 2014, pp. 38-45.

[39] Abhay B. Lingayat, Yogesh R. Suple, "Review on Phase Change Material as Thermal Energy Storage Medium: Materials," Application, International Journal of Engineering Research and Applications (IJERA), Vol. 3, Issue 4, Jul-Aug 2013, pp.916-921.

[40] S. R. Karale, Dr. G.K Awari, "Thermal Analysis of Energy storage system for federal facilities using phase change material: a Review," IRACST Engineering Science and Technology: An International Journal (ESTIJ), Vol.2, No. 5, October 2012, pp.875-880.

[41] Lavinia Gabriela Socactu, "Thermal Energy Storage with Phase Change Material," Leonardo Electronic Journal of Practices and Technologies, Issue 20, January-June 2012, p. 75-98.

[42] Uros Stritih, Eneja Osterman, Hunay Evliya, VincencButala, HalimePaksoy, "Exploiting solar energy potential through thermal energy storage in Slovenia and Turkey," Renewable and Sustainable Energy Reviews25(2013)442461.

[43] Parfait Tatsidjodoung, NolwennLePierres, LingaiLuo, "A review of potential materials for thermal energy storage in building applications," Renewable and Sustainable Energy Reviews 18 (2013) 327349.

[44] Yejun Zhu, "Modeling and Optimization of Phase Change Material Composites for Latent Heat Storage," Ph.D Thesis (2015), Hong Kong.

[45] E. Or, A. de Gracia , A. Castell , M.M. Farid , L.F. Cabeza, "Review on phase change materials (PCMs) for cold thermal energy storage applications," Applied Energy 99 (2012) 513533.

[46] Akgn, M., O. Aydn, and K. Kaygusuz, "Experimental study on melting/solidification characteristics of a paraffin as PCM. Energy Conversion and Management," 2007. 48(2): p. 669-678.

[47] He Bo, E. Mari Gustafsson, "Fredrik Setterwall, Tetradecane and hexadecane binary mixtures as phase change materials (PCMs) for cool storage in district cooling systems," Energy 24 (1999) 10151028.

[48] Hasnain, S.M., "Review on sustainable thermal energy storage technologies; Part I: Heat storage materials and techniques," Energy Convers. Manag. 1998, 39, 11271138.

[49] A. Hasan, S.J. McCormack, M.J. Huang, B. Norton, "Characterization of phase change materials for thermal control of photovoltaics using Differential Scanning Calorimetry and Temperature History Method," Energy Conversion and Management 81 (2014) 322329.

[50] A. Shukla, Karunesh Kant, Atul Sharma, "Solar still with latent heat energy storage: A review, Innovative Food Science and Emerging Technologies," 41 (2017) 3446.

[51] Ahmet Sari, Murat Akcay, Mustafa Soylak, Adem Onl, "Polymer-stearic acid blends as form-stable phase change material for thermal energy storage," Journal of Scientific and Industrial Research, Vol. 64, December 2005, pp. 991-996.

[52] Ahmet Sari, Cemil Alkan, and Alper Bicer, "Development, Characterization, and Latent Heat Thermal Energy Storage Properties of Neopentyl Glycol-Fatty Acid Esters as New SolidLiquid PCMs," Ind. Eng. Chem. Res. 2013, 52, 1826918275.

[53] H Ambarita, I Abdullah, C A Siregar, R E T Siregar, A D Ronowikarto, "Experimental Study on Melting and Solidification of Phase Change Material Thermal Storage," IOP Conf. Series: Materials Science and Engineering 180 (2017) 012030.

[54] B. Kanimozhi, A. Prabhu. M. Anish, P. K. Harish Kumar, "Review on Heat Transfer Enhancement Techniques in Thermal Energy Storage Systems," Int. Journal of Engineering Research and Applications, Vol. 4, Issue 2(Version 1), February 2014, pp.144-149.

[55] Nicole Pfleger, Thomas Bauer, Claudia Martin, Markus Eck and Antje Wrner, "Thermal energy storage overview and specific insight into nitrate salts for sensible and latent heat storage," Beilstein J. Nano technol. 2015, 6, 14871497.

[56] Belen Zalba , Jose Ma Marn , Luisa F. Cabeza , Harald Mehling, "Review on thermal energy storage with phase change: materials, heat transfer analysis and applications," Applied Thermal Engineering 23 (2003) 251283.

[57] Benjamin Sponagle, Simon Maranda, "Investigation of the thermal behaviour of thin phase change material packages as a solution to temperature control in electronics," Proceedings of the ASME 2017 Summer Heat Transfer Conference, HT2017,July, 2017, pp. 1-10.

[58] Dinu G Thomasa, Sajith Babu Cb, Sajith Gopic, "Performance Analysis of a Latent Heat Thermal Energy Storage System for Solar Energy Applications," Procedia Technology 24 (2016) 469 476.

[59] Eunsoo Choi, Young I. Cho, and Harold G. Lorsch, "Thermal analysis of the mixture of laboratory and commercial grades hexadecane and teradecane," Int comm. Heat mass transfer, Vol. 19, pp.1-15,1992

[60] Hiroyuki Kumano, Akio Saito, Seiji Okawa, Kazunari Takeda, Atsuko Okuda, "Study of direct contact melting with hydrocarbon mixtures as the PCM," International Journal of Heat and Mass Transfer 48 (2005) 32123220.

[61] Hisham Ettouney, Hisham El-Dessouky,and Eman Al-Kandari, "Heat Transfer Characteristics during Melting and Solidification of Phase Change Energy Storage Process," Ind. Eng. Chem. Res. 2004, 43, 5350-5357.

[62] Irena Paunovic, Anil K. Mehrotra, "Liquid-solid phase transformation of C16H34, C28H58 and C41H84 and their binary and ternary mixtures," Thermochimica Acta 356 (2000) 27-38.

[63] Jaume Gasia, Marc Martin, Aran Sol , Camila Barreneche and Luisa F. Cabeza, "Phase Change Material Selection for Thermal Processes Working under Partial Load Operating Conditions in the Temperature Range between 120C and 200C," Appl. Sci. 2017, 7, 722.

[64] Jong Chan Choi and Sang Done Kim, "Heat transfer characteristics of a latent heat storage system using $MgCl_2.6H_2O$, Energy," Vol. 17, No. 12, pp. 1153-1164, 1992.

[65] Kota Nakano, Yasuaki Masuda, and Hirofumi Daiguji, "Crystallization and Melting Behavior of Erythritol In and Around, Two-Dimensional Hexagonal Mesoporous Silica," J. Phys. Chem. C 2015, 119, 47694777.

[66] M. Rahimi, A. A. Ranjbar, D. D. Ganji, K. Sedighi, and M. J. Hosseini, "Experimental Investigation of Phase Change inside a Finned-Tube Heat Exchanger," Journal of Engineering Volume 2014, Article ID 641954, pp. 1-11.

[67] Nan Ren Yu-ting Wu Tao Wang Chong-fang Ma, "Experimental study on optimized composition of mixed carbonate for phase change thermal storage in solar thermal power plant," J Therm Anal Calorim (2011) 104:12011208.

[68] Yifei Wang, Liang Wang, Haisheng Chen, Ningning Xie, Zheng Yand and Lei Chai, "Numerical study on thermal performance characteristics of a cascaded latent heat storage unit," J Power and Energy 2016, Vol. 230(1) 126137.

[69] R. Meenakshi Reddy, N. Nallusamy, and K. Hemachandra Reddy, "Experimental Studies on Phase Change Material-Based Thermal Energy Storage System for SolarWater Heating Applications," Journal of Fundamentals of Renewable Energy and Applications,Vol. 2 (2012), Article ID R120314.

[70] R. Sakmoto, M. Kamimoto, Y. Takahashi, Y. Abe, K. Kanari, and T. Ozawa, "Investigation of latent heat-thermal energy storage materials. III. Thermoanalytical evaluation of pentaerythritol, Thermochimica Acta," 71 (1984) 241-249.

[71] Stella P. Jesumathy, M. Udayakumar and S. Suresh, "Heat transfer characteristics in latent heat storage system using paraffin wax," Journal of Mechanical Science and Technology 26 (3) (2012) 959-965.

[72] Stephan H., Andreas K.H and Dieter B., "Thermophysical Characterization of $MgCl2.6H2O$, Xylitol and Erythritol as Phase Change Materials (PCM) for Latent Heat Thermal Energy, Materials Storage (LHTES)," 2017, 10, 444; doi:10.3390 /ma10040444.

[73] Y. Takahashi, M. Kamimoto, Y. Abe, R. Sakamoto, K. Kanari and T. Ozawa, "Investigation of latent heat thermal energy storage materials V. thermoanalytical evaluation of binary eutectic mixtures and compounds of $NaOH$ with $NaNO_3$ or $NaNO_2$, Thermochimica Acta," 123 (1988) 233-245.

[74] Yifei Wang, Liang Wang, Ningning Xie, Xipeng Lin, Haisheng Chen, "Experimental study on the melting and solidification behavior of erythritol in a vertical shell-and-tube

latent heat thermal storage unit," International Journal of Heat and Mass Transfer 99 (2016) 770781.

[75] Zhongliang Liu, Xuan Sun, Chongfang Ma, "Experimental study of the characteristics of solidification of stearic acid in an annulus and its thermal conductivity enhancement," Energy Conversion and Management 46 (2005) 971984.

[76] Murat M. Kenisarin, "High-temperature phase change materials for thermal energy storage," Renewable and sustainable energy reviews 14(2010)955-970.

[77] Thomas Bauer, Doerte Laing, and Rainer Tamme "Overview of PCMs for concentrated solar power in the temperature range 200 to 350 C," Advances in Science and Technology Vol. 74 (2010) pp 272-277.

[78] C. Villada, F. Bolvar, F. Jaramillo, J.G. Castao and F. Echeverra "Thermal evaluation of molten salts for solar thermal energy storage," International Conference on Renewable Energies and Power Quality (ICREPQ14), No.12, 2014.

[79] Bruno Cardenas, Noel Leon, "High temperature latent heat thermal energy storage: Phase change materials, design considerations and performance enchancement techniques," Renewable and sustainable energy reviews 27(2013)724-737.

[80] Sumitomo, H., Kado, S., Nozalo, T., Fushinobu, K. and Okazaki, K. (2015) "Energy Enhancement of Low-Temperature Waste Heat by Methanol Steam Reforming for Hydrogen Production," 8th Asian Hydrogen Energy Conference, Beijing, China, 26-27 May 2005, 26-27.

[81] MyoungJun Kim, JikSu Yu, GyuHoon Chea, "Fundamental study on development of latent heat storage material for waste heat recovery of biomass gasification," Journal of the Korean Society of Marine Engineering, Vol. 38, No. 5 pp. 533 540, 2014.

[82] Japan Society of Thermophysical Properties, Thermophysical Properties Handbook, pp.119-124, 1990.

[83] Inaba, H. and Sato, K. (2000) Latent Cold Heat Energy Storage Characteristics by Means of Direct-Contact-Freezing between Oil Droplets and Cold Water Solution. International Journal of Heat and Mass Transfer, 40, 3189-3200.

[84] Kiatsiriroat, T., Vithayasai, S., Vorayos, N., Nuntaphan, A. and Vorayos, N. (2003) Heat Transfer Prediction for a Direct Contact Ice Thermal Energy Storage. Energy Conversion and Management, 44, 497-508.

[85] Kiatsiriroat, T., Tiansuwan, J., Suparos, T. and Na Thalang, K. (2000) Performance Analysis of a Direct-Contact Thermal Energy Storage Solidification. Renewable Energy, 20, 195-206.

[86] Kaizawa, A., Kamano, H., Kawai, A., Jozuka, T., Senda, T., Maruoka, N. and Akiyama, T. (2008) Thermal and Flow Behaviors in Heat Transportation Container Using Phase Change Material. Energy Conversion and Management, 49, 698-706.

[87] Baran, G. and Sari, A. (2003) Phase Change and Heat Transfer Characteristics of a Eutectic Mixture of Palmitic and Stearic Acids as PCM in a Latent Heat Storage System. Energy Conversion and Management, 44, 3227-3246.

[88] Hidaka, H., Yamazaki, M., Yabe, M., Kakiuchi, H., Pona, E., Kojima, Y. and Matsuda, H. (2004) New PCMs Prepared from Erythritol-Polyalcohols Mixtures for Latent Heat Storage between 80°C and 100°C. Journal of Chemical Engineering of Japan, 37, 1155-1162.

[89] Gubanova, T.V. and Garkushin, I.K. (2007) LiF-LiCl-LiVO3-Li2SO4-Li2MoO4 System. Russian Journal of Inorganic Chemistry, 52, 1624-1628.

[90] Elena Palomo Del Barrio, Rgis Cadoret, Julien Daranlot, Fouzia Achchaq, "New sugar alcohols mixtures for long-term thermal energy storage applications at temperatures between 70 °C and 100°C," Solar Energy Materials & Solar Cells 155 (2016) 454468.

[91] Horibe, A., Jang, H., Haruki, N., Sano, Y., Habara, H. and Takahashi, K. (2015) "Melting and Solidification Heat Transfer Characteristics of Phase Change Material

in the Latent Heat Storage Vessel: Effect of Perforated Partition Plate," International Journal of Heat and Mass Transfer, 82, 259-266.

[92] Horibe, A., Yu, J., Haruki, N., Kaneda, A., Machida, A. and Kato, A.M. (2011) Melting Characteristic of Mixture of Two Kinds of Latent Heat Storage Material. Netsu Bussei, 25, 136-142.

[93] Mitsubishi Chemical Engineering, The Document of Heat Storage Division, 1999.

[94] A. Hoshi and T. S. Saitoh, "A study of the solar steam accumulator with high-temperature latent heat thermal energy storage (1st Report; High melting point phase change material)," Journal of Japan Solar Energy Society, vol. 27, no. 5, pp. 34-40, 2001.

[95] http://www.k-tanac.co.jp/msdsdl.cgi?d=TSF458-100_MSDS_J.pdf, http://www.k-tanac.co.jp/pdsdl.cgi?d=MPMtsf458.pdf, .http://silicones.momentive.jp/data_sheet/pds/Pdf/Jp/MPMtsf451.pdf

[96] JikSu yu, "Research on melting and solidification behaviors of mixed latent heat storage material Erythritol and Mannitol," Ph.d Thesis(2013)

Appendix A. Detail Drawings of Indirect Contact Device

Test section

(a) Top plate

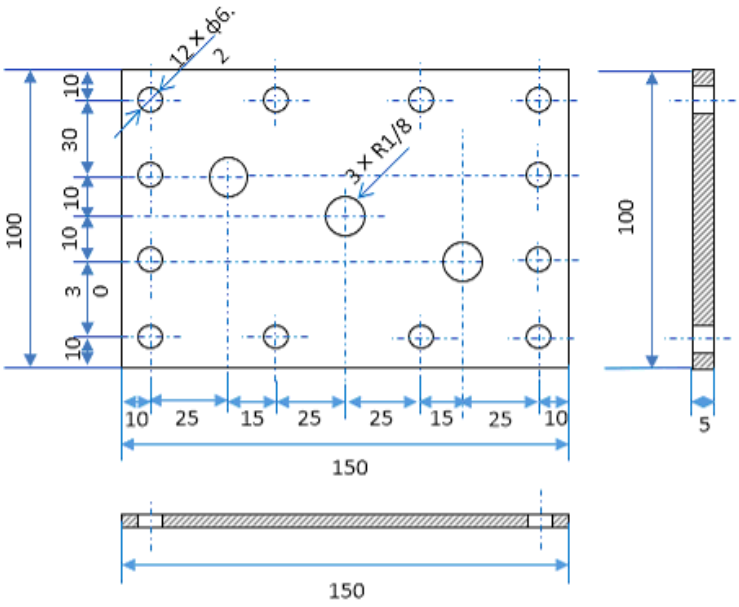

(b) Top lid

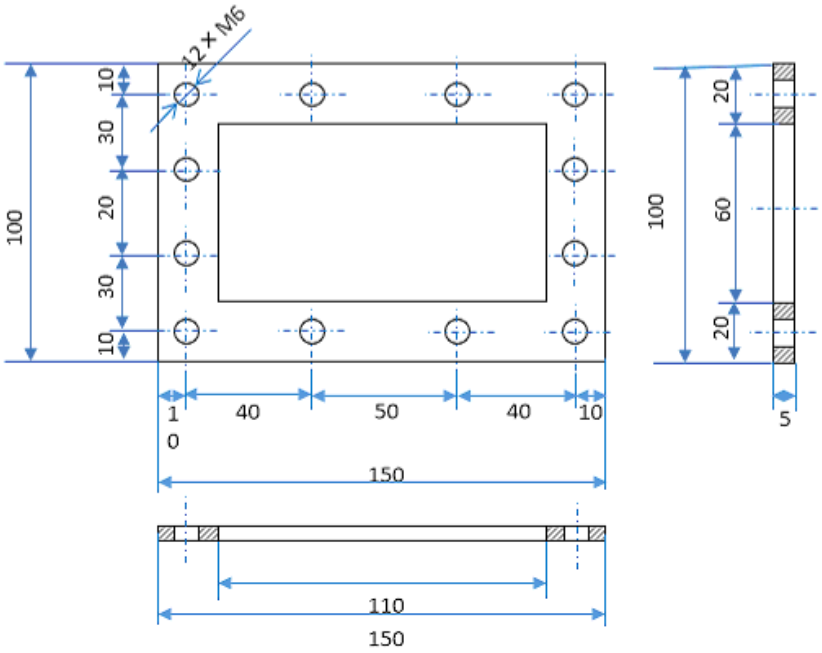

(c) Glass frame

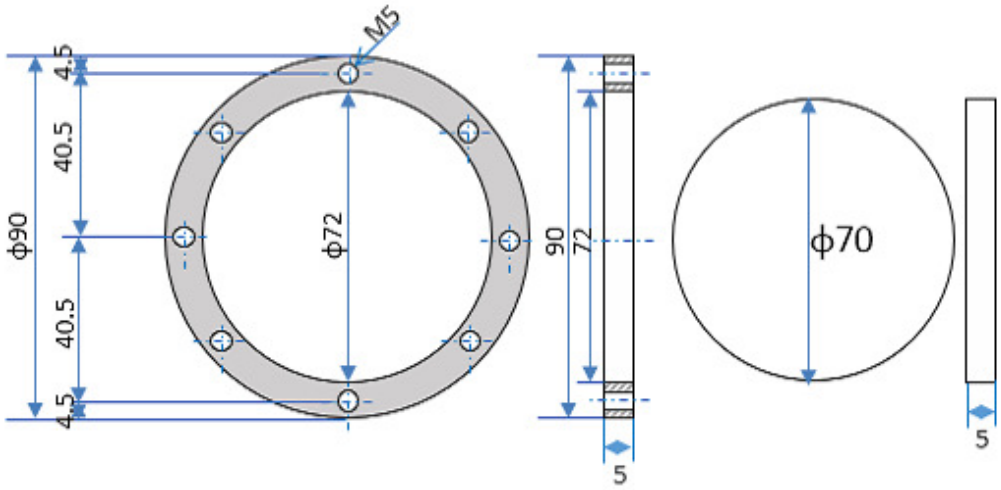

(d) Glass stopper

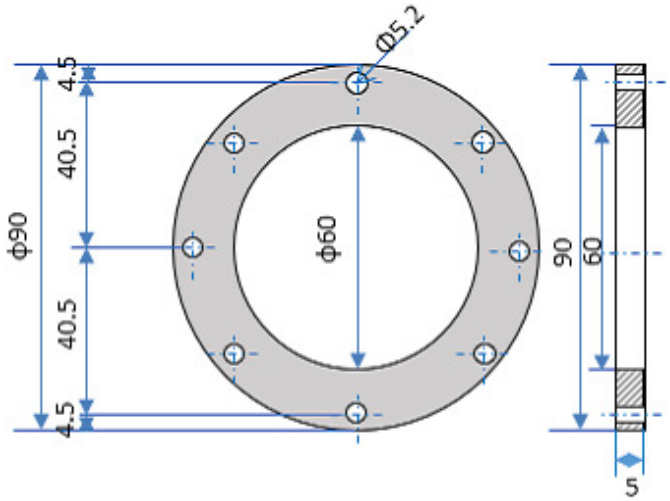

(e) Front plate

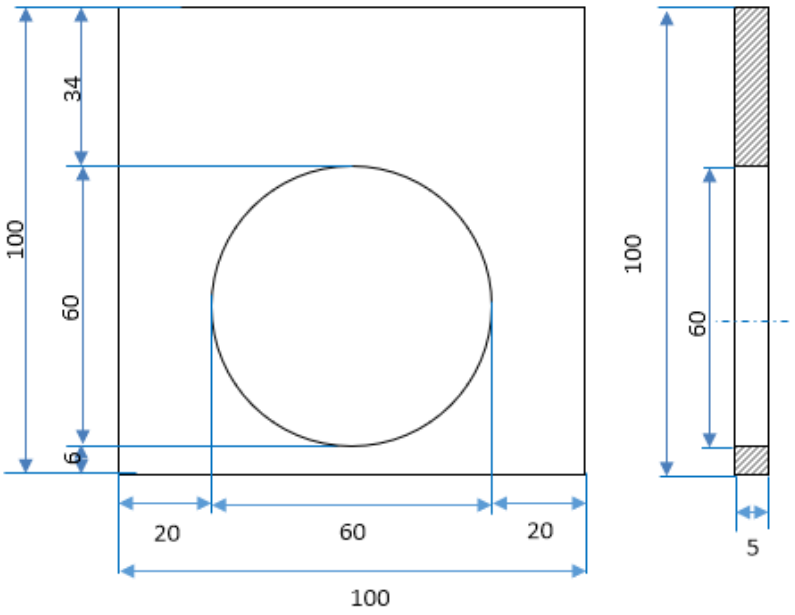

(f) Back plate

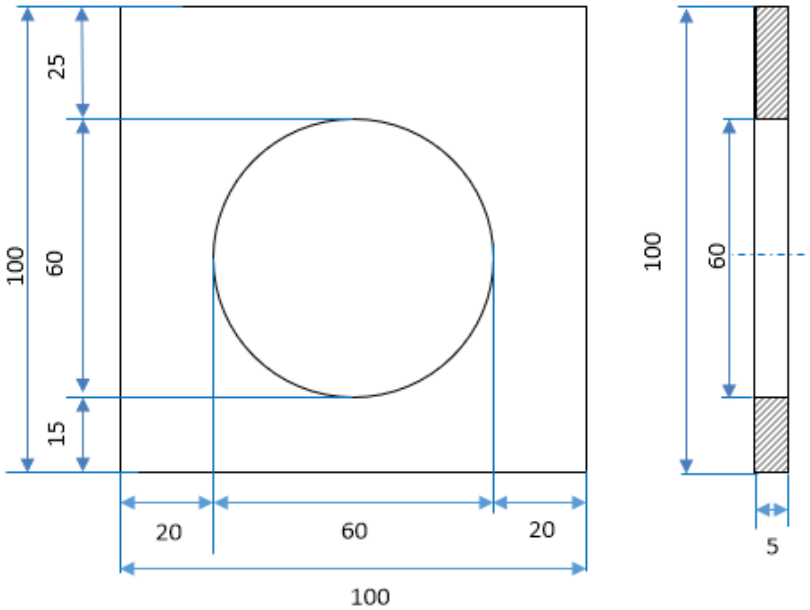

(g) Lower plate

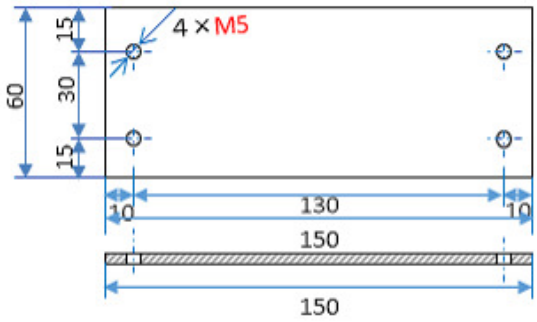

Cooling system

(a) upper plate

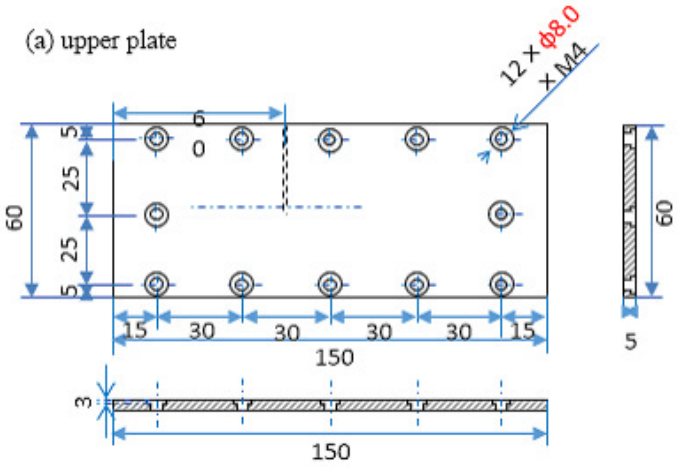

(b) upper lid

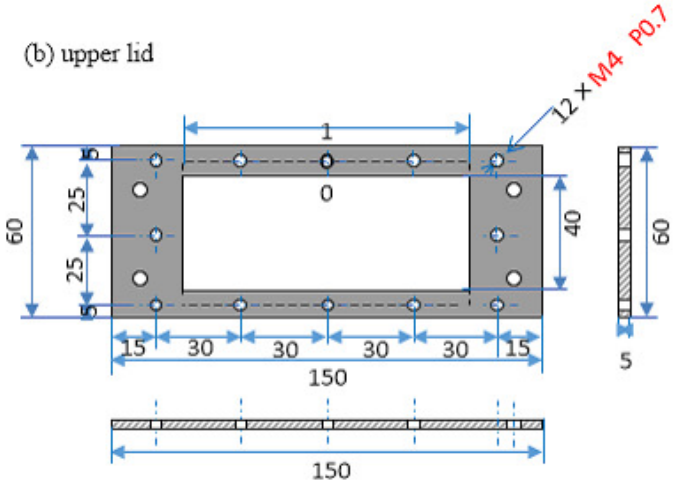

(c) Front and back plate

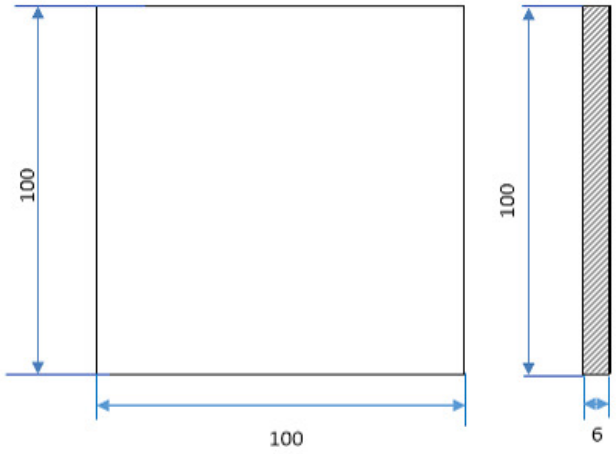

(d) Side plate

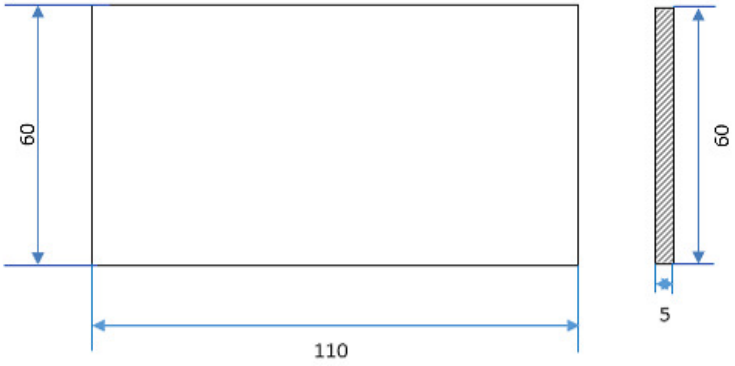

(e) Inside plate

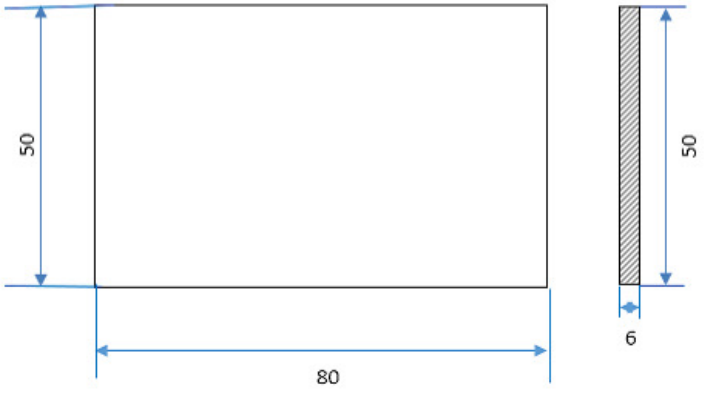

(f) Oil inlet side plate

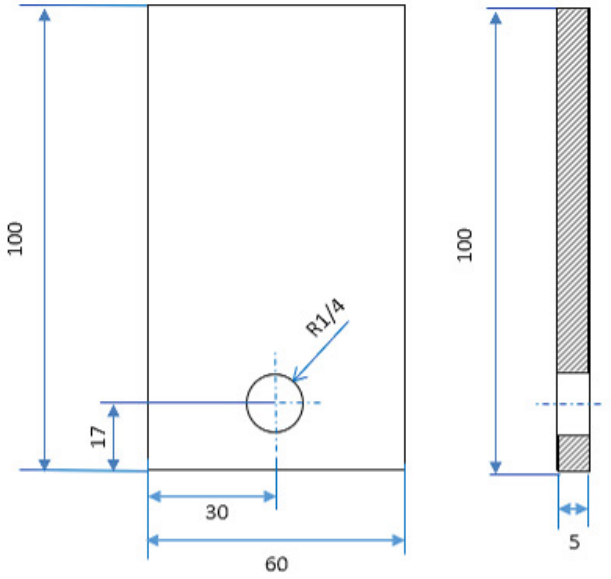

(g) Oil outlet side plate

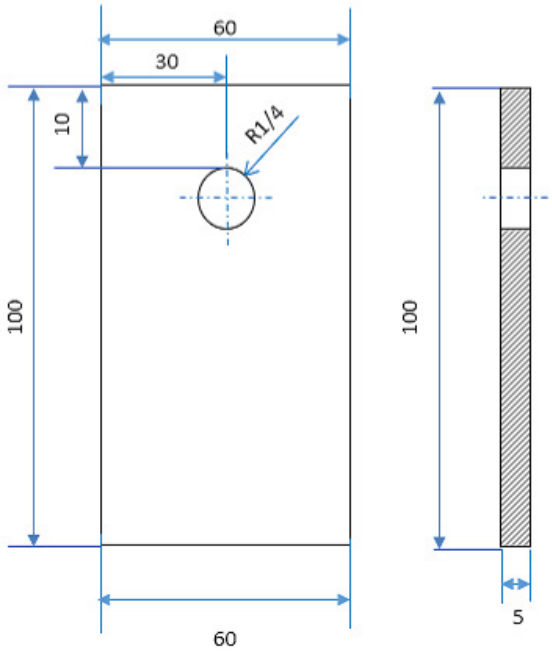

Appendix B. Some Microsopic Photos of Corrosion Test

Titanium with NaCl0%

Before test

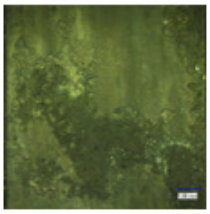

inside after test

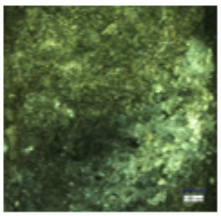

outside after test

Titanium with NaCl23%

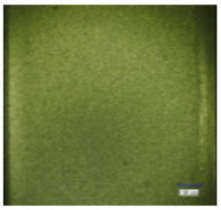

Before test

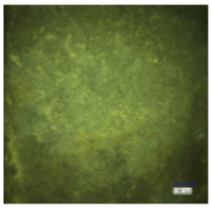

inside after test

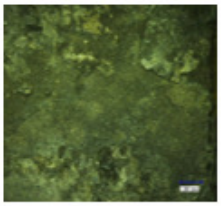

outside after test

Nickel with NaCl0%

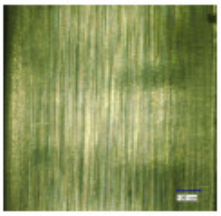

Before test

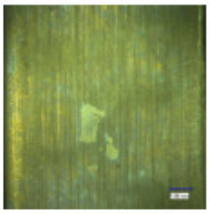

inside after test

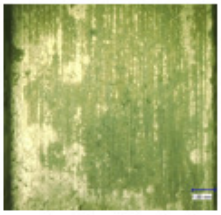

outside after test

Nickel with NaCl23%

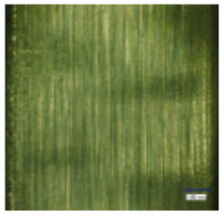

Before test

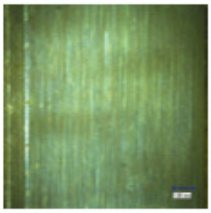

inside after test

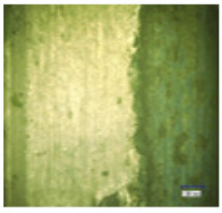

outside after test

Carbon steel with NaCl0%

Before test

After test
in PCM region

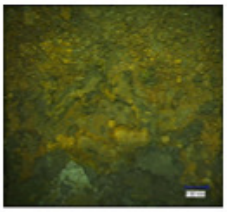

After test
outside PCM region

Carbon steel with NaCl23%

Before test

After test
in PCM region

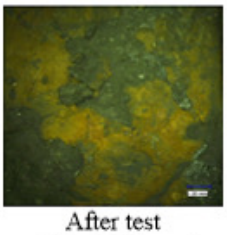

After test
outside PCM region

Aluminum with NaCl0%

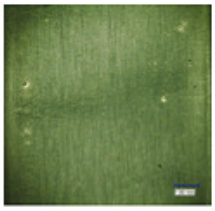

Before test

After 3rd test

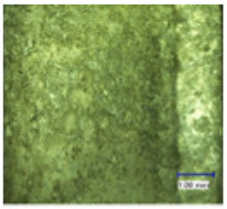

After 4th test

Aluminum with NaCl23%

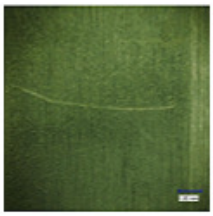

Before test

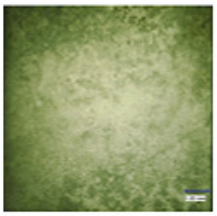

After 3rd test

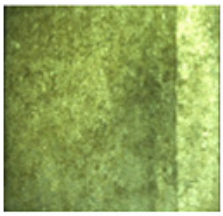

After 4th test

Molybdenum with NaCl0%

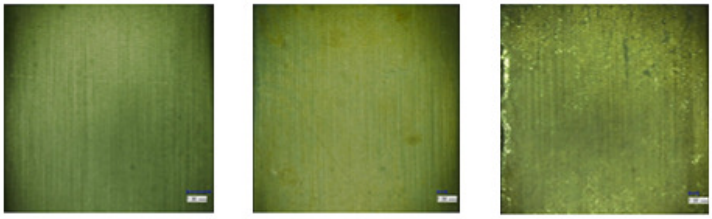

Before test | After test in PCM region | After test outside PCM region

SS310 with NaCl0%

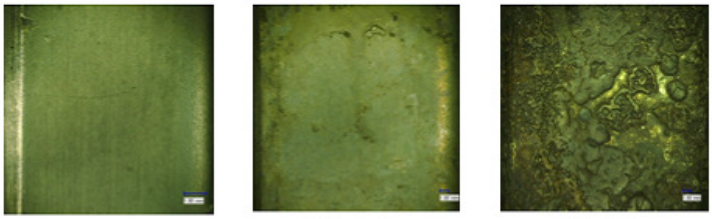

Before test | After test in PCM region | After test outside PCM region

Copper with NaCl0%

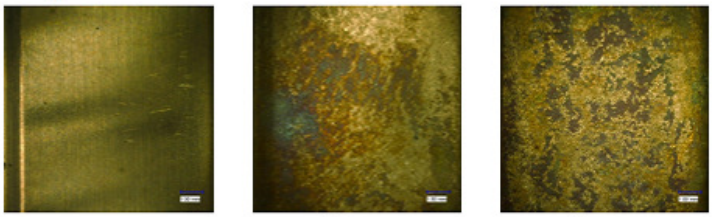

Before test | After test in PCM region | After test outside PCM region

Brass with NaCl0%

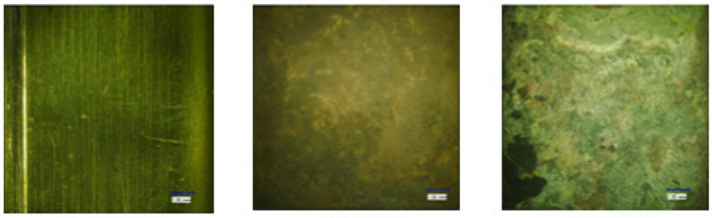

Before test | After test in PCM region | After test outside PCM region